ABSTRACT

CHANGES IN THE U.S. HURRICANE DISASTER LANDSCAPE:
THE RELATIONSHIP BETWEEN RISK AND EXPOSURE

Ashley Irizarry, M.S.
Department of Geography
Northern Illinois University, 2016
Walker S. Ashley, Director

This research appraises how residential built-environment growth influences coastal exposure and how this fundamental component of societal vulnerability contributes to tropical cyclone impact and disaster potential. Historical and future demographic projections from a high-resolution, spatial allocation model illustrate that the area within 50 km of the U.S. Atlantic and Gulf Coastlines has the greatest housing unit density of any physiographic region in the U.S., with residential development in this particular region outpacing non-coastal areas. The growing development footprint and residential densification in a region that has a very high risk to tropical cyclone hazards suggests intensifying disaster potential for U.S. coastal communities. At the local scale, tropical cyclone exposure for six at-risk metropolitan statistical areas (MSAs) along the U.S. Atlantic and Gulf Coasts is assessed. All six MSAs evaluated are distinct in their development character, yet all experience statistically significant growth from 1940 through 2100. Using a worst-case scenario framework, the historical and future residential data for the six MSAs are intersected with synthetic hurricane wind swaths generated from contemporary landfalling events. Of the six metropolitan regions examined, the New York City MSA contains the greatest residential built-environment exposure, but Miami is the most rapidly changing MSA and has the greatest potential for hurricane disaster occurrence based on the juxtaposition of climatological risk and exposure. A disaster potential metric illustrates that all six MSAs will experience significant increases in disaster possibility during the 21st century. This analysis facilitates a detailed spatiotemporal assessment of U.S. coastal region vulnerability, providing decision makers with essential information that may be used to evaluate the potential for tropical cyclone disasters, mitigate tropical cyclone hazard impacts, and build community resilience for these and other hazards in the face of environmental and societal change.

NORTHERN ILLINOIS UNIVERSITY
DE KALB, ILLINOIS

AUGUST 2016

CHANGES IN THE U.S. HURRICANE DISASTER LANDSCAPE: THE RELATIONSHIP BETWEEN RISK AND EXPOSURE

BY

ASHLEY IRIZARRY

A THESIS SUBMITTED TO THE GRADUATE SCHOOL

IN PARTIAL FULFILLMENT OF THE REQUIREMENTS

FOR THE DEGREE

MASTER OF SCIENCE

DEPARTMENT OF GEOGRAPHY

Thesis Director:
Dr. Walker S. Ashley

ACKNOWLEDGEMENTS

First, I would like to thank my advisor and mentor, Dr. Walker Ashley, from whom I have learned to become a better scientist, a better writer, and who has helped me on every step of this research process. I also thank Stephen Strader for his continuous advice and assistance throughout this research project. I would also like to thank my committee members, Dr. David Changnon, Dr. Andrew Krmenec, and Dr. Thomas Pingel for all of their suggestions, support, and encouragement. Lastly, I would like to thank my friends and family, especially my fiancé Justin for motivating and inspiring me to follow my dreams.

TABLE OF CONTENTS

LIST OF TABLES

LIST OF FIGURES

Figure Page

CHAPTER 1

INTRODUCTION

Losses from tropical cyclones are expected to double every 10 years; a rate that suggests that losses in 2050 will be 15 times greater than those in 2006 (Pielke 2007). One key factor in increasing tropical cyclone losses is population and affiliated built-environment growth. Trends in population, population density, and the number of housing units indicate expanding development across the U.S., especially along the coasts (Wilson and Fischetti 2010). By 2040, the U.S. population is projected to reach 400 million, with more than 60% of the population located in the nation's 10 "mega-regions" (Nelson and Lang 2007a; Nelson and Lang 2007b). Three of these "mega-regions" are located along the Gulf and Atlantic Coasts. Naturally, more housing units will be built to accommodate the growth of population along the coast. As population increases, cities swell outward to allow room for growth, in turn, expanding the area's overall developed footprint (Hall and Ashley 2008). Expansion of the human-built environment of a city increases the risk of a geophysical hazard impact and disaster potential (Ashley et al. 2014; Strader and Ashley 2015). The conceptual disaster framework known as the "expanding bull's-eye effect" suggests that increasing and expanding residential built environment leads to more "targets" for hazards to impact. Employing this concept to tropical cyclones, it is likely that the vulnerability of coastline counties will increase over time, which, in turn, will magnify the likelihood of future tropical cyclone disasters. This begs the question: What impact will tropical cyclones have on coastline exposure in the future and, in turn, how will the tropical cyclone disaster landscape change? This is an important inquiry since both tropical cyclone risk and exposure to the hazard are likely to shift—and potentially magnify—in a warming world.

The research suggests that continued development across the U.S. Atlantic and Gulf Coasts will increase exposure to tropical cyclones, and, consequentially, inflate their vulnerability to disasters now and in the future. This study uses residential built environment output from a fine-scale, spatial allocation model to investigate how coastal exposure to tropical cyclones has changed since the mid-20th century and how it is forecast to evolve through 2100. Synthetic hurricane models are developed based on historical storm attributes, permitting an observationally grounded approach to evaluate future disaster "what if" scenarios. The synthetics are employed to simulate possible hurricane impacts across a spatially diverse risk landscape. The goal of the work is to deliver a methodology and set of results that may be used by catastrophe analysts, emergency managers, and policy makers to evaluate how their portfolio and/or community may be affected by future tropical cyclone events. The information may be used by these important groups to reduce vulnerabilities and build resilience in the face of both environmental and societal change.

CHAPTER 2

BACKGROUND

Hurricane Climatology

A tropical cyclone is a large, long-lasting, low pressure system that forms over relatively warm oceans. These storms can produce damaging winds, storm surges, flooding, and tornadoes, all of which can cause substantial damage to both the built and natural environment (Czajkowski et al. 2011; Cangialosi and Berg 2012). These powerful storms are thermodynamic systems that rely on the presence of warm sea-surface temperatures, moisture, and instability. Tropical cyclones can vary in size and intensity, reaching over 1,500 km (932 miles) in diameter (e.g., Hurricane Sandy in 2012; Rasch et al. 2006) with sustained wind speeds as high as 80 m s-1 (178 mph) (e.g., Hurricane Wilma in 2005; Blake et al. 2013). Historically, in the U.S., eight of the ten costliest disasters were due to hurricanes (Smith 2013). Hurricane Katrina in 2005 was the costliest disaster from 2000 to 2010, causing an estimated $81 billion in insured damages (Pielke et al. 2008). The destruction of a tropical cyclone is not limited to coastal counties; tropical cyclones and their hazards can threaten human life well removed from the coast (Georgiou 1986; Czajkowski et al. 2011).

The Saffir-Simpson Hurricane Wind Scale categorizes the hurricane based on the sustained wind speed of the storm. The original Saffir-Simpson scale was based on wind, central pressure, and storm surge criteria; around 1990, the National Hurricane Center (NHC) implemented new criteria that categorizes hurricanes based only on the maximum one-minute sustained wind speed at the surface (Blake and Gibney 2011). Tropical cyclones are assigned a hurricane category when wind speeds exceed 33 m s-1 (74 mph). The lowest classification of hurricanes is Category 1; the highest classification is Category 5, which is given to storms that have sustained winds exceeding 70 m s-1 (157 mph) (Table 1). Category 3, 4, and 5 hurricanes exceed 111 mph (50 m s-1) and are considered major hurricanes (Cangialosi and Berg 2012).

Table 1. The Saffir-Simpson Hurricane Wind Scale

Storm Type	1-Min. Sustained Wind (mph)	(m s^{-1})	(kts)
Tropical Depression	0-38	0-16	0-32
Tropical Storm	39-73	17-32	33-63
Category 1	74-95	33-42	64-82
Category 2	96-110	43-49	83-95
Category 3	111-129	50-58	96-112
Category 4	130-156	59-69	113-136
Category 5	≥157	≥70	≥137

In the North Atlantic, tropical cyclones typically form between June and November, with the climatological peak in September (Blake and Gibney 2011; Cangialosi and Berg 2012). From 1851 through 2010, there were 284 hurricanes that made landfall on the U.S. mainland. On average, there were 17.8 hurricanes that occurred each decade, six of which were considered major hurricanes. In this period, Category 1 hurricanes account for 39.3% of all events, while major landfalling hurricanes account for 33.7%. Some coastal states are impacted by tropical cyclones more than others. For instance, from 1960 through 2008, 86 hurricanes impacted the U.S. Atlantic and Gulf Coasts, with the states of Louisiana, Florida, and North Carolina experiencing 11 or more landfalling hurricanes (Wilson and Fischetti 2010). Overall, Florida is affected by twice as many of these types of storms than any other state in the country (Table 2; Brettschneider 2008; Blake and Gibney 2011).

Table 2. Number of landfalling tropical cyclones from 1900 through 2006 within 50 km of the state (after Brettschneider 2007).

Location	Number of Storms
Louisiana	84
North Carolina	86
Texas	86
Florida	165

Disaster Losses and Trends

An upward trend in hurricane losses is evident when assessing the storm damages over time in the U.S (Pielke 2007; Pielke et al. 2008; Burton 2010; Mendelsohn et al. 2012). While major hurricanes are climatologically rare, they account for 85% of the total damage from 1900 through 2005 (Pielke et al. 2008). To examine historical tropical cyclone damages, Pielke et al. (2008) employed a set of normalization methods on estimated damage costs to control for changes in society (e.g., wealth, inflation, etc.). The Great Miami Hurricane of 1926 caused an estimated $105 million in damages as well as 370 fatalities and over 6,000 injuries. Due to inflation, societal changes, and amplifying exposure, a similar hurricane impacting the same region in contemporary times would likely cause over $160 billion in losses (Table 3). For perspective, Hurricane Katrina in 2005 caused an estimated $81 billion in damages, over $70 billion less than the projected loss from a repeat of the Great Miami Hurricane along today's southeast Florida coast. Overall, results revealed no change in normalized losses, suggesting that societal factors are likely responsible for the trends found in non-normalized tropical cyclone losses (Pielke et al. 2008; Miller et al. 2008; Bouwer 2011) and that losses are not solely based on the frequency or intensity of the hazard (Pielke et al. 2008; Sutter 2009; Bouwer 2011; Weinkle et al. 2012; Bouwer 2013).

Table 3. Top ten storms with the highest normalized damages (after Pielke et al. 2008).

Rank	Hurricane	Year	State	Category	PL05 damage (US$ billions)	CL05 damage (US$ billions)		AIR top 10 events (US$ billions)	
1	Great Miami (6)	1926	FL-FL,AL	4-3	157	(1)	139.5	(1)	160
2	Katrina	2005	LA,MS	3	81	(2)	81	(3)	82
3	Galveston (1)	1900	TX	4	78	(3)	71.9	(6)	66
4	Galveston (2)	1915	TX	4	61.7	(4)	54.1	-	-
5	Andrew	1992	FL-LA	5-3	57.7	(5)	54.3	(2)	84
6	New England (4)	1938	CT,MA,NY,RI	3	39.2	(6)	37.3	(4)	70
7	11	1944	FL	3	38.7	(7)	35.6	-	-
8	Lake Okeechobee	1928	FL	3	33.6	(8)	31.8	(6)	66
9	Donna	1960	FL-NC,NY	4-3	29.6	(9)	31.9	(8)	52
10	Camille	1969	LA,MS	5	21.2	(10)	24	-	-

The potential for climate change to influence hurricane frequency and magnitude is an ongoing debate that leaves researchers unsure of how storm behavior will evolve in the future. After accounting for past changes in intensity, frequency, or duration, the consensus is that frequency of storms may remain constant, but intensity could increase in the future (Knutson et al. 2010; IPCC 2012, Wong et al. 2014; NAS 2016). Other studies indicate that anthropogenic climate change may promote stronger tropical cyclones globally; however, climate influence on global frequency is likely to remain constant or decrease (Bender et al. 2010; Knutson et al.

2010; Nordhaus 2010; Christensen et al. 2013). Research shows that not all records used to describe historical trends are of sufficient length or homogenous, which causes inconsistencies in assessing future climate influence on storm intensity and frequency (Shepherd and Knutson 2007). Any trends in hurricane activity are dependent on the start date of the historical record (IPCC 2012). Pielke (2014) exemplifies this by examining tropical cyclone activity (frequency, intensity, and duration) in the North Atlantic in three time intervals: 1900 to 2013, 1950 to 2013, and 1970 to 2013. Pielke found that, for both frequency and intensity, no trends existed from 1900 and 1950. An upward trend exists when examining tropical cyclone activity from 1970 to 2013; however, this time period does not prove sufficient to assess activity trends. Overall, the broad consensus is that it is likely that tropical storm wind speed and precipitation will increase and storm frequency will remain unchanged or decrease (Knutson et al. 2010; Nordhaus 2010; IPCC 2012; NAS 2016; Walsh et al. 2016).

Coastline Demographic Trends

Coastal counties (excluding Alaska) comprise less than 10% of the total land area of the U.S; however, in 2010, approximately 39% of the nation's population lived in these areas (State of the Coast 2013). The U.S. coastal population amplified from 47 million in 1960 to 87 million in 2008, which exceeds the population change for non-coastline counties by 20% (Wilson and Fischetti 2010; Figure 1). A number of coastline counties have experienced greater than 1,000% growth in population from 1960 through 2008, with many of those counties in Florida (Table 4). In conjunction with the rapid population growth, the population density of Florida increased 260% during the same period (Figure 2). To accommodate the swelling population, there has

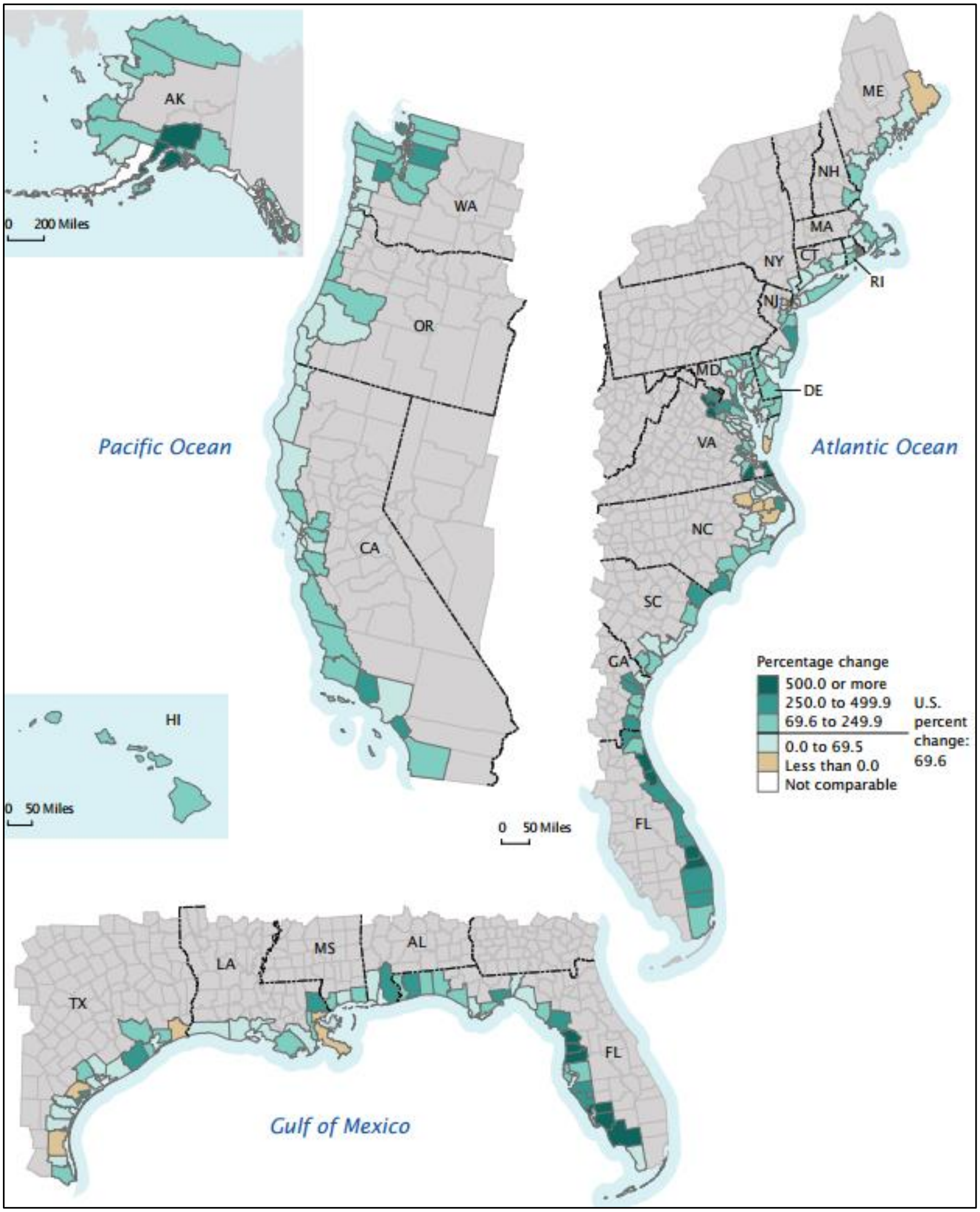

Figure 1. Percentage changes in coastal population from 1960 to 2008 (from Wilson and Fischetti 2010).

Table 4. Coastal counties with the largest percentage population change: 1950 to 2008 (after Wilson and Fischetti 2010).

County and State	Coastline Region	Population 1960	2008	Change, 1960 to 2008
Collier County,FL	Gulf of Mexico	15,753	315,258	1,901.30
Flagler County, FL	Atlantic	4,566	91,247	1,898.40
Matanuska-Susitna Borough, AK	Pacific	5,188	85,458	1,547.20
Hernando County, FL	Gulf of Mexico	11,205	171,689	1,432.30
Citrus County, FL	Gulf of Mexico	9,268	141,416	1,425.90
Pasco County, FL	Gulf of Mexico	36,785	471,028	1,180.50
Charlotte County, FL	Gulf of Mexico	12,594	150,060	1,091.50
Lee County, FL	Gulf of Mexico	54,539	593,136	987.5
Kenai Peninsula Borough, AK	Pacific	6,097	53,409	776
Martin County, FL	Atlantic	16,932	138,660	718.9
Prince William County, VA	Atlantic	50,164	364,734	627.1
Stafford County, VA	Atlantic	16,876	121,736	621.4
St. Lucie County, FL	Atlantic	39,294	265,108	574.7
St. Johns County, FL	Atlantic	30,034	181,540	504.4
Wakulla County, FL	Gulf of Mexico	5,257	31,089	491.4
St. Tammany Parish, LA	Gulf of Mexico	38,643	228,456	491.2
Dare County, NC	Atlantic	5,935	33,584	465.9
Calvert County, MD	Atlantic	15,826	88,698	460.5
Palm Beach County, FL	Atlantic	228,106	1,265,293	454.7
James City County, VA	Atlantic	11,539	62,414	440.9

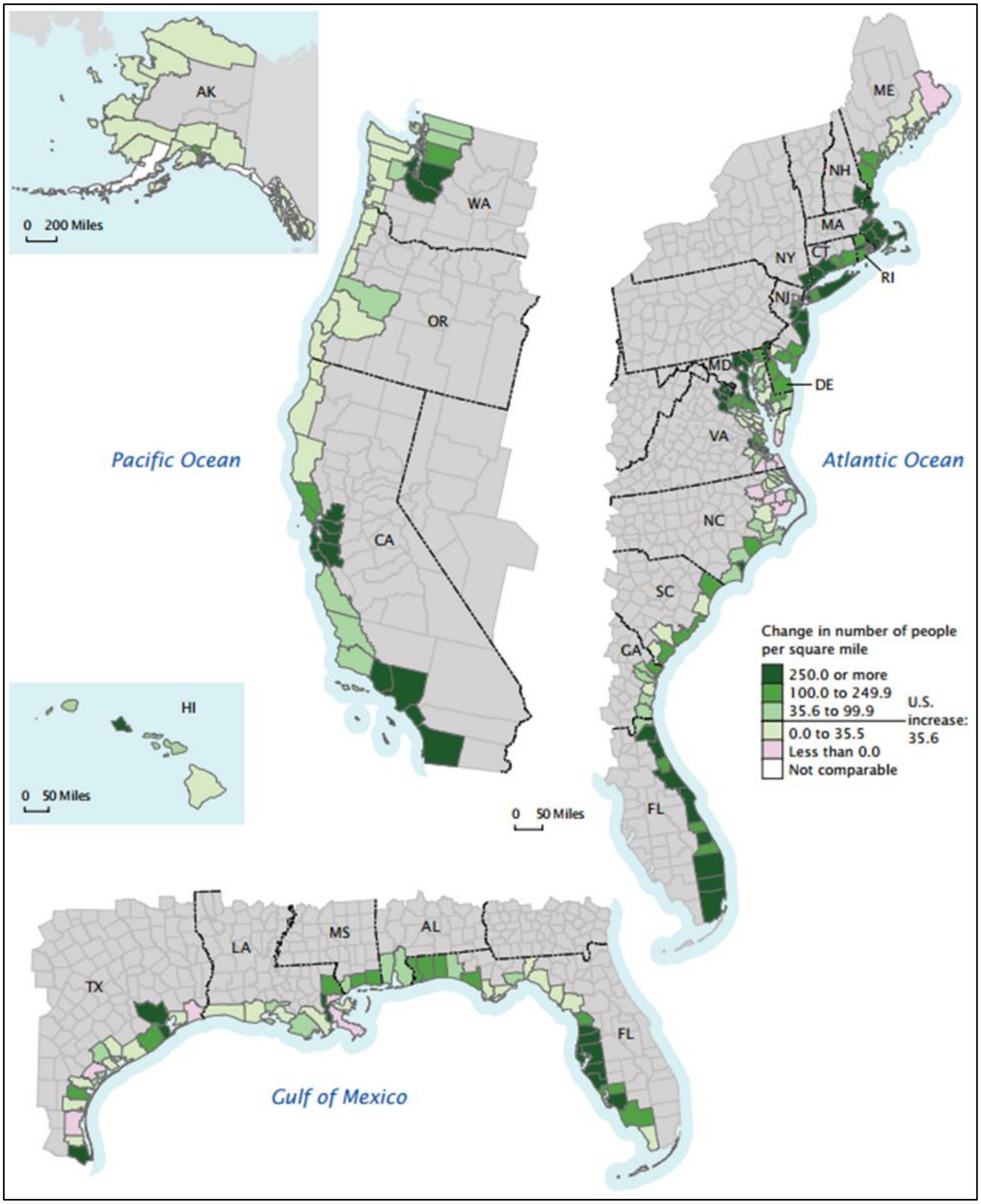

Figure 2. Change in coastal population density from 1960 to 2008 (from Wilson and Fischetti 2010).

been a corresponding amplification in the number of housing units along the coastline, with coastal counties collectively increasing their residential development by roughly 300% during the 48-year period. In conjunction with forecast population growth in the future, the residential built environment is expected to swell. U.S. urban and suburban regions are expected to experience a population influx, increasing between 19% and 23% by 2100, expanding the developed footprint of these regions (Bierwagen et al. 2010).

Migration is an important component of increasing population along the coasts (Cutter et al. 2007). People choose to migrate to the coasts because of their idyllic features, despite the risk of tropical storms and other hazards. The Southeast, especially Florida, is an attractive destination for job-seekers, as well as retirees (Crossett et al. 2004). From 1970 to 2000, coastal counties frequently impacted by hurricanes have increased in elderly (ages 65+) and Hispanic populations, two particularly vulnerable demographics (Cutter et al. 2007). Elderly population increased from 10.6% to 14.6% of the total population; Hispanic population surged from 4.9% to 9.8%. The elderly tend to remain in their homes in the event of a storm due to their inability to move and/or hesitance to leave (Cutter et al. 2003). For some ethnic minorities there exists a language barrier, which hinders this group's ability to receive evacuation or storm information (Cutter et al. 2003). In addition to demographic changes along the coastline, the percentage of mobile homes as residences has inflated from 8.4% to 23.2% from 1970 to 2000 in coastal counties, which increases this important vulnerability constituent of the built environment (Cutter et al. 2007). In 2014, 9.2% of the housing units in Florida were mobile homes (U.S. Census Bureau 2014). The demographic changes that are occurring along the Atlantic and Gulf

Coastlines are influencing the vulnerability of these locations and, ultimately, could escalate the potential for a tropical cyclone disaster.

Vulnerability: Exposure and Risk

Vulnerability can be broadly defined as the susceptibility of people or places to loss or harm (Cutter 1996, Cutter 2003, Borden et al. 2007; Morss et al. 2011). There are many different and complex factors that contribute to vulnerability. For example, mitigation, structure construction, demographics, and rising populations are factors that can increase or decrease a region's vulnerability (Cutter and Emrich 2005; Pielke et al. 2005; Borden et al. 2007; Pielke 2007; Miller et al. 2008; Burton 2010). Conceptually, vulnerability to hurricanes and other hazards is a function of three primary components: exposure, sensitivity, and adaptive capacity (Morss et al. 2011). Exposure involves the conditions of natural or human-built environment that are subject to potential losses. Sensitivity, or susceptibility, is the degree to which coastal regions coastline is affected by hurricanes, while adaptive capacity is the ability of a system (e.g. political, social, structural, environmental) to cope or adapt to hurricanes. Population growth, urban density, and housing all have an influence on vulnerability, indicating that future growth could enhance hurricane impact in the future (Borden et al. 2007).

Risk is the likelihood or probability of an event occurring in space and time (Cutter et al. 2009). The risk for tropical storms varies along the coastline—e.g., Florida has a higher risk of landfalling hurricanes than states in the Northeast. Additionally, locations experience different climatological peaks for tropical storms. For instance, the Northeast is most likely to see hurricane activity in September or October, while regions along the Gulf Coast are likely to experience tropical cyclones as early as June and as late as December (Cangialosi and Berg 2012). A tropical cyclone is a hazard and could potentially cause harm; however, if the storm never landfalls, there is, for the most part, no risk of a storm to the coastline or interior. This exemplifies that risk can be defined by the climatology of tropical cyclones and the probability of landfall.

Changes in the Human-Built Environment

Population growth, wealth, and demographic shifts play a major role in losses from weather extremes (Changnon et al. 2000; Cutter and Emrich 2005; Pielke at al. 2005; Borden et al. 2007; Pielke 2007; Changnon 2008; Pielke et al. 2008; Burton 2010; Mendelsohn et al. 2012; Ashley et al. 2014; Noy 2016). The "expanding bull's-eye effect" exhibits increasing development and population spreading over time. Regardless of the change of storm characteristics, the growing "targets"—people, property, and built environments—amplify exposure to hazards and increase the odds of disaster (Ashley et al. 2014; Strader and Ashley 2015). For example, the Washington, IL tornado of 17 November 2013 caused catastrophic damage in the northwest region of the community, an area that was undeveloped 20 years prior to the event. The tornado would have traversed through mostly farm land had the area been left undeveloped (Figure 3). Thus, the incremental expansion of the community through development magnified the tornado disaster. Mendelsohn et al. (2012) suggested that the recent global impact of tropical cyclones was largely due to increasing vulnerability and exposure. As population increases along the coastlines, exposure to hurricanes will grow, resulting in a magnified tropical cyclone disaster potential.

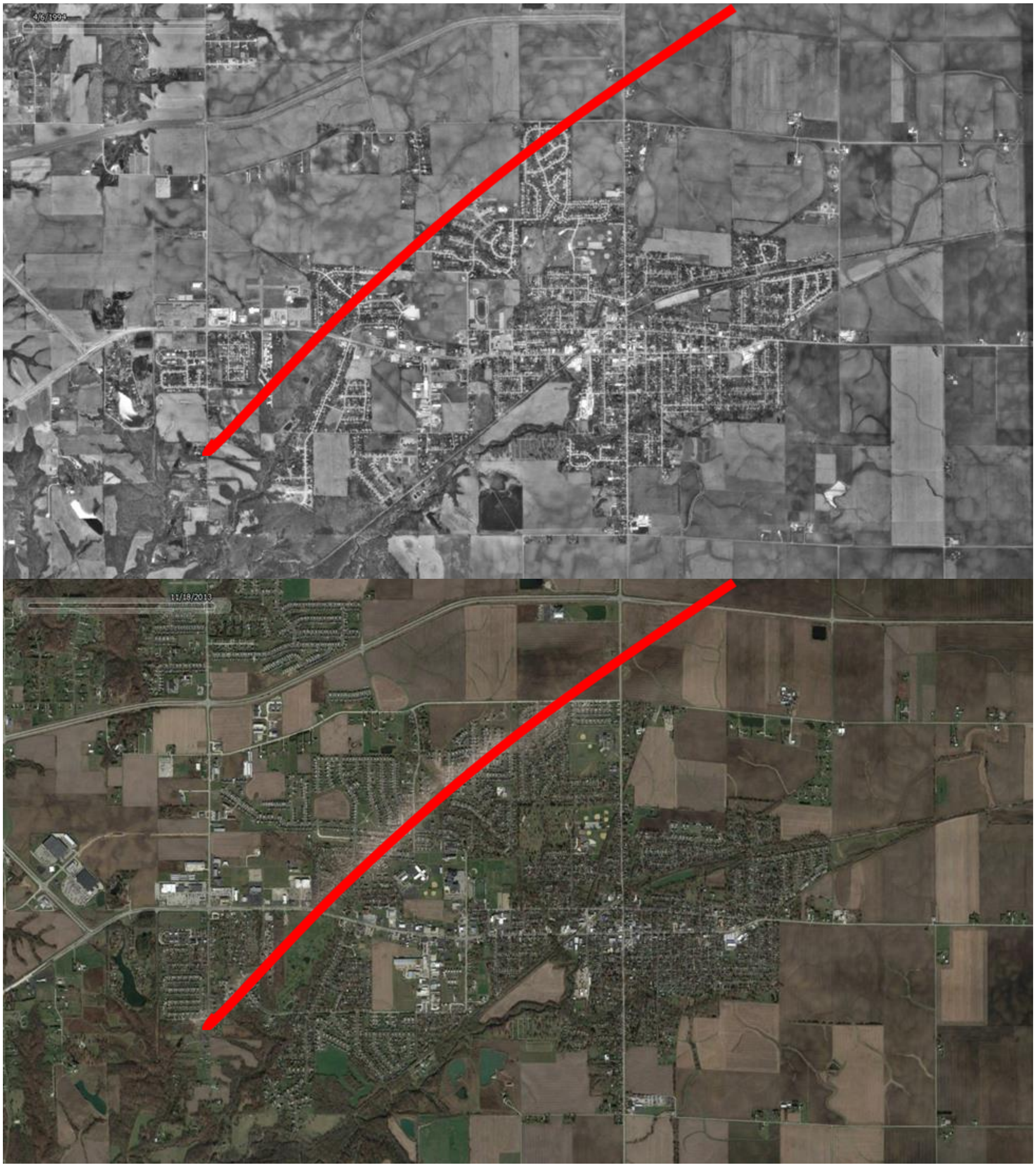

Figure 3. The 17 November 2013 Washington, IL tornado path (red) overlaid atop 1994 (top) and 2013 (bottom) satellite images (Google Earth).

In addition to population and housing unit increase, the pattern of development has an influence on vulnerability. According to Cutter et al. (2003), the density of the built environment is a significant factor in vulnerability to disasters. The clustering of populations are likely to lead to more damages from disasters, especially large scale hazards, such as hurricanes. Additionally, urban sprawl, distinct from traditional urban growth, could expand the area of impact and increase the vulnerability to potential hazards (Hall and Ashley 2008). The growth of human and built-environments along coastal counties can increase the vulnerability and exposure to hurricane impacts. In turn, this causes the potential for greater losses, especially if a growth trend persists or accelerates.

Future sea-level rise is also likely to increase coastal vulnerability. A rise in sea-level by 0.82 meters by 2100 increases storm surge inundation by 7 to 20% (Maloney and Preston 2014; Hay et al. 2015; Carson et al. 2016). The number of housing units along the Gulf and East coasts exposed to storm surge is currently 4.1 million for Category 1 storms and is projected to increase by 83% to 230% through the year 2100. Potential increases in tropical cyclone intensity are likely to promote stronger storm surges and are a concern when assessing future tropical cyclone exposure (Maloney and Preston 2014; Carson et al. 2016; Walsh et al. 2016). The rise in sea-level is a hazard concern, especially if housing unit growth continues to increase along the coastline in the future.

Hazard Synthetics: Importance and Use

The development of hypothetical hazard scenarios—e.g., overlaying a hazard such as a hurricane wind swath over an exposure surface—allows users to create "what if" events to examine the variation of impact, including an extreme, “worst-case” event (Clarke 2005). The modeling of a “worst-case” scenario conveys the idea of a possible disaster occurring and promotes preparation for a future extreme event. Previous studies have exemplified the benefits of hazard synthetics in assessing potential disasters to the human-built environment, primarily for the tornado hazard (Wurman et al. 2007; Hall and Ashley 2008; Paulikas and Ashley 2011; Ashley et al. 2014; Strader et al. 2014). Hurricane synthetics have been used to evaluate simulated lifecycle and intensity through historical storm data (Casson and Coles 2000; Vickery 2000; Emanuel 2006; Emanuel et al. 2006; Hall and Jewson 2007; Hallegate 2007; Rumpf et al. 2007; Rumpf et al. 2009; Yonekura and Hall 2011; Nakamura at al. 2015). Hallegate (2007) found that a 10% increase in intensity would increase the annual hurricane damage by 54%, indicating that losses are influenced by tropical cyclone intensity. While previous synthetic studies focused on simulating storm lifecycles and track projections, there is a dearth of research that focuses on the simulated impact of storms on the built environment. Changing intensity, risk, and societal factors are fundamental contributors to the potential for increasing damage losses over time (Hallegate 2007; Pielke et al. 2008; Miller et al. 2008; Bouwer 2011).

CHAPTER 3

DATA AND METHODS

The study area of this research includes coastline metropolitan statistical areas (MSAs) of the U.S. that have historically been impacted by tropical cyclones that form and traverse the North Atlantic basin, specifically focusing on areas with extensive development. The study uses six MSAs as cases of assessment, including: New York City-Newark-Jersey City (New York City), Charleston-North Charleston (Charleston), Miami-Fort Lauderdale-West Palm Beach (Miami), Tampa-St. Petersburg-Clearwater (Tampa), New Orleans-Metairie (New Orleans), and Houston-The Woodlands-Sugar Land (Houston) (Figure 4).

Tropical Cyclone Data

The National Hurricane Center (NHC) provides best track storm analysis data (HURDAT2) that includes attributes of historical storms from their genesis to dissipation. The archive includes all observed tropical systems (depressions, post tropical cyclones, named storms, and hurricanes) from 1851 to 2014. HURDAT2 provides the basic attributes for each storm—i.e., location, maximum sustained wind speed, and minimum pressure—every six hours, as well as special timestamps upon landfall or during other important storm life events. Additionally, the dataset includes wind radii of the storm for each quadrant throughout its lifetime. The wind radii show the extent of the wind speeds at 17.5 m s^{-1} (34 knots; tropical cyclone classification), 25.7 m s^{-1} (50 knots), and 32.9 m s^{-1} (64 knots; Category 1 hurricane

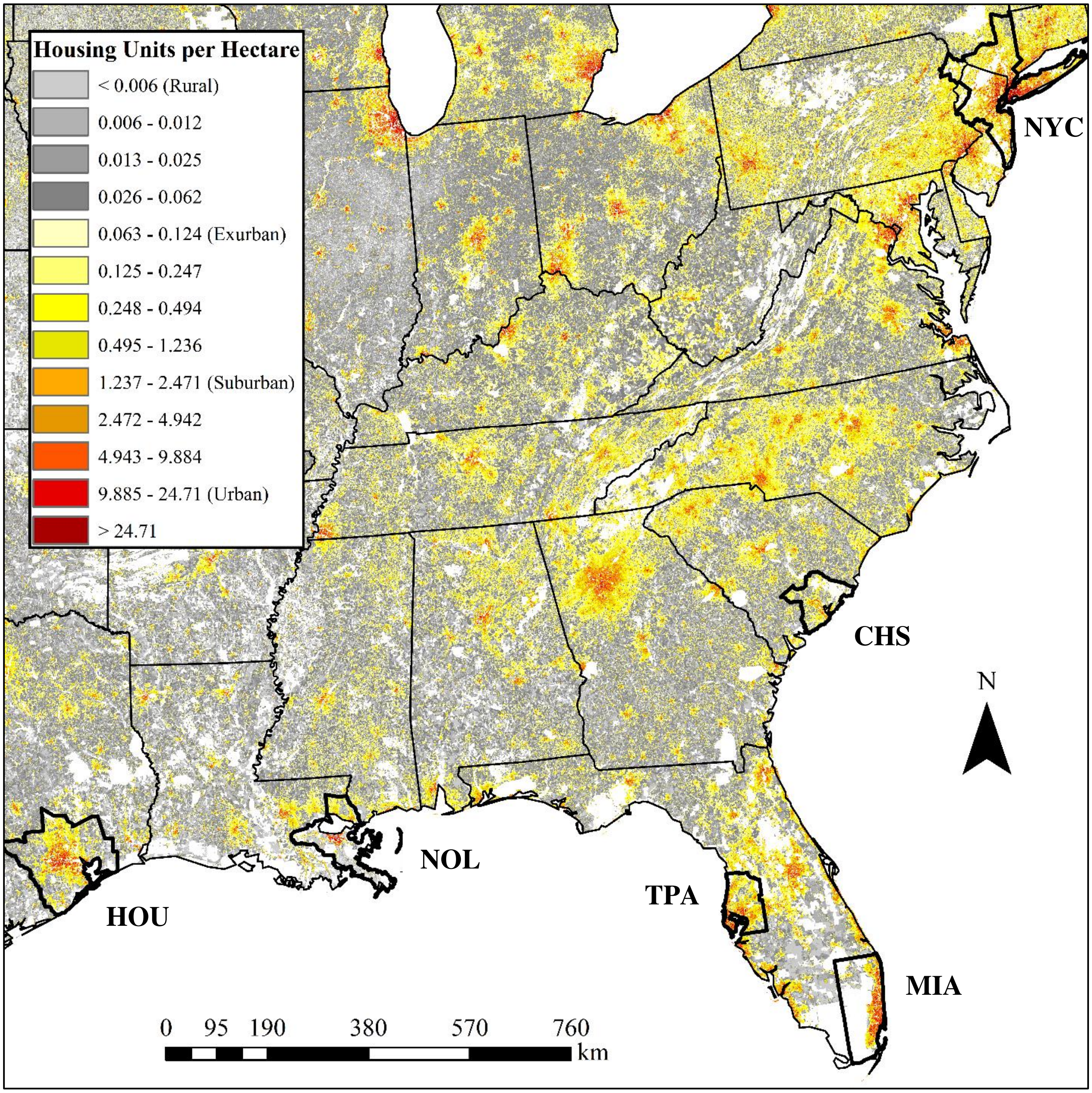

Figure 4. Eastern U.S. housing unit density for 2010 base case. The six MSAs employed in this study are bounded by thick black lines and are labeled as follows: Houston (HOU), New Orleans (NOL), Tampa (TPA), Miami (MIA), Charleston (CHS), and New York City (NYC).

classification). The radii of historical landfalling storms from 2004 to 2014 on the Gulf and East coasts are used for the synthetic wind swaths and placed across historical and forecast residential built-environment cost surfaces. Because HURDAT2 only provides radii at three wind speeds—34 knots, 50 knots, and 64 knots—the extended best track data provided by Demuth et al. (2006) is used in conjunction with the HURDAT2 radii. The extended best track includes additional storm parameters supplementing HURDAT2, such as the radius of the maximum wind at each timestamp. This hypothetical framework will be used as a basis for simulating both historical and future hurricane impacts.

Population and Housing Unit Data

Models have long been used to estimate and forecast mortality, fertility, and migration within demography (Coale and Trussell 1996). Simulations are becoming more precise due to the ability to verify and correct the models over time. The Integrated Climate and Land-Use Scenarios (ICLUS) has employed a demographic and spatial allocation model to examine population growth scenarios (Bierwagen et al. 2010). The ICLUS scenarios are based on the Intergovernmental Panel on Climate Change (IPCC) Special Report on Emissions Scenarios (SRES), which describes potential socioeconomic and environmental trajectories for the future. The ICLUS scenarios for the U.S. consist of county population, housing density, and impervious surface estimates. The spatial allocation model employed in ICLUS is the Spatially Explicit Regional Growth Model, or SERGoM, which relates historical development trends to predict future growth of population and housing units (cf. Theobald 2005). There are binary storylines along two axes in which the SRES describes population growth in the model: economic vs.

environmentally-driven development (A-B) and global vs. regional development (1-2). The matrix produces scenarios in which the future housing unit density layer will behave: A1, A2, B1, and B2. A1 represents low population growth but rapid economic development, encouraging flexible migration (U.S. EPA 2009; Bierwagen et al. 2010). The A2 scenario assumes the highest fertility and the highest mortality of the SRES storylines, resulting in steadily increasing economic growth. The B1 storyline is similar to A1, except B1 focuses on environmentally sustainable economic growth. B2 focuses on local environmental and economic issues, and illustrates a regionally-oriented landscape. Additionally, there is a “base case” scenario where all of the influencing parameters (fertility, mortality, and migration) are set to “medium” (U.S. EPA 2009) (Table 5). Scenario A2 has the highest projected increase in population at 164% from 2010 to 2100 for the contiguous U.S., while scenario B1 has the lowest at 60% (Figure 5). Each scenario includes housing unit density data that are allocated at a 100-m resolution with a semi-decadal temporal resolution from 1940 to 2100. With the housing density projections, future population scenarios are used to assess potential residential exposure within a spatiotemporal framework.

Table 5. SRES scenarios and projected global average surface warming by 2100 (IPCC 2007).

	Global (homogeneous world)	Regional (heterogeneous world)
Economic	**A1** Rapid Economic Growth **1.4 – 6.4 °C**	**A2** Regionally Oriented Economic Development **2.0 – 5.4 °C**
Environmental	**B1** Global Environmental Sustainability **1.1 – 2.9 °C**	**B2** Local Environmental Sustainability **1.4 – 3.8 °C**

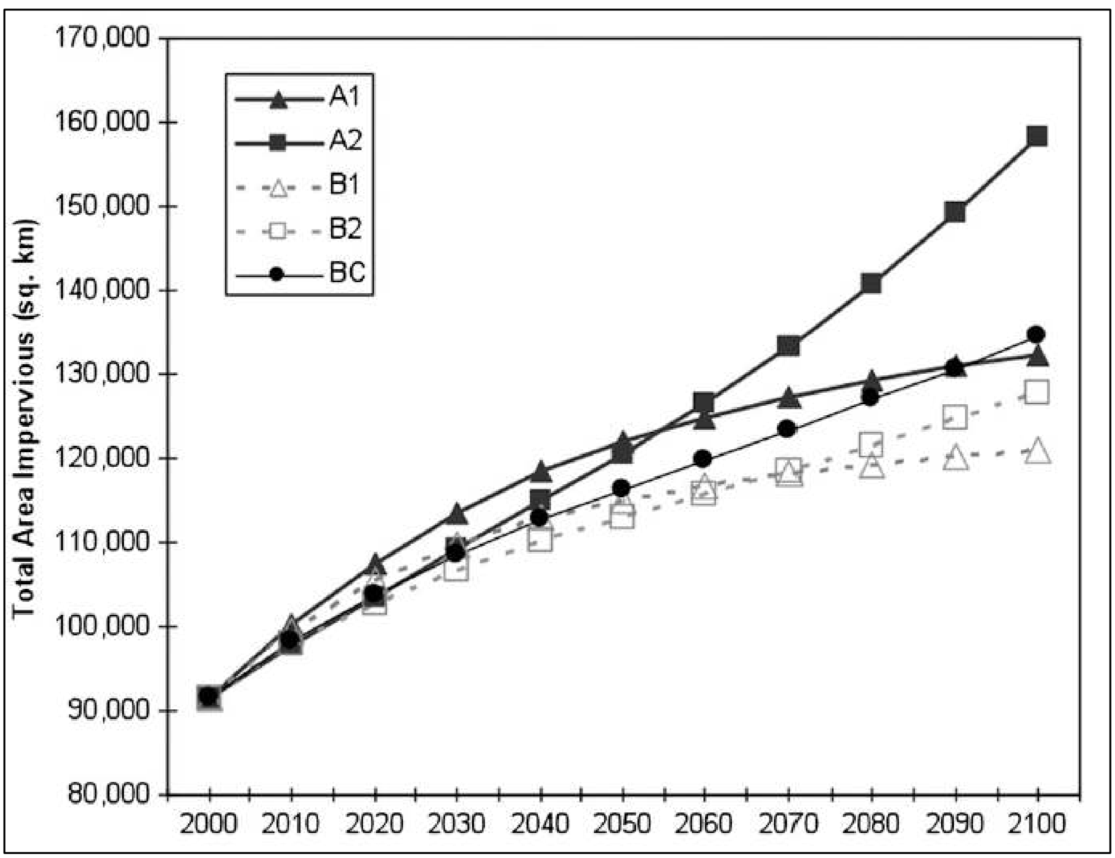

Figure 5. Area covered by impervious surfaces for the conterminous U.S. for all scenarios (from Bierwagen et al. 2010).

The accuracy of the SERGoM forecast model is revealed by examining historical housing patterns to the model's hindcasts (Theobald 2005). Since the projected housing pattern is based on the previous year, Theobald (2005) tested the model at 1980 to estimate the housing pattern for 1990 and 2000. After, he compared the model runs to the historical development patterns for the two years. For 1990, the model resulted in 93.0%, 91.2%, and 99.0% accuracy for urban, exurban, and rural coverage, respectively. The results indicate that the model is a relatively accurate estimator for housing density growth and can be used to assess the spatiotemporal differences in the human-built environment.

Methods

What impact will hurricanes have on coastline exposure and how will the hurricane disaster landscape change? First, buffers are created along the Gulf and Atlantic coast at 50 km increments up to 200 km to assess the historical and future HU development. Next, the housing development is examined at a local scale, analyzing the development of six high-risk MSAs along the coast. Using criteria developed by Theobald (2005), four different LU classifications are employed in this study, including: rural (<0.062 HU per hectare), exurban (0.062-1.236 HU per hectare), suburban (1.236-9.884 HU per hectare), and urban (>9.884 HU per hectare). Storms that made landfall from 2004 through 2014 along the Atlantic Coast are compiled to construct two hurricane synthetics: an "all" synthetic and a "major" synthetic. The "all" synthetic comprises all of the landfalling storms on the Gulf and East Coasts, while the "major" synthetic comprises only the major landfalling storms. Since HURDAT2 does not provide radius data prior to 2004, storm data are collected from 2004 through 2014 (Table 6;Table 7).

Thereafter, the synthetics are used to assess changes in housing exposure on the coasts by overlapping the storm synthetics with the built environment layer in *ArcGIS* from 1940 through 2100. To construct the synthetics, the mean radii wind swaths for each landfalling storm is extracted for each quadrant. The area of the mean swath (A_{swath}) is calculated by equation 1,

$$A_{swath} = \frac{\pi}{4}\sum_{i=1}^{4} {r_i}^2 \tag{1}$$

where r_1 is the radius in the northeast quadrant, r_2 is the radius in the southeast quadrant, r_3 is the radius in the southwest quadrant, and r_4 is the radius in the northwest quadrant. A_{swath} is used to find the radius of the synthetic swath (r_{synth}) by equation 2 (Figure 6).

$$r_{synth} = \sqrt{\frac{A_{swath}}{\pi}} \tag{2}$$

The result is a storm synthetic that has a uniform radius over all quadrants. This method is applied to the 6-hr and landfall timestamps provided by HURDAT2, creating a smooth wind swath from -24 hr to dissipation (Figure 7). Including dissipation in the study provides an analysis on the tropical cyclone impacts on both the coastal and surrounding counties.

H*Wind and HAZUS are other sources that provide hurricane data. H*Wind provides wind swath shapefiles, but the process of compiling the shapefiles into a synthetic is complex. Additionally, H*Wind did not have a complete dataset that was required for the study. HAZUS hurricanes are track-based and they do not provide the hurricane extent data. Because HURDAT2 provides the extent of the wind swath, the data are easier to compile into synthetic

Table 6. U.S. landfalling hurricanes from 2004 to 2014 by category at landfall.

U.S. Landfalls by Category from 2004 to 2014

Cat 1	Cat 2	Cat 3	Cat 4	Cat 5	Total	Majors (3,4,5)
7	4	6	1	0	18	7
Percent of Total						
38.9%	22.2%	33.3%	5.6%	0.0%	100.0%	38.9%

Table 7. Observed hurricanes used for creating the "all" synthetic. Asterisk indicates the storms employed in constructing the "major" synthetic.

Name	Year	Category	Max. Sustained Winds (m/s)	Pressure (mb)
Charley*	2004	4	66.82	941
Frances	2004	2	46.26	960
Gaston	2004	1	33.41	985
Ivan*	2004	3	53.97	946
Jeanne*	2004	3	53.97	950
Cindy	2005	1	33.41	991
Dennis*	2005	3	53.97	946
Katrina*	2005	3	56.54	920
Rita*	2005	3	51.4	937
Wilma*	2005	3	53.97	950
Humberto	2007	1	41.12	985
Dolly	2008	2	38.55	967
Gustav	2008	2	46.26	954
Ike	2008	1	48.83	950
Irene	2011	1	38.55	952
Isaac	2012	1	35.98	967
Sandy	2012	1	35.98	945
Arthur	2014	2	43.69	973

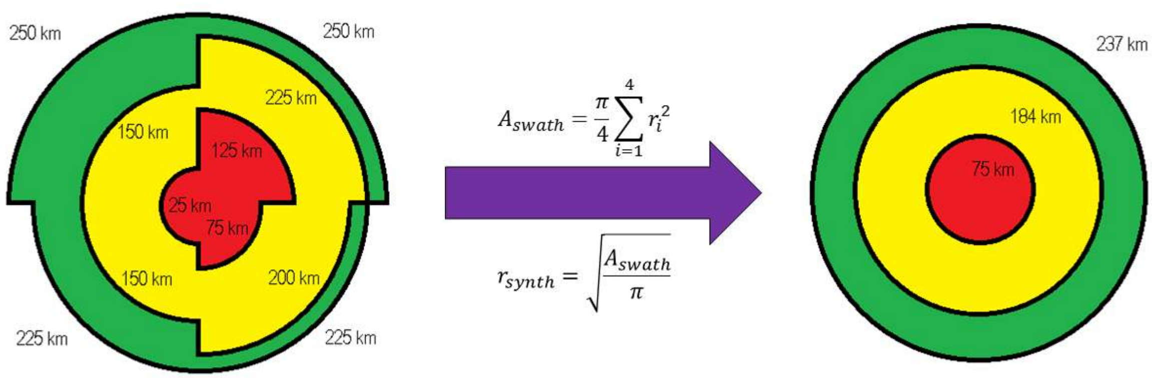

Figure 6. An example of how the synthetic hurricanes are created at each time step. In this figure, green is the 17 m s^{-1} wind swath (Tropical Storm), yellow is the 25 m s^{-1} wind swath, and the red is the 32 m s^{-1} (Cat 1) wind swath. The figure on the left represents the hurricane wind distribution at one time step and the radial extent of the swath in each quadrant. The figure on the right represents the same storm at one time step, where the wind distribution is uniform throughout.

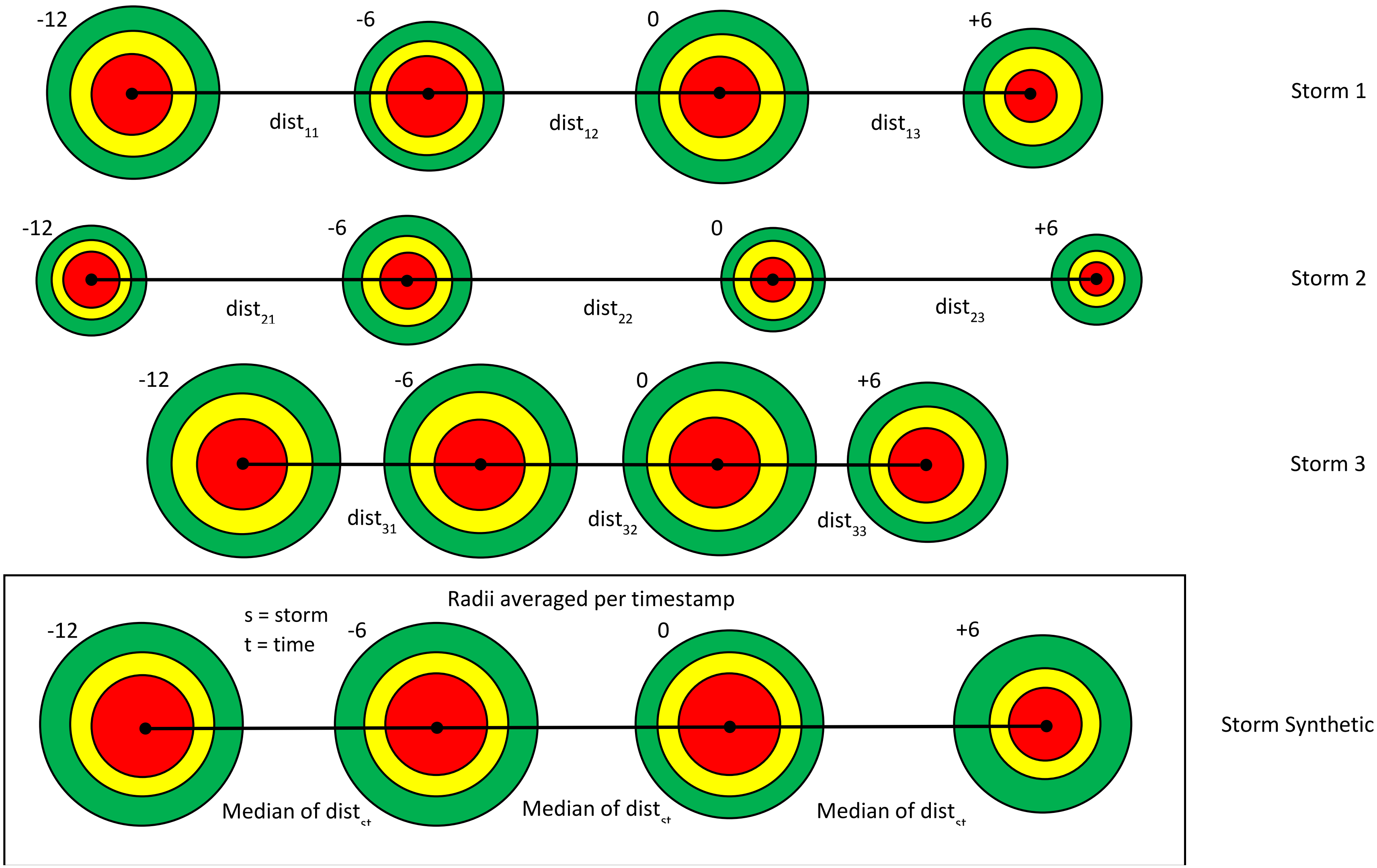

Figure 7. The creation of the storm synthetics after calculating the uniform wind radii (Figure 6) at each time step (-12, -6, 0, +6, etc.). The median of the distances between each time step is used as the distance between each time step of the hurricane synthetic. The radii are averaged for to produce the radii of the wind swaths within the synthetic.

hurricanes.

There are five SRES scenarios in which the housing unit projections will behave, each with semi-decadal projections up to 2100 per region. The Extract by Mask Spatial Analyst tool in *ArcGIS* permits the extraction of the cells within the region polygon in the housing scenario raster, resulting in the number of housing units in the specified region. The housing unit raster provides a value for each cell, indicating the number of housing units within one hectare. Given the MSA polygon and the projection raster, the values are extracted by the polygon to find the number of housing units per year and scenario. This method works similarly for the hurricane synthetic and is used to extract housing units within the extent of the storm. Using this method assesses the impact potential if a storm impacted the regions in the future with the mean wind swaths.

CHAPTER 4

RESULTS

As of 2016, there was a net gain of one person approximately every 17 seconds in the U.S., which is nearly 1.8 million people per year (U.S. Census Bureau 2010a). More housing units (HUs) are constructed to accommodate the increase in people over time, which can lead to growing exposure of the residential built environment to hazards. Since 2010, HU growth in the U.S. has varied between approximately 400,000 to one million HU per year (United States Census Bureau 2010b). From 2011 to 2014, the median growth per year was 549,288 HU (μ=675,738; σ=209,545; n=4), which indicates there are around half a million more HU that are exposed to a variety of atmospheric and geophysical hazards in the country each year. The increase in the human and built environment has led to a greater potential for disasters, as well as magnitude of those disasters, when they occur, especially along the Atlantic and Gulf Coasts. Despite the risk for tropical, extratropical, and other geophysical hazards in this coastal region, population and HUs are continuing to increase. This research examines how the number and distribution of HUs have grown, and will continue to change, along the Atlantic and Gulf Coasts (hereafter, coastline). Specifically, the study uses the hurricane hazard as an instrument in a scenario based framework to assess and compare exposure and its influence on hurricane disaster potential across both historical and future periods (1940-2100).

This chapter is separated into three main analyses: buffer analysis, MSA analysis, and hurricane scenarios. The first analysis focuses on historical and forecast HU changes within different distances, or buffers, from the coastline. The second analysis investigates six at-risk MSAs along the coastline and examines historical and forecast HU within each of the MSAs. The third analysis explores the outcome of two hurricane synthetics on the six MSAs to reveal HU impacts from plausible worst-case hurricane disaster scenarios. Thereafter, the exposure and climatological risk of the MSAs are incorporated into a disaster metric that can provide insight on the changes in disaster potential in the future.

Buffer Analysis

In 2010, about 40% of the U.S. population lived in coastal counties, resulting in an increase in the number of HUs along the coast (National Ocean Service 2014, Lindsey 2015). To assess how the HU growth changed near the coastline, buffers were placed at 50-km increments, starting on the coastline and applied inland iteratively thereafter (Figure 8). In 1940, there were approximately 17 million HUs in the contiguous U.S. (CONUS) with 38% of HUs located within 50 km of the coastline. By 2000, the number of HUs grew to 115 million, with 36% of HUs located in the 50-km buffer region. The percentage of HUs within 50 km of the coastline did not vary greatly over time; however, the total number of HUs increased 500% from 1940 to 2000 (Figure 9). The number of HU decreases inland nearly exponentially, which is similar to the coastal growth pattern elsewhere around the globe (Nicholls and Small 2002). The number of HUs located within 50 km is about twice the number of HU within the other three analyzed buffer zones (i.e., 50-200 km inland), combined.

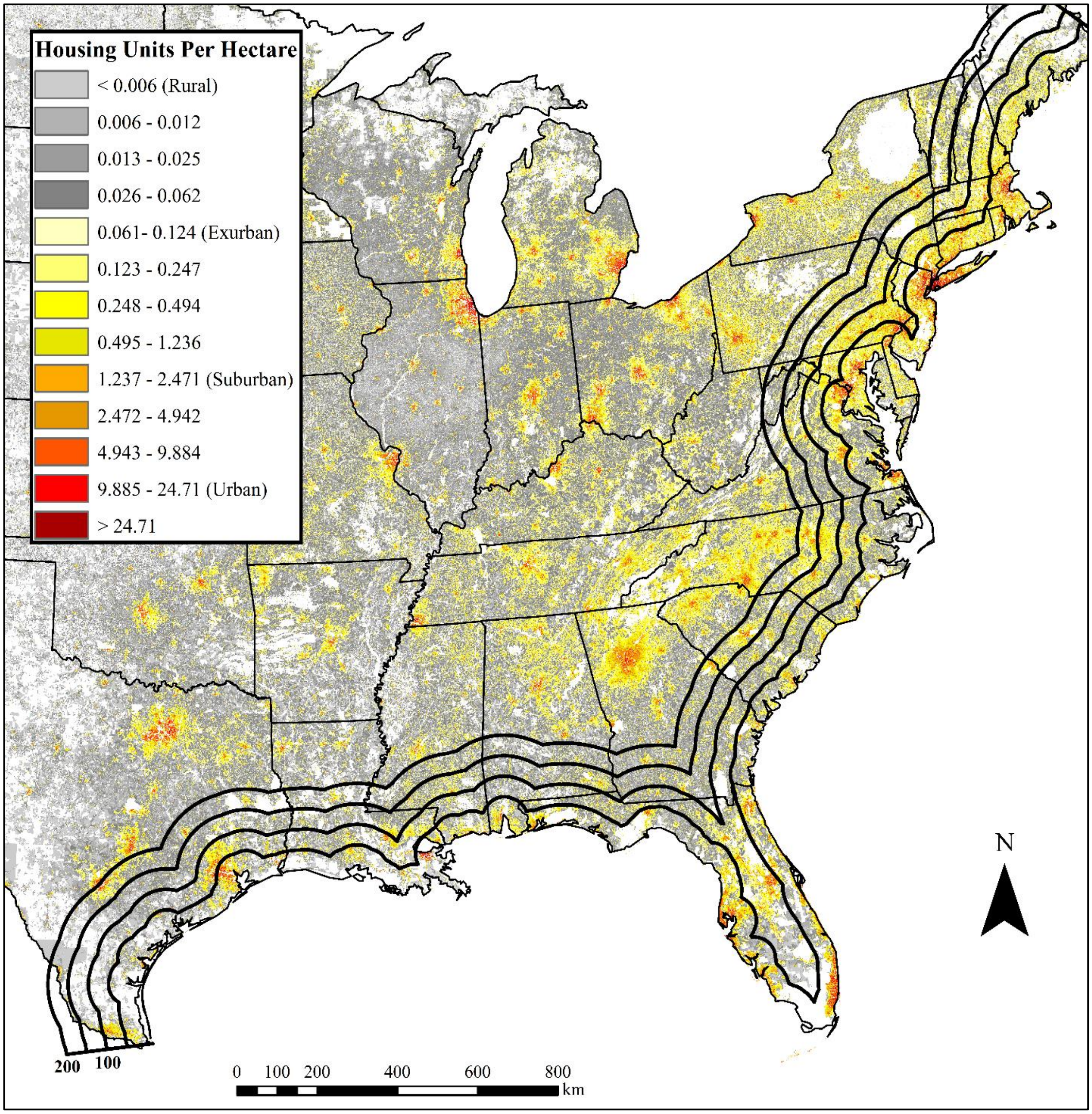

Figure 8. Total housing units per hectare in 2010, as well as the land-use classification (after Theobald 2005), superimposed with the coastal buffers measured every 50 km (i.e., 50 km, 100 km, 150 km, and 200 km) from the coastline.

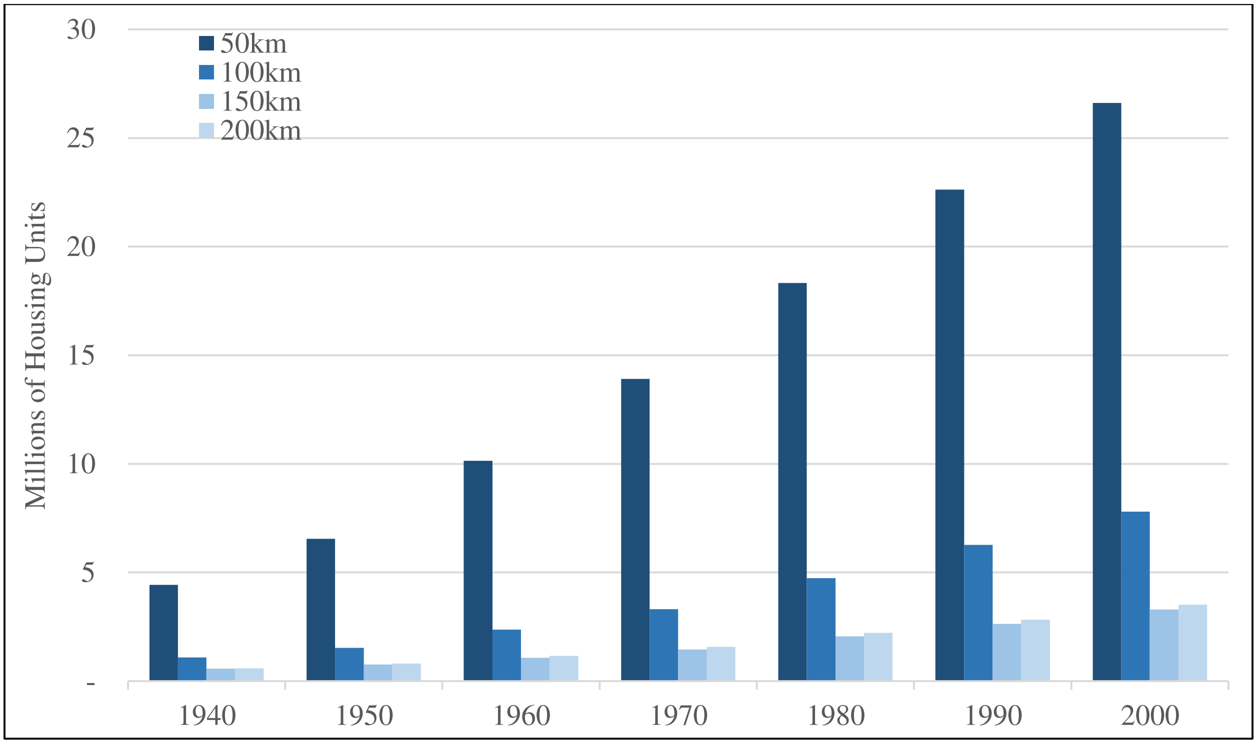

Figure 9. The number of housing units from 1940 to 2000 for the four different buffer regions illustrated in Figure 8.

HU density within the 50-km buffer greatly surpasses the HU density for the 200-km region (i.e., 0-200 km inland), as well as the HU density for the CONUS. In 2000, the HU density for the CONUS, excluding the 200-km region, was approximately 11 HU km-2, while the HU density for the 200-km region was approximately 40 HU km-2. The HU density for the 50-km buffer zone was approximately 78 HU km-2, but had the smallest land area compared to the other two regions. These higher density locations—such as the 50-km buffer region—are more at risk and vulnerable to coastal hazards due to their proximity to the ocean, resulting in greater structural loss potential (Cutter 2003). The growth and density near the coastline aligns more people and their property to the greatest risks from tropical cyclone hazards—including hurricane induced storm surge and winds—which could cause more frequent, and higher magnitude, disasters in the future. Further, the various ICLUS projections suggest that areas within the 50-km buffer region are expected to incur from 63% to 117% HUs growth through 2100 (Figure 10). Ultimately, these buffer results reveal that HU growth is greatest, and exposure is the highest, in the areas that typically experience the most extreme tropical cyclone hazard risk and affiliated hazards.

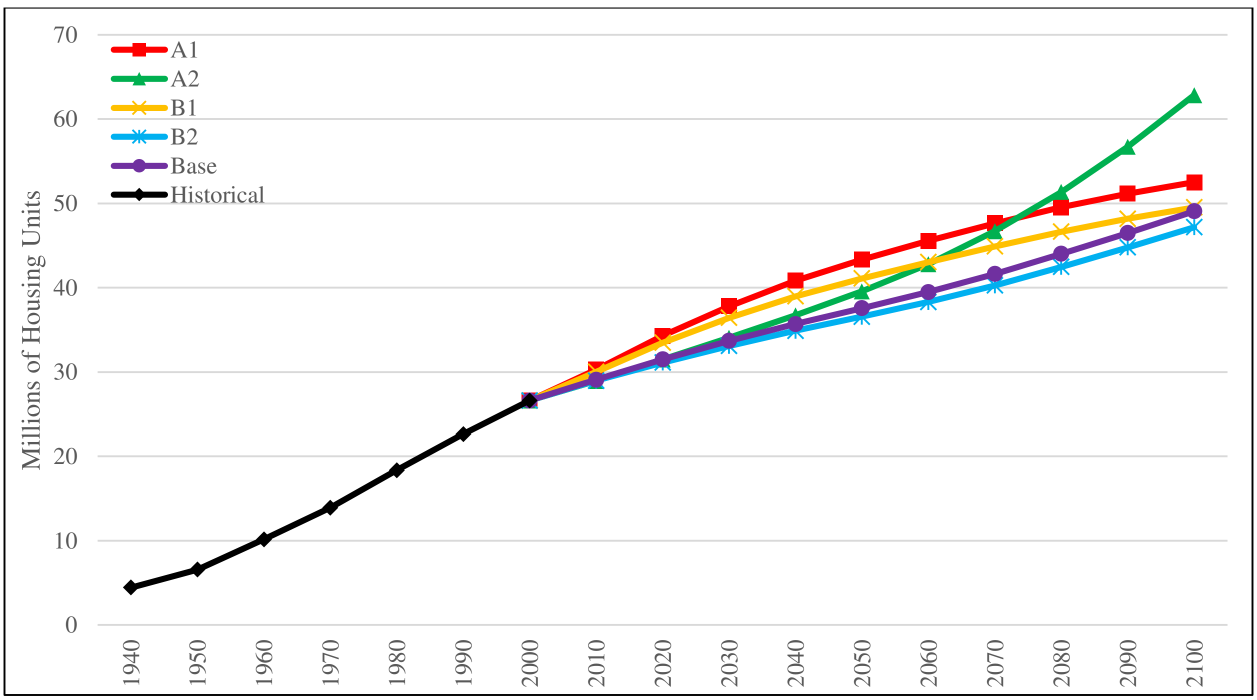

Figure 10. The number of housing units (HUs) within the coastal 50-km buffer region (Figure 8) from 1940 to 2000 and the projected number of HUs within the same region through 2100 for the various ICLUS simulations.

The 50-km buffer region was examined further by investigating the land use (LU) classification over time to provide detail on the character of the human-built environment. In 1940, 80% of the developable land in the 50-km buffer region was classified as rural, but, by 2000, only 46% of the region was rural (Figure 11). The decrease in rural LU is largely due to the increased conversion of developable rural land to more densely populated exurban and suburban morphologies. From 1940 to 2000, the percentage of developable land within 50 km of the coastline increased from 17% to 41% exurban, while suburban increased from 3% to 10%. More land has been converted to exurban than any other classification; however, the absolute changes in HUs for suburban and urban (high density) exceeds that of exurban, indicating that the greatest potential for catastrophic impact are in the suburban and urban regions (Ashley et al. 2014; Ashley and Strader 2016). Suburban and urban grew nearly 20 million HUs collectively from 1940 to 2000 within the 50-km buffer region, while exurban increased 2.2 million. The change in HU magnitude and its footprint expansion are important factors when understanding exposure and its contribution to disasters. Future projections indicate that HUs are expected to continue growing, further increasing exposure to tropical cyclones and associated hazards.

Since the A1 ICLUS projection for 2010 aligns more closely with the 2010 Census than the other projections (U.S. Census Bureau 2010b), A1 is examined further to assess LU development up to 2100. Initially, A1 is the steepest HU growth projection and indicates the fastest rate of growth (Figure 10). Overtime, A1 begins to decelerate, and nearly plateaus, by 2100. While A1 is the not the largest HU projection in 2100, A1 exhibits continual HU growth into the future. By 2100, the number of HUs in the 50-km buffer region is projected to rise by approximately 22.2 million HUs, a 73% increase from 2010. Further, rural and exurban LU morphologies are projected to decline by -10% and -6%, respectively, within the 50-km buffer region from 2010 to 2100. The 50-km region remains mostly exurban up to 2100; however, urban is projected to grow by 92%, indicating future expansion of high-density regions. Additionally, the number of HUs within urban regions is projected to increase by 32.4 million HUs, or 100%, by the end of the century, further increasing the density along the coastline.

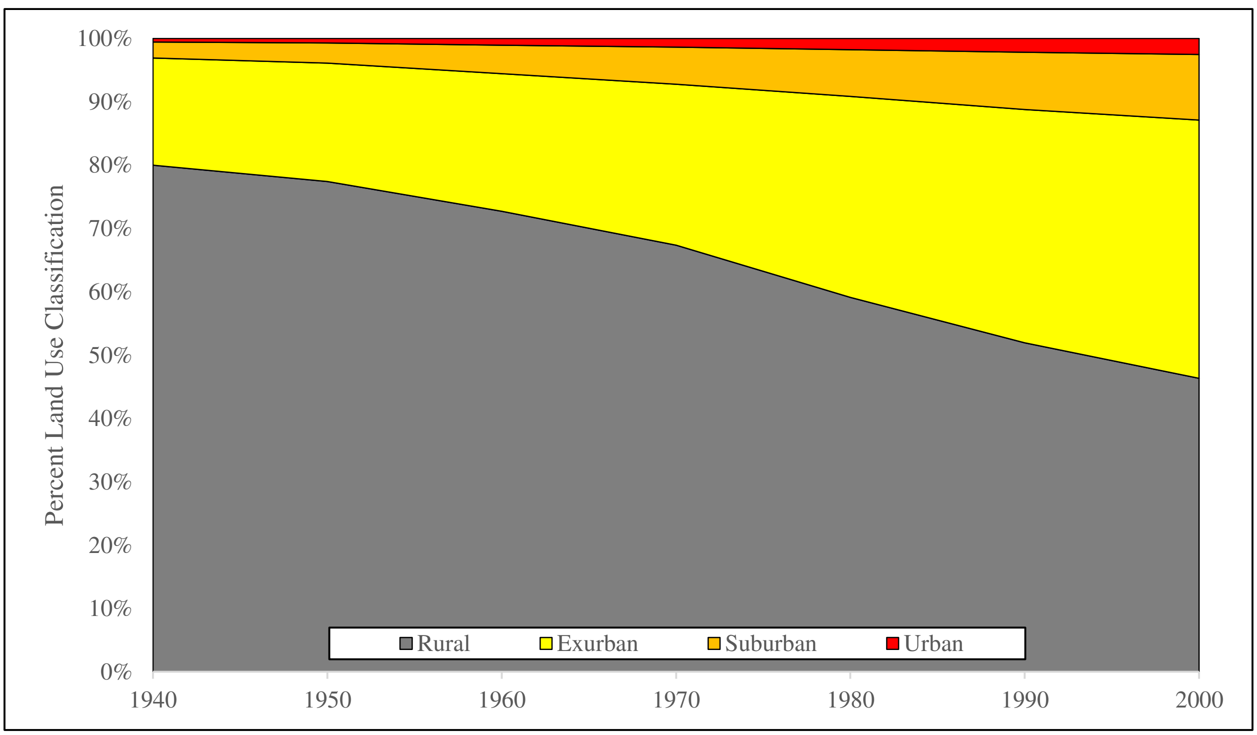

Figure 11. The percentage of rural, exurban, suburban, and urban land use from 1940 to 2000 for the coastal 50-km buffer region (Figure 8).

Since disasters are partially a product of a hazard interacting with the built environment, this study defines the macroscale (or coastal region), worst-case scenario as the projection with the largest number of HU in a defined coastal buffer that could be impacted by tropical hazards at any given time (Clarke 2005). Starting in 2010, A1 begins as the worst-case scenario within the 50-km region, but by 2070, A2 surpasses A1 and begins to grow exponentially. By 2100, the number of HUs in A2 exceeds the other projections, indicating that growth will continue into the 22nd century. A2 appears aggressive as the projection approaches the latter part of the 21st century, revealing the potential difficulty in extrapolating the changes in HUs after 2010. From 2010 through 2100, the number of HUs within the 50-km region is projected to increase by 33.9 million HUs, or 117%. Additionally, A2 shows a much more dramatic decrease (increase) in rural and exurban morphologies (suburban and urban) compared to A1 for the century. For both projections, the 50-km region is predominantly exurban; however the number of HUs in urban is greater than the number of HUs for rural, exurban, and suburban, cumulatively. The greatest catastrophic impact exists within suburban and urban regions from both projections: A1 from 2010 to 2070, A2 from 2070 to 2100. It is unknown exactly how the coastal built environment will grow in the future and how it will align with the A1 or A2 projections; however, the scenario data permits at least an exploration of tangible possibilities. Given that the number of HUs within coastal zones is trending toward A1, the coastline is currently developing within the worst-case scenario based on the five projections. Because development and density are not uniform across the coastline, the six high-risk MSAs along the coast are examined to further understand the built-environment change now and in the future.

MSA Analysis

The U.S has experienced rapid HU growth and LU transformations that have altered the disaster potential landscape, especially along its Atlantic and Gulf Coasts. To assess historical and forecast changes in HU growth and developmental characteristics along this vulnerable coastline, six coastal MSAs were investigated, including: Houston, New Orleans, Tampa, Miami, Charleston, and New York City (Figure 12). MSA geographic boundaries were defined by the Office of Management and Budget's 2013 delineations (OMB 2013), with MSAs assessed in this research based on the metropolitan region's size, propensity for historical tropical cyclone impacts, potential for catastrophic events under worst case scenarios, and their facilitation of robust measures of disaster potential for the U.S. coastline. Because the MSAs are unique in HU composition and LU typologies, the analysis provides a spectrum of change, indicating that each MSA is exposed differently than the other MSAs. This section provides an analysis of the historical HU growth and LU change, as well as projected HUs through 2100 based on an ensemble of societal pathways for each MSA.

The 2010 ICLUS projections are validated with the 2010 U.S. Census data to assess how close the modeled projections are to Census reports for the same enumerations (U.S. Census Bureau 2010b; Figure 13). The U.S Census provides HU counts for each MSA; however, since MSAs change over time, the U.S Census HU counts for the MSAs were not used. Instead, the number of HUs within the counties in each study area were summed to provide a total HU count for the MSA (Table 8). The base case was the most accurate projection for New York City, and A1 was the most accurate for the other MSAs. For consistency, A1 is used herein to explore

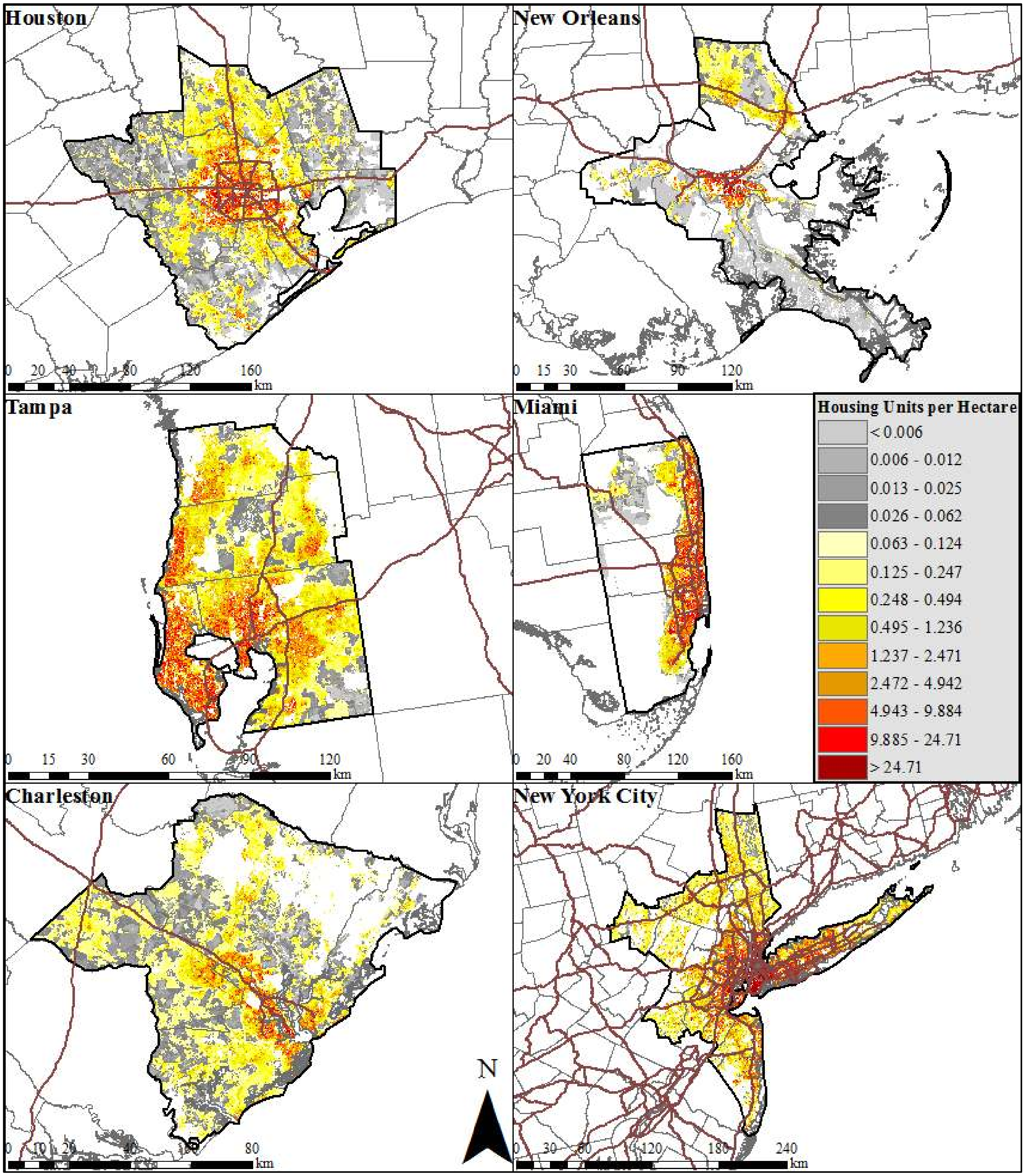

Figure 12. The six MSAs investigated and their housing unit density and land use distribution for 2010 base case.

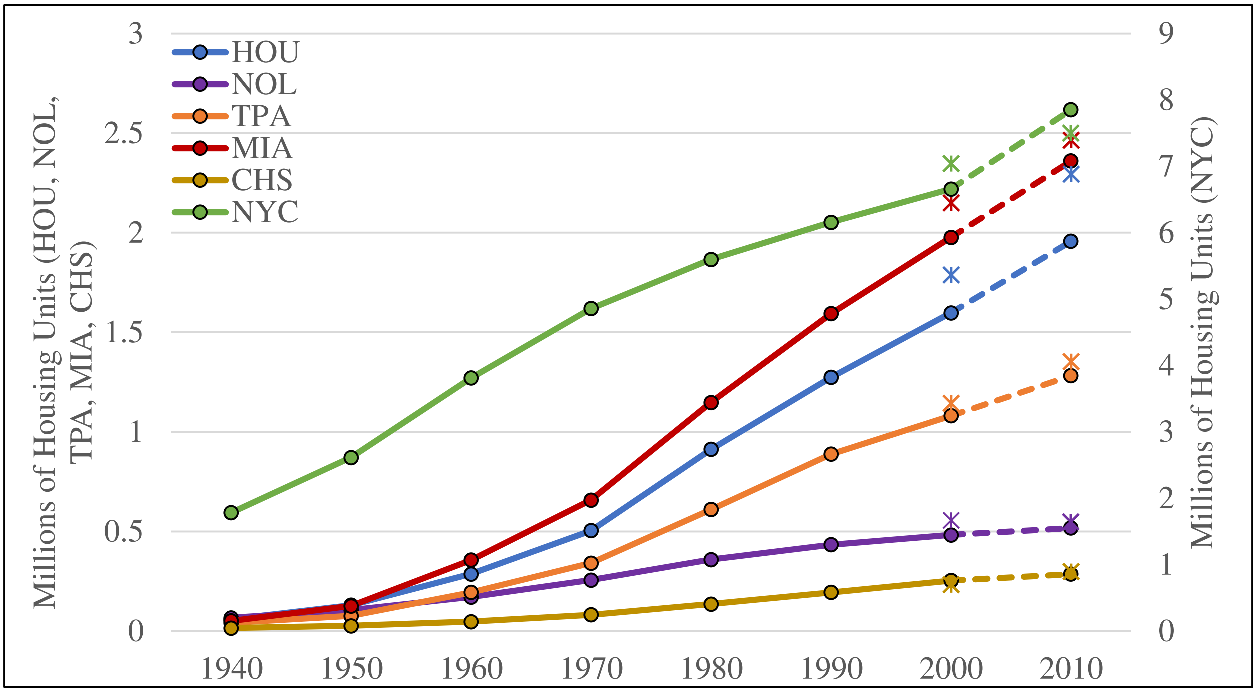

Figure 13. The number of housing units within each MSA from 1940 to 2000 and the A1 projection for 2010. The asterisks indicate the number of housing units observed in 2000 and 2010 by the U.S Census (U.S. Census Bureau 2010b).

Table 8. The counties or parishes for each MSA studied, including each enumeration's 2000 and 2010 U.S. Census housing unit counts and MSA totals (U.S. Census 2010).

MSA	County/Parish	2000 HU	2010 HU
HOU	Austin	10,205	12,926
	Waller	11,955	15,839
	Montgomery	112,770	177,647
	Harris	1,298,130	1,598,698
	Liberty	26,359	28,759
	Chambers	10,336	13,291
	Galveston	111,733	132,492
	Brazoria	90,628	118,336
	For Bend	115,991	197,030
	Total	**1,788,107**	**2,295,018**
NOL	St. James	7,605	8,455
	St. John	15,532	17,510
	St. Charles	17,430	19,896
	Jefferson	187,907	189,135
	St. Bernard	26,790	16,794
	St. Tammany	75,398	95,412
	Orleans	215,091	189,896
	Plaquemines	10,481	9,596
	Total	**556,234**	**546,694**
TPA	Hernando	62,727	84,504
	Pasco	173,717	228,928
	Hillsborough	425,962	536,092
	Pinellas	481,573	503,634
	Total	**1,143,979**	**1,353,158**
MIA	Palm Beach	556,428	664,594
	Broward	741,043	810,388
	Miami-Dade	852,278	989,447
	Total	**2,149,749**	**2,464,429**

MSA	County/Parish	2000 HU	2010 HU
CHS	Berkeley	54,717	73,372
	Dorchester	37,237	55,186
	Charleston	141,031	169,984
	Total	**232,985**	**298,542**
NYC	Suffolk	522,323	569,985
	Nassau	458,151	468,346
	New York	798,144	847,090
	Bronx	490,659	511,896
	Queens	817,250	835,127
	Kings	930,866	1,000,293
	Richmond	163,993	176,656
	Hudson (NJ)	240,618	270,340
	Middlesex (NJ)	273,637	294,800
	Monmouth (NJ)	240,884	258,410
	Ocean (NJ)	248,711	278,052
	Somerset (NJ)	112,023	123,127
	Hunterdon (NJ)	45,032	49,487
	Morris (NJ)	174,379	189,842
	Union (NJ)	192,945	199,489
	Essex	23,115	25,603
	Bergen (NJ)	339,820	352,388
	Westchester	349,445	370,821
	Putnam	35,030	38,224
	Dutchess	106,103	118,638
	Orange	122,754	137,025
	Rockland	94,973	104,057
	Passaic (NJ)	170,048	175,966
	Sussex (NJ)	56,528	62,057
	Pike (PA)	34,681	38,350
	Total	**7,042,112**	**7,496,069**

historical (2010) and future projections for each MSA. Overall, the historical data for 2000 underestimates the number of HUs for all MSAs, except Charleston. The validation reports a 90% accuracy or better for the MSAs, which is consistent with other validation analysis (Theobald 2005). In 2010, the accuracy of A1 increases to about 95% for all MSAs, while Houston is 85% accurate. Since the number of HUs is a function of five spatial inputs (2000 census, undevelopable lands, road and groundwater well density, county population projections and commercial and industrial LU), there are various factors that can alter the results of the model, such as job market, high rates of immigration, and zoning laws. After calculating the total number of HUs within the counties of the MSA, the validation reveals that Houston is growing much more rapidly than the five projections. This could be due to unexpected immigration from Hurricane Katrina and Hurricane Rita in 2005 (Frey and Singer 2006), or other factors. Because the model does not account for the underlying causes of population or HU change, the future projections should be used as guidance, rather than a deterministic solution.

All MSAs experienced substantial growth between 1940 and 2010. While it is important to assess the number of HUs within the MSAs, the percentage of growth and density must also be considered. The number of HUs in New York City increased about 6 million HUs, or 341%. Comparatively, Miami gained a relatively lower 2.3 million HUs, but experienced 4,526% growth. The number of HUs in Charleston increased about 270,000, or 1,871%, from 1940 to 2010. Charleston experienced the least absolute growth in HU, but had a greater percentage change than New York City and New Orleans. Although New York City had the smallest HU change from 1940 to 2010, New York City remained the densest MSA in this study through the 70-year period. In 1940, New Orleans was the second densest MSA at 7.9 HU km-2 behind New

York City at 82.9 HU km-2, while Charleston was the least dense at 2.15 HU km-2. By 2010, New York contained the greatest density at 365.4 HU km-2. Additionally, Tampa and Miami surpassed New Orleans in density during this recent decade, becoming the second and third most dense MSAs at 196.6 HU km-2 and 179.5 HU km-2, respectively. From 1940 to 2010, Miami densified most rapidly, shifting from 3.88 HU km-2 to 179.5 HU km-2. Based on the percent change of HU and density change, Miami is the most rapidly changing MSA in this study. Miami's disaster potential landscape is changing far more rapidly than the other MSAs, indicating that it may be difficult to adapt to potential hurricane and other geophysical hazards (Adger et al. 2003; Cutter et al. 2003; Borden et al. 2007; Satterthwaite 2007; Haurer et al. 2015) now and in the future. Overall, there is a statically significant (paired-t=2.41; p=0.03) increase in the number of HUs from 1940 to 2000 for all MSAs.

The majority of the growth within the MSAs has been in the exurban and suburban morphologies at the expense of rural (Table 9; Figure 14), especially in the Tampa, Charleston, and New York City MSAs. These locations had a negative change in rural character from 1940 to 2010, indicating that the rural landscape is developing into a higher density zone in these MSAs. In 1940, all of the MSAs were mostly rural, including New York City; by 2010, Tampa, Charleston, and New York City were mostly suburban. Houston and New Orleans remained mostly rural in the historical 70-year period, but experienced rapid suburban and urban development. Miami is nearly split evenly between rural, exurban, and suburban, with urban the smallest morphology by proportion; however, Miami experienced 13,747% increase of the number of HU within urban classification from 1940 to 2010. The percentage of urban within Miami has grown from 0.3% to 12.2%, resulting in an urban footprint about 140 times larger

Table 9. The total land use (LU) area, percentage LU (rural, exurban, suburban, and urban) classification of total developable land, percent change in LU classification, total number of housing units (HUs), percentage of total HUs by LU classification, and percent change in HUs by LU classification for the MSAs from 1940 to 2010, where 2010 is based on the A1 projection.

MSA	LU	Area (km^2)		% LU		% Change LU 1940-2010	Total HUs (x1,000)		% of Total HUs		% Change HU 1940-2010
		1940	2010	1940	2010		1940	2010	1940	2010	
HOU	Ru.	7287.6	8201.2	90.7	44.8	12.5	4.9	15.3	8.4	0.8	215.3
	Ex.	661.7	7523.0	8.2	41.1	1036.9	17.9	262.8	30.8	13.4	1371.3
	Su.	82.7	2100.9	1.0	11.5	2439.5	26.7	808.6	46.0	41.3	2929.4
	Ur.	5.3	489.5	0.1	2.7	9066.7	8.6	870.0	14.8	44.5	10066.0
NOL	Ru.	1517.8	3166.9	82.8	59.8	108.6	1.4	3.0	2.1	0.6	122.4
	Ex.	246.5	1591.2	13.5	30.0	545.6	7.0	48.5	10.5	9.4	595.5
	Su.	49.5	386.9	2.7	7.3	681.2	19.2	157.3	29.0	30.4	721.1
	Ur.	18.5	153.6	1.0	2.9	729.9	38.6	308.2	58.4	59.6	697.6
TPA	Ru.	1757.5	787.6	78.1	14.7	-55.2	1.9	2.2	4.8	0.2	14.3
	Ex.	427.4	2811.2	19.0	52.4	557.7	11.8	127.4	29.2	9.9	981.3
	Su.	61.8	1456.9	2.7	27.2	2256.4	18.9	549.2	46.8	42.9	2805.3
	Ur.	4.3	305.6	0.2	5.7	6990.5	7.8	601.9	19.2	47.0	7644.6
MIA	Ru.	868.6	1641.7	59.4	29.3	89.0	1.2	2.2	2.3	0.1	82.6
	Ex.	503.7	1632.1	34.4	29.2	224.0	15.7	85.5	30.7	3.6	445.6
	Su.	85.4	1640.4	5.8	29.3	1821.9	25.3	731.8	49.5	31.0	2797.7
	Ur.	4.9	684.1	0.3	12.2	13747.2	8.9	1539.8	17.4	65.3	17227.8
CHS	Ru.	2810.6	1916.1	93.8	36.6	-31.8	2.1	5.3	14.3	1.9	158.0
	Ex.	169.8	2930.8	5.7	56.0	1626.5	3.7	73.1	25.5	25.7	1885.7
	Su.	12.8	343.1	0.4	6.6	2584.4	4.1	123.6	28.6	43.4	2891.8
	Ur.	2.4	45.2	0.1	0.9	1775.9	4.6	82.5	31.6	29.0	1709.3
NYC	Ru.	7502.9	791.4	53.4	5.1	-89.5	16.3	2.7	0.9	0.0	-83.2
	Ex.	4999.3	8574.9	35.6	55.6	71.5	144.4	362.7	8.1	4.6	151.2
	Su.	1188.9	4455.2	8.5	28.9	274.7	431.5	1683.6	24.2	21.4	290.2
	Ur.	360.1	1589.2	2.6	10.3	341.4	1188.6	5802.6	66.7	73.9	388.2

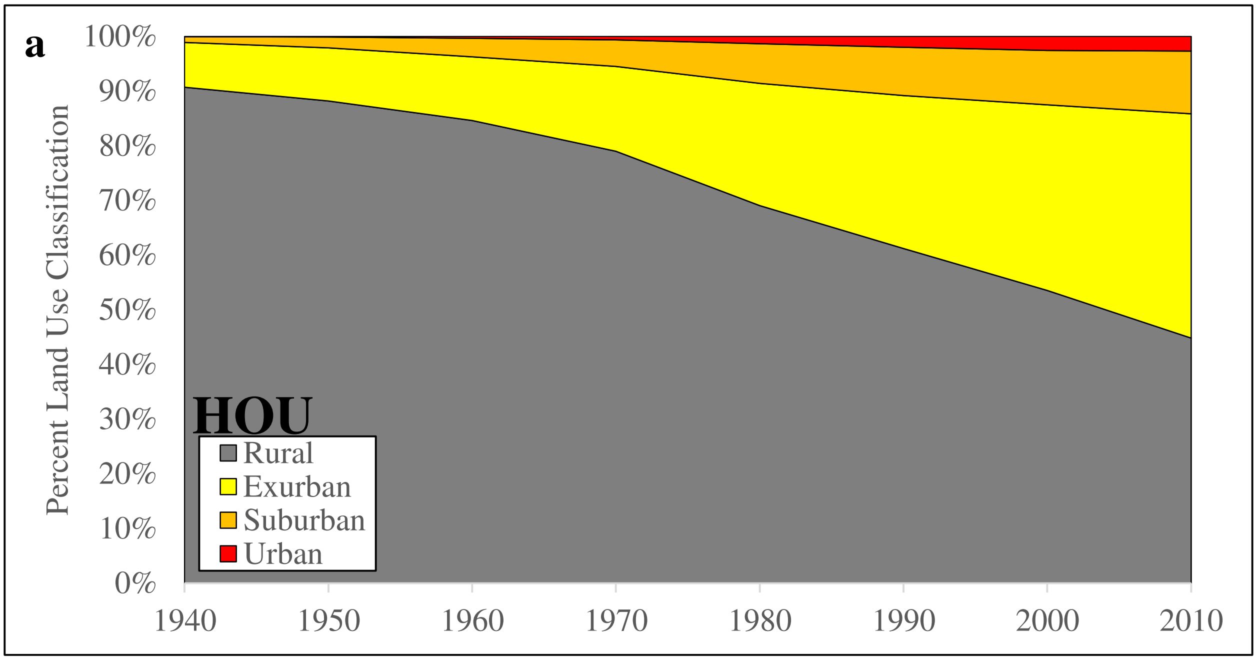

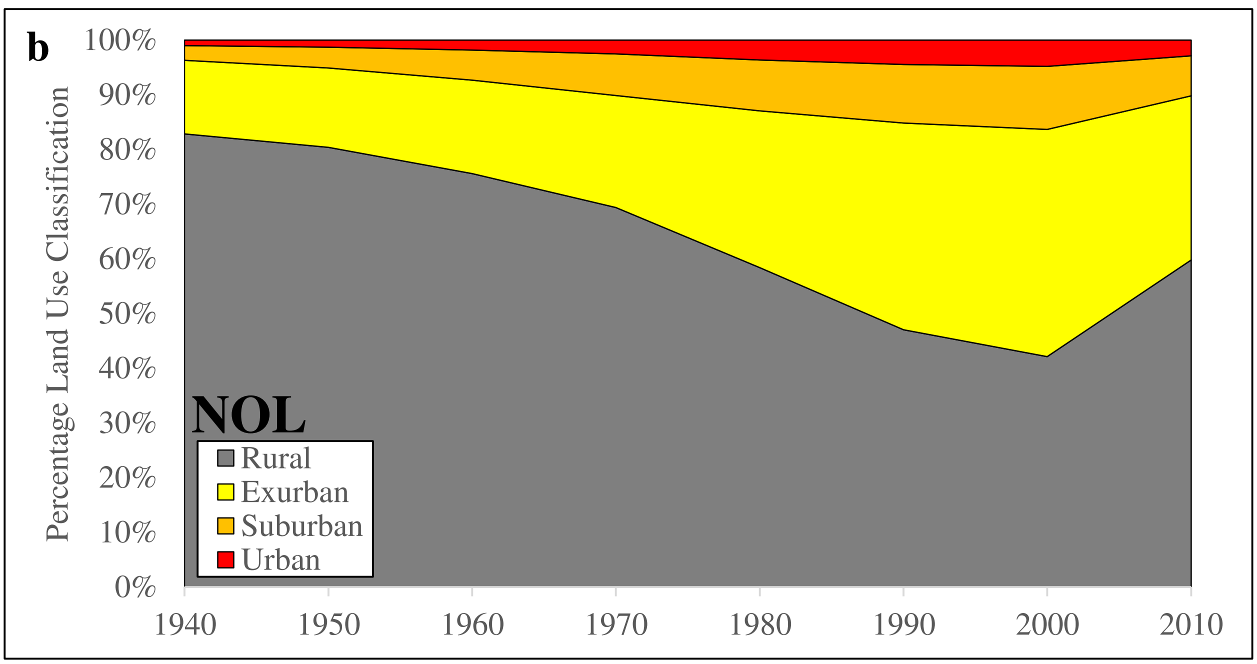

Figure 14. The percentage land use classification from 1940 to 2010 for a Houston, b New Orleans, c Tampa, d Miami, e Charleston, and f New York City MSAs where 2010 is the A1 projection

(continued on following page)

Figure 14 (continued)

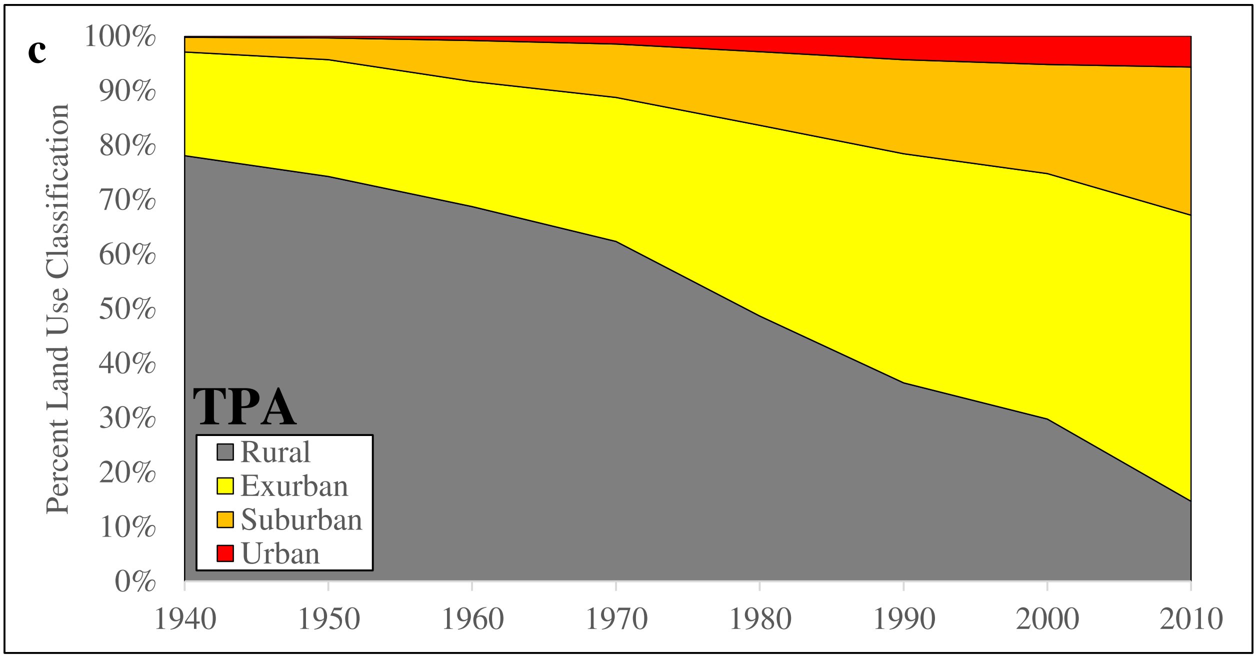

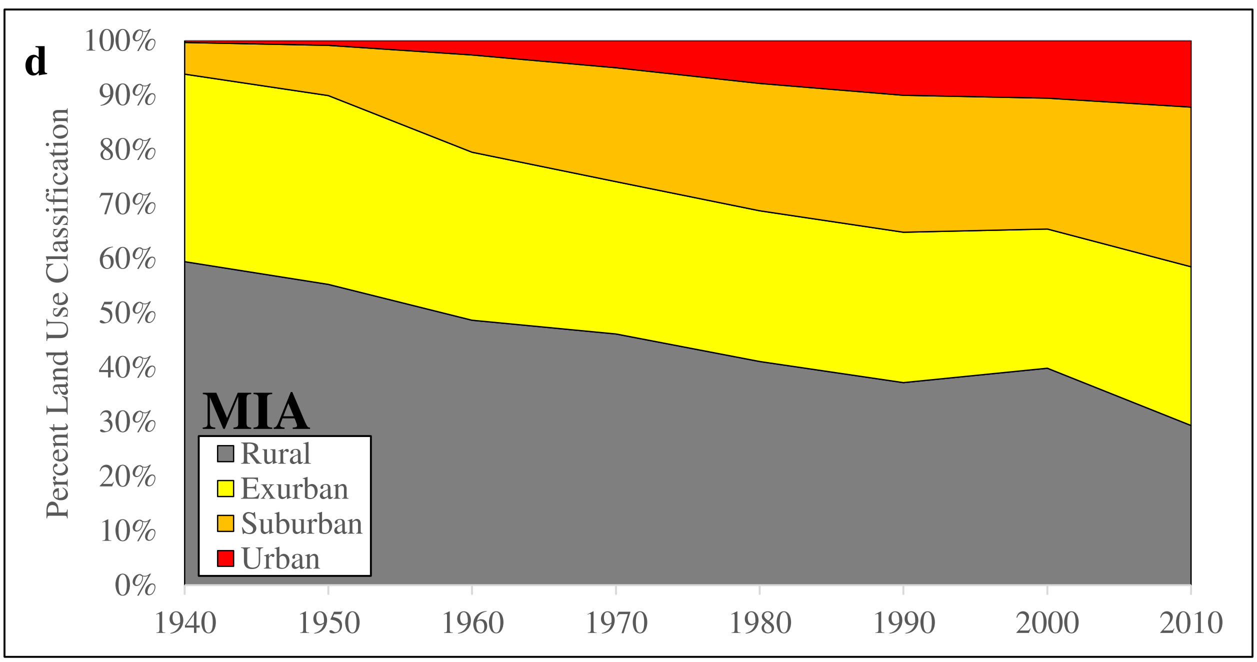

(continued on following page)

Figure 14 (continued)

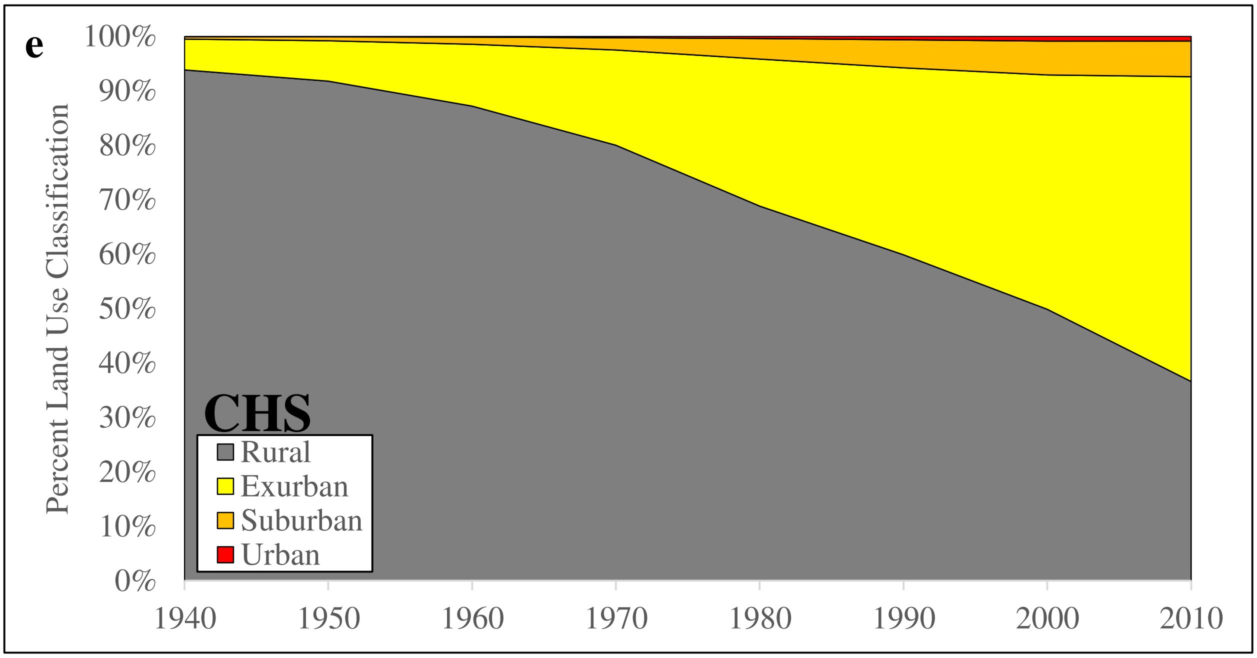

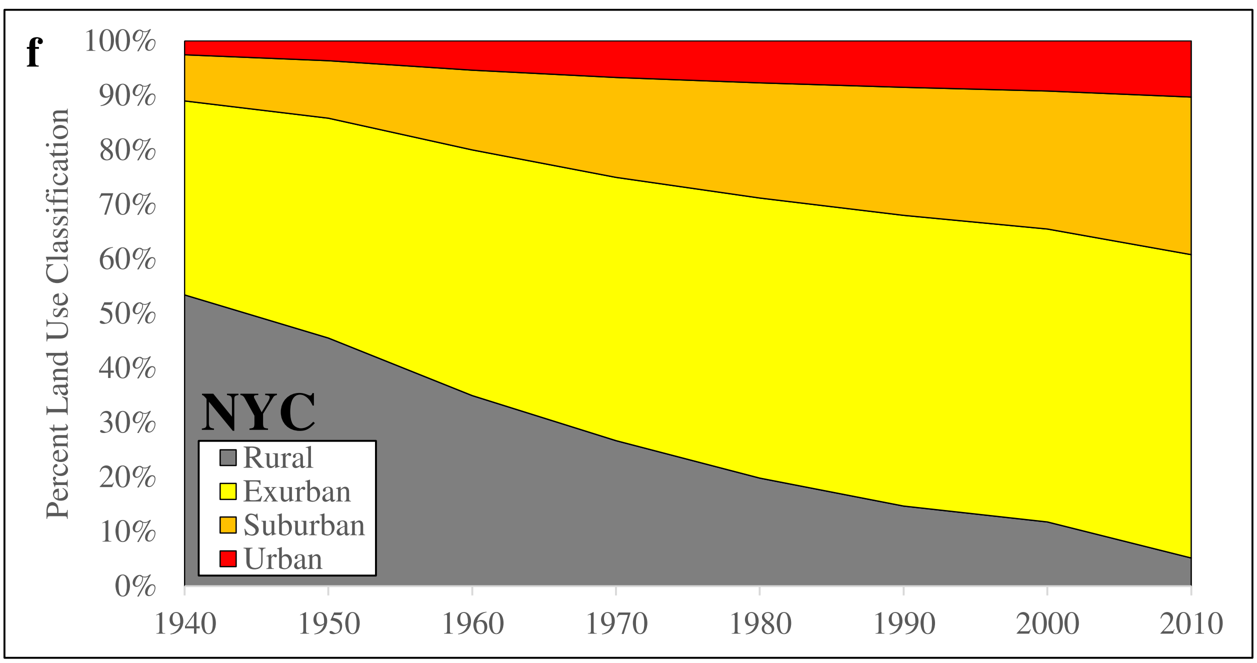

than that of 1940. Because of the Everglades Wildlife Management Area west of Miami, the expansion of Miami may be limited, or halted; however, the MSA will likely densify and become largely suburban and urban over time. Rural LU in New Orleans decreased from 1940 to 2000, but was projected to increase from 2000 to 2010 (Figure 14). It is possible that the destructive nature of Hurricane Katrina in 2005 may have been the cause of the LU shift, thus altering how the built environment will grow now and in the future (Vigdor 2008).

All MSAs are projected to increase in HUs into the future (Figure 15); however, they are all unique in their growth patterns and magnitudes. Houston, New Orleans, and Charleston exhibit a fanning pattern with their projections, indicating the number of HUs may vary greatly by 2100. Under the B1 scenario, the number of HUs for Houston, New Orleans, and Charleston remains constant, resulting in no growth from about 2030 to 2100. The other MSAs—Tampa, Miami, and New York City—exhibit a clustered pattern of future HU growth MSAs. HUs grow in a quasi-linear fashion, with an increase in HU across all scenarios. The A1 scenario indicates an exponential growth for all MSAs, similar to the previous buffer analysis. Overall, the fanning pattern could exhibit greater variability in HU growth, while the narrow pattern indicates that the scenario input parameters do not greatly alter the projections. Miami is projected to increase in HUs between 109% and 146% from 2010 to 2100; although the growth is large, the window of potential increase is narrow. Conversely, the number of HUs in Houston is projected to increase between 33% and 140%, a large range for potential HU growth under the various societal pathways modeled. Regardless of the uncertain forecast growth for Houston, New Orleans, and Charleston, Miami's A2 projection has the largest change scenario of the MSAs and simulation assessed. By 2100, under the A2 scenario, Miami is projected to increase by 3.2 million HUs.

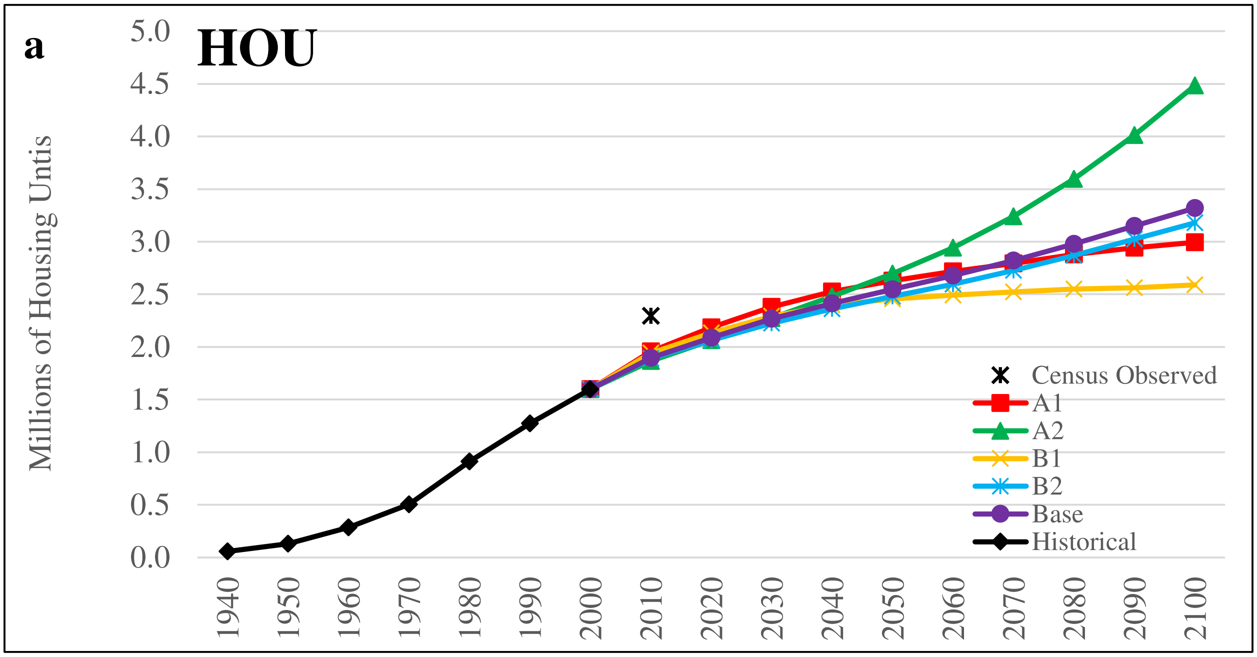

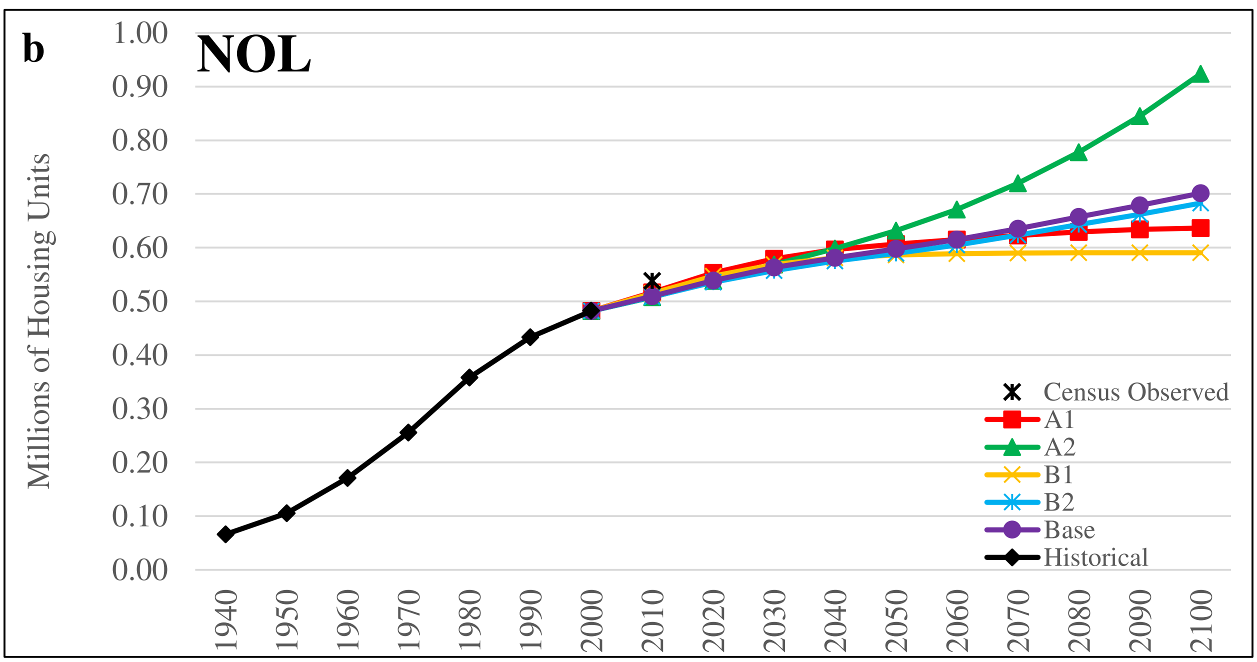

Figure 15. The number of housing units (HUs) for a Houston, b New Orleans, c Tampa, d Miami, e Charleston, and f New York City from 1940 to 2010 and the potential number of HUs within the MSA through 2100. Asterisk indicates Census-observed HUs in 2010 for each MSA.

(continued on following page)

Figure 15 (continued)

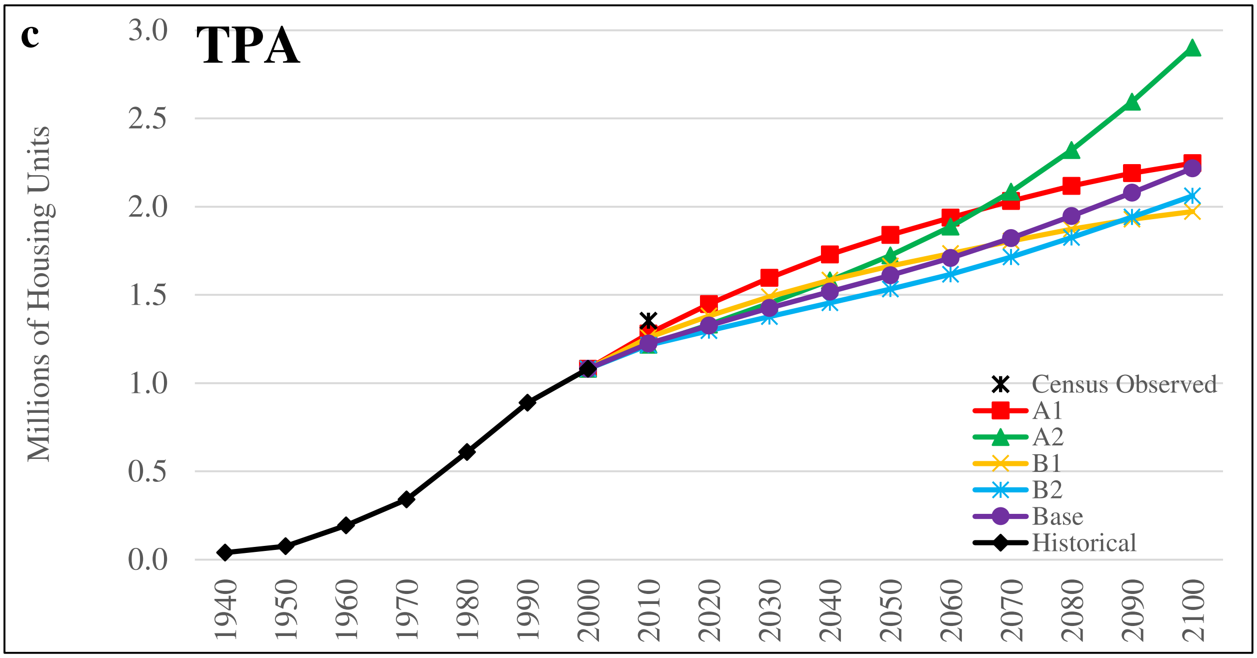

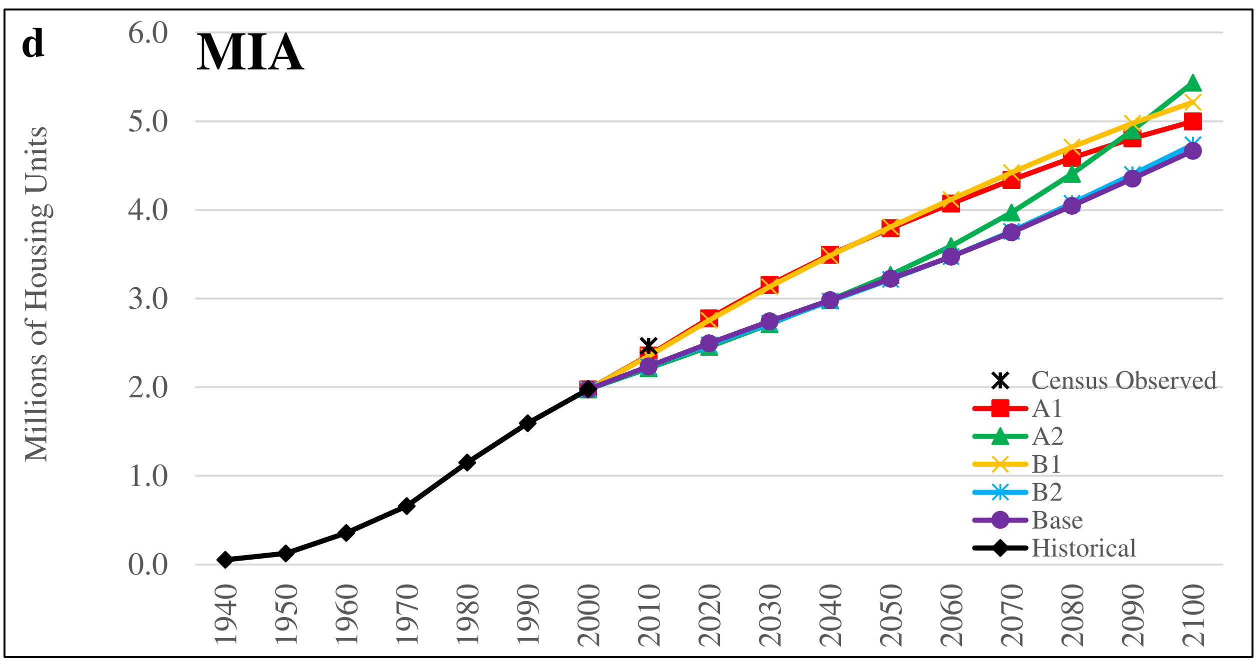

(continued on following page)

Figure 15 (continued)

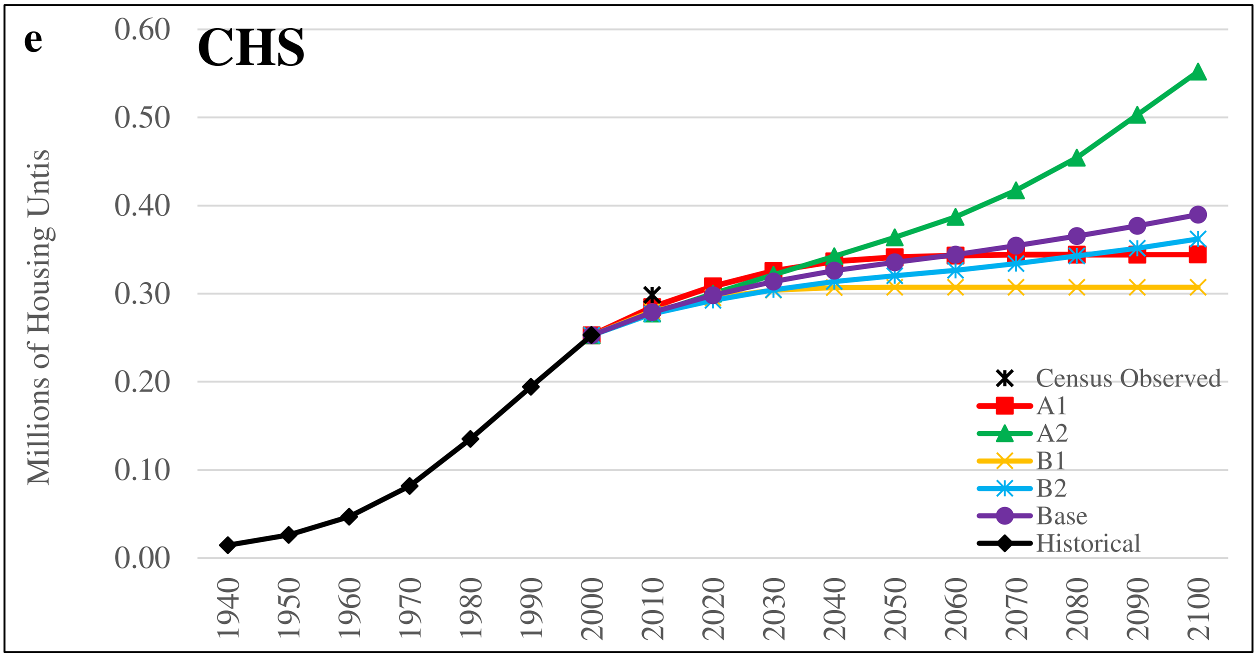

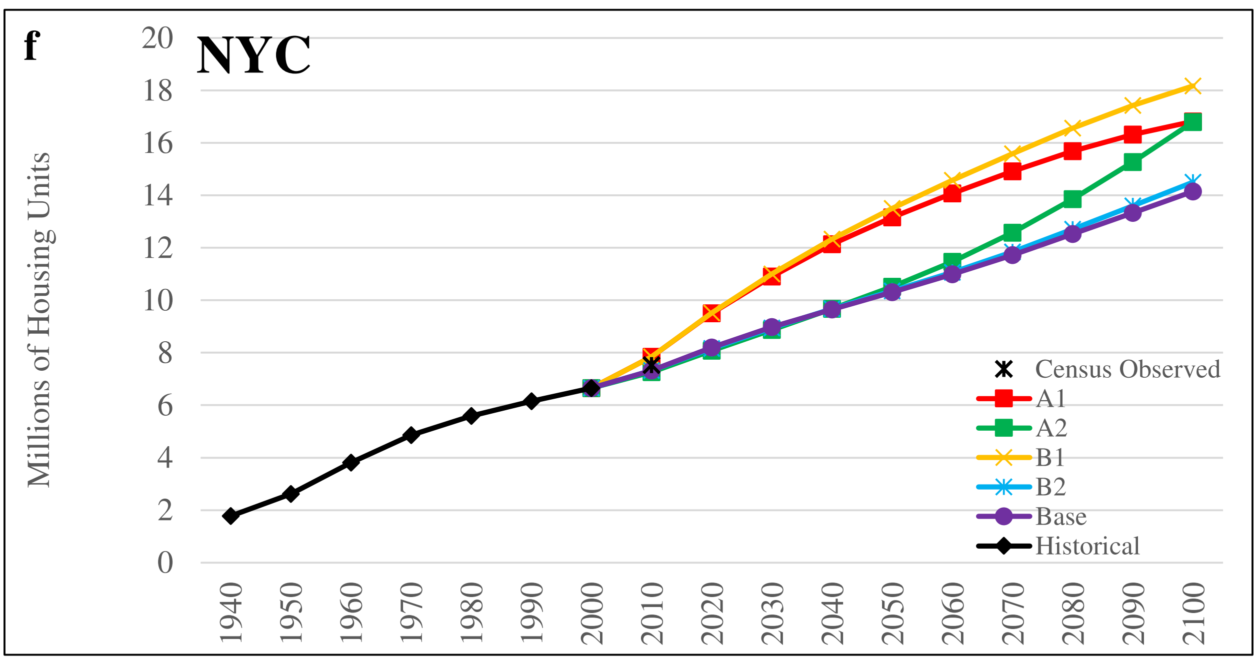

The MSAs exhibit different LU growth patterns for all five projections (Tables 10 through 15). Every MSA is projected to experience a decrease in rural area and rural-classified HUs from 2010 to 2100 for all scenarios. Tampa (Table 12) is expected to have a decrease in rural and exurban area for all scenarios, indicating that HU growth will largely be of suburban and urban character. Miami (Table 13) is expected to decrease in rural, exurban, and suburban area, and become largely urban for all scenarios by 2100. While exurban and suburban growth varies per MSA, all MSAs exhibit an increase in urban development. Houston, New Orleans, and Charleston are likely to see the most growth in suburban area than the other LU types for all projections; Tampa, Miami, and New York will experience the most growth in urban area. By 2100, Miami will be the only MSA in this study to be more than 30% urban for all projections. Tampa will be about 37% to 53% suburban by 2100, while New York City is expected to be suburban and/or exurban and Houston is expected to be exurban and/or rural. Charleston will be approximately 60% exurban and New Orleans will be about 55% rural for all projections. The historical and potential growth of the MSAs illustrates the diversity of the HU growth in time and space.

Each MSA has a unique spatiotemporal growth pattern that influences the potential impact of tropical cyclone hazards (Figure 16). Houston, Tampa, Charleston, and New York City experienced tremendous exurban and suburban growth from 1950 to 2000 and are projected to expand further by 2100. New Orleans does not exhibit considerable variation in LU changes throughout the 21st century, which is likely due to Wildlife Management protected lands and surrounding lakes (i.e., Lakes Ponchartrain, Borgne, Maurepas, and Salvador). After 2000, New Orleans remains about 55% rural, 32% exurban, 10% suburban, and 3% urban up to 2100.

Table 10. The total land use (LU) area, percentage LU (rural, exurban, suburban, and urban) classification of total developable land, percent change in LU classification, total number of housing units (HUs), percentage of total HUs by LU classification, and percent change in HUs by LU classification for Houston MSA and the ICLUS scenarios from 2010 to

HOU	LU	Area (km^2)		% LU		% Change LU 2010-2100	Total HUs (x1,000)		% of Total HUs		% Change HU 2010-2100
		2010	2100	2010	2100		2010	2100	2010	2100	
A1	Ru.	8201.2	5540.9	44.8	30.0	-32.4	15.3	8.7	0.8	0.3	-43.4
	Ex.	7523.0	8351.4	41.1	45.2	11.0	262.8	437.1	13.4	14.6	66.3
	Su.	2100.9	3934.6	11.5	21.3	87.3	808.6	1445.3	41.3	48.3	78.8
	Ur.	489.5	642.8	2.7	3.5	31.3	870.0	1103.7	44.5	36.9	26.9
A2	Ru.	8325.6	4571.5	46.0	24.8	-45.1	15.7	7.2	0.8	0.2	-54.5
	Ex.	7332.1	6508.9	40.5	35.4	-11.2	241.1	398.5	12.9	8.9	65.3
	Su.	1954.5	6342.4	10.8	34.5	224.5	767.1	2417.5	41.1	53.9	215.1
	Ur.	472.9	986.0	2.6	5.4	108.5	843.6	1661.0	45.2	37.0	96.9
B1	Ru.	8333.1	7179.4	45.7	39.2	-13.8	15.8	12.4	0.8	0.5	-21.6
	Ex.	7305.1	7322.2	40.1	40.0	0.2	251.7	276.8	13.0	10.7	10.0
	Su.	2088.8	3171.3	11.5	17.3	51.8	804.2	1221.7	41.4	47.2	51.9
	Ur.	489.7	621.7	2.7	3.4	27.0	870.7	1079.6	44.8	41.7	24.0
B2	Ru.	8519.8	7251.1	46.9	39.6	-14.9	16.0	12.3	0.8	0.4	-22.7
	Ex.	7180.1	6218.3	39.5	34.0	-13.4	239.6	234.9	12.7	7.4	-2.0
	Su.	2000.0	4044.7	11.0	22.1	102.2	778.8	1593.4	41.2	50.1	104.6
	Ur.	480.0	774.0	2.6	4.2	61.2	855.0	1338.4	45.3	42.1	56.5
Base	Ru.	8480.7	5460.7	46.4	29.5	-35.6	15.9	8.5	0.8	0.3	-46.7
	Ex.	7331.2	8155.8	40.1	44.1	11.2	245.9	457.1	13.0	13.8	85.9
	Su.	2002.2	4149.3	10.9	22.4	107.2	779.3	1570.7	41.1	47.3	101.5
	Ur.	479.8	744.6	2.6	4.0	55.2	854.4	1281.4	45.1	38.6	50.0

Table 11. As in Table 10, except for New Orleans MSA.

NOL	LU	Area (km^2)		% LU		% Change LU 2010-2100	Total HUs (x1,000)		% of Total HUs		% Change HU 2010-2100
		2010	2100	2010	2100		2010	2100	2010	2100	
A1	Ru.	3166.9	2824.2	59.8	53.3	-10.8	3.0	2.2	0.6	0.3	-26.4
	Ex.	1591.2	1762.9	30.0	33.3	10.8	48.5	83.5	9.4	13.1	72.2
	Su.	386.9	539.0	7.3	10.2	39.3	157.3	207.1	30.4	32.5	31.7
	Ur.	153.6	173.6	2.9	3.3	13.0	308.2	343.9	59.6	54.0	11.6
A2	Ru.	3228.9	2860.7	61.1	54.0	-11.4	3.0	2.2	0.6	0.2	-28.1
	Ex.	1529.8	1482.4	28.9	28.0	-3.1	45.1	53.8	8.9	5.8	19.4
	Su.	377.2	681.5	7.1	12.9	80.7	154.3	327.5	30.4	35.5	112.2
	Ur.	152.1	273.4	2.9	5.2	79.7	305.2	540.2	60.1	58.5	77.0
B1	Ru.	2999.1	2854.6	58.8	56.0	-4.8	3.0	2.7	0.6	0.5	-9.5
	Ex.	1561.0	1586.4	30.6	31.1	1.6	47.0	52.8	9.1	8.9	12.4
	Su.	383.1	483.4	7.5	9.5	26.2	156.4	185.0	30.4	31.3	18.3
	Ur.	153.7	174.4	3.0	3.4	13.5	308.7	350.0	59.9	59.3	13.4
B2	Ru.	3010.3	2803.5	59.5	55.3	-6.9	3.0	2.6	0.6	0.4	-13.7
	Ex.	1522.9	1496.6	30.1	29.5	-1.7	45.0	52.6	8.9	7.7	16.8
	Su.	377.4	568.8	7.5	11.2	50.7	154.7	221.6	30.4	32.4	43.3
	Ur.	152.3	201.6	3.0	4.0	32.4	305.9	406.3	60.1	59.5	32.8
Base	Ru.	3215.3	2958.2	60.7	55.8	-8.0	3.0	2.4	0.6	0.3	-20.9
	Ex.	1548.7	1564.9	29.2	29.5	1.0	45.8	53.1	9.0	7.6	16.1
	Su.	378.5	573.7	7.1	10.8	51.6	154.8	242.3	30.4	34.5	56.6
	Ur.	152.3	202.5	2.9	3.8	33.0	305.7	403.6	60.0	57.5	32.0

Table 12. As in Table 10, except for Tampa MSA.

TPA	LU	Area (km^2)		% LU		% Change LU 2010-2100	Total HUs (x1,000)		% of Total HUs		% Change HU 2010-2100
		2010	2100	2010	2100		2010	2100	2010	2100	
A1	Ru.	787.6	525.6	14.7	9.8	-33.3	2.2	1.3	0.2	0.1	-41.9
	Ex.	2811.2	1782.5	52.4	33.2	-36.6	127.4	80.1	9.9	3.6	-37.1
	Su.	1456.9	2526.3	27.2	47.1	73.4	549.2	1212.3	42.9	54.0	120.7
	Ur.	305.6	534.1	5.7	9.9	74.8	601.9	953.1	47.0	42.4	58.4
A2	Ru.	883.3	494.5	16.5	9.2	-44.0	2.4	1.1	0.2	0.0	-53.6
	Ex.	2883.6	1223.4	53.8	22.8	-57.6	122.5	53.7	10.1	1.9	-56.1
	Su.	1302.6	2888.6	24.3	53.8	121.8	509.1	1533.1	41.8	52.8	201.1
	Ur.	293.9	762.5	5.5	14.2	159.5	583.7	1313.0	47.9	45.3	124.9
B1	Ru.	889.7	831.2	16.6	15.5	-6.6	2.5	2.3	0.2	0.1	-7.3
	Ex.	2758.6	1999.0	51.4	37.3	-27.5	122.9	78.2	9.8	4.0	-36.4
	Su.	1413.5	2029.9	26.3	37.9	43.6	536.2	980.6	42.6	49.7	82.9
	Ur.	302.5	502.6	5.6	9.4	66.1	596.6	911.8	47.4	46.2	52.8
B2	Ru.	941.0	860.1	17.6	16.0	-8.6	2.6	2.3	0.2	0.1	-10.5
	Ex.	2818.5	1860.0	52.6	34.7	-34.0	121.2	73.0	10.0	3.5	-39.8
	Su.	1307.5	2113.2	24.4	39.4	61.6	509.1	1030.3	41.9	50.0	102.4
	Ur.	293.4	529.6	5.5	9.9	80.5	582.8	956.1	47.9	46.4	64.0
Base	Ru.	872.9	600.9	16.3	11.2	-31.2	2.4	1.5	0.2	0.1	-39.8
	Ex.	2873.0	1800.5	53.5	33.5	-37.3	123.9	79.4	10.1	3.6	-36.0
	Su.	1324.5	2420.3	24.7	45.1	82.7	513.9	1156.8	41.9	52.2	125.1
	Ur.	294.7	545.7	5.5	10.2	85.2	584.9	979.2	47.7	44.2	67.4

Table 13. As in Table 10, except for Miami MSA.

MIA	LU	Area (km^2)		% LU		% Change LU 2010-2100	Total HUs (x1,000)		% of Total HUs		% Change HU 2010-2100
		2010	2100	2010	2100		2010	2100	2010	2100	
A1	Ru.	1641.7	1359.6	29.3	24.2	-17.2	2.2	1.5	0.1	0.0	-31.6
	Ex.	1632.1	871.2	29.2	15.5	-46.6	85.5	37.3	3.6	0.7	-56.3
	Su.	1640.4	1496.5	29.3	26.7	-8.8	731.8	724.5	31.0	14.5	-1.0
	Ur.	684.1	1883.5	12.2	33.6	175.3	1539.8	4234.6	65.3	84.7	175.0
A2	Ru.	1714.2	1317.0	30.6	23.5	-23.2	2.2	1.4	0.1	0.0	-38.6
	Ex.	1690.2	609.0	30.2	10.8	-64.0	77.4	23.8	3.5	0.4	-69.2
	Su.	1556.8	1510.2	27.8	26.9	-3.0	681.7	864.6	30.8	15.9	26.8
	Ur.	635.2	2179.6	11.4	38.8	243.1	1450.8	4546.7	65.6	83.6	213.4
B1	Ru.	1701.7	1598.1	30.5	28.6	-6.1	2.3	2.1	0.1	0.0	-10.0
	Ex.	1572.0	810.0	28.1	14.5	-48.5	84.0	34.6	3.6	0.7	-58.8
	Su.	1630.6	1336.5	29.2	23.9	-18.0	728.2	642.3	31.0	12.3	-11.8
	Ur.	681.1	1845.3	12.2	33.0	171.0	1534.8	4536.2	65.3	87.0	195.6
B2	Ru.	1735.1	1620.8	31.1	29.0	-6.6	2.3	2.1	0.1	0.0	-10.8
	Ex.	1632.6	717.4	29.2	12.8	-56.1	77.8	29.7	3.5	0.6	-61.9
	Su.	1575.1	1402.6	28.2	25.1	-11.0	690.5	742.5	30.9	15.7	7.5
	Ur.	640.8	1848.2	11.5	33.1	188.4	1461.7	3959.9	65.5	83.6	170.9
Base	Ru.	1703.7	1423.8	30.4	25.4	-16.4	2.3	1.6	0.1	0.0	-29.9
	Ex.	1673.7	792.9	29.9	14.1	-52.6	78.3	33.0	3.5	0.7	-57.9
	Su.	1581.5	1538.4	28.2	27.4	-2.7	692.4	816.9	31.0	17.5	18.0
	Ur.	641.8	1850.6	11.5	33.0	188.4	1463.5	3815.1	65.4	81.8	160.7

Table 14. As in Table 10, except for Charleston MSA.

CHS	LU	Area (km^2)		% LU		% Change LU 2010-2100	Total HUs (x1,000)		% of Total HUs		% Change HU 2010-2100
		2010	2100	2010	2100		2010	2100	2010	2100	
A1	Ru.	1916.1	1321.9	36.6	25.2	-31.0	5.3	3.2	1.9	0.9	-39.5
	Ex.	2930.8	3421.3	56.0	65.2	16.7	73.1	97.5	25.7	28.3	33.3
	Su.	343.1	450.8	6.6	8.6	31.4	123.6	153.7	43.4	44.6	24.3
	Ur.	45.2	50.2	0.9	1.0	10.9	82.5	90.1	29.0	26.2	9.2
A2	Ru.	2065.4	1308.2	39.5	25.0	-36.7	5.6	3.1	2.0	0.6	-45.7
	Ex.	2781.6	3120.1	53.2	59.5	12.2	68.6	92.2	24.7	16.7	34.4
	Su.	335.7	722.8	6.4	13.8	115.3	121.5	306.3	43.8	55.5	152.1
	Ur.	44.7	92.0	0.9	1.8	105.7	81.8	150.4	29.5	27.2	83.9
B1	Ru.	2061.0	1765.9	39.4	33.8	-14.3	5.6	4.7	2.0	1.5	-16.1
	Ex.	2784.4	3035.0	53.2	58.0	9.0	69.8	82.2	24.9	26.7	17.7
	Su.	340.7	382.8	6.5	7.3	12.4	122.9	134.8	43.8	43.9	9.7
	Ur.	45.0	47.2	0.9	0.9	4.9	82.2	85.6	29.3	27.9	4.2
B2	Ru.	2131.3	1793.8	40.7	34.3	-15.8	5.8	4.7	2.1	1.3	-17.9
	Ex.	2718.3	2855.7	52.0	54.6	5.1	67.7	91.2	24.4	25.2	34.7
	Su.	336.8	532.7	6.4	10.2	58.1	121.8	172.3	44.0	47.6	41.5
	Ur.	44.8	52.6	0.9	1.0	17.5	81.8	93.8	29.5	25.9	14.6
Base	Ru.	2037.1	1406.5	38.9	26.9	-31.0	5.6	3.4	2.0	0.9	-39.3
	Ex.	2814.0	3218.2	53.8	61.4	14.4	69.5	89.2	24.9	22.9	28.4
	Su.	337.2	554.2	6.4	10.6	64.3	121.9	194.0	43.7	49.8	59.1
	Ur.	44.8	59.2	0.9	1.1	32.4	81.8	103.2	29.4	26.5	26.1

Table 15. As in Table 10, except for New York City MSA.

NYC	LU	Area (km^2)		% LU		% Change LU 2010-2100	Total HUs (x1,000)		% of Total HUs		% Change HU 2010-2100
		2010	2100	2010	2100		2010	2100	2010	2100	
A1	Ru.	791.4	668.8	5.1	4.3	-15.5	2.7	2.3	0.0	0.0	-16.6
	Ex.	8574.9	5941.7	55.6	38.6	-30.7	362.7	219.0	4.6	1.3	-39.6
	Su.	4455.2	5889.3	28.9	38.2	32.2	1683.6	3007.9	21.4	17.9	78.7
	Ur.	1589.2	2913.0	10.3	18.9	83.3	5802.6	13593.6	73.9	80.8	134.3
A2	Ru.	977.7	808.8	6.3	5.2	-17.3	3.3	2.7	0.0	0.0	-17.4
	Ex.	8678.2	5128.8	56.3	33.3	-40.9	356.3	176.8	4.9	1.1	-50.4
	Su.	4249.9	5769.4	27.6	37.4	35.8	1626.3	3321.1	22.4	19.8	104.2
	Ur.	1497.0	3700.7	9.7	24.0	147.2	5278.1	13290.2	72.7	79.2	151.8
B1	Ru.	908.7	844.6	5.9	5.5	-7.1	3.1	2.8	0.0	0.0	-8.0
	Ex.	8525.9	6635.4	55.3	43.1	-22.2	356.8	246.6	4.5	1.4	-30.9
	Su.	4397.0	5392.4	28.5	35.0	22.6	1663.5	2421.0	21.2	13.3	45.5
	Ur.	1579.8	2538.8	10.3	16.5	60.7	5818.4	15499.5	74.2	85.3	166.4
B2	Ru.	1029.7	946.3	6.7	6.1	-8.1	3.4	3.1	0.0	0.0	-8.7
	Ex.	8630.5	6328.3	56.0	41.1	-26.7	354.7	227.0	4.8	1.6	-36.0
	Su.	4239.1	5715.2	27.5	37.1	34.8	1621.0	2627.4	22.2	18.1	62.1
	Ur.	1505.6	2418.2	9.8	15.7	60.6	5338.4	11639.4	73.0	80.3	118.0
Base	Ru.	949.8	822.5	6.2	5.3	-13.4	3.3	2.8	0.0	0.0	-13.7
	Ex.	8687.3	6007.4	56.4	39.0	-30.8	358.2	215.2	4.9	1.5	-39.9
	Su.	4259.3	6062.4	27.6	39.3	42.3	1628.1	2930.6	22.2	20.7	80.0
	Ur.	1508.3	2516.6	9.8	16.3	66.8	5335.5	10994.2	72.8	77.7	106.1

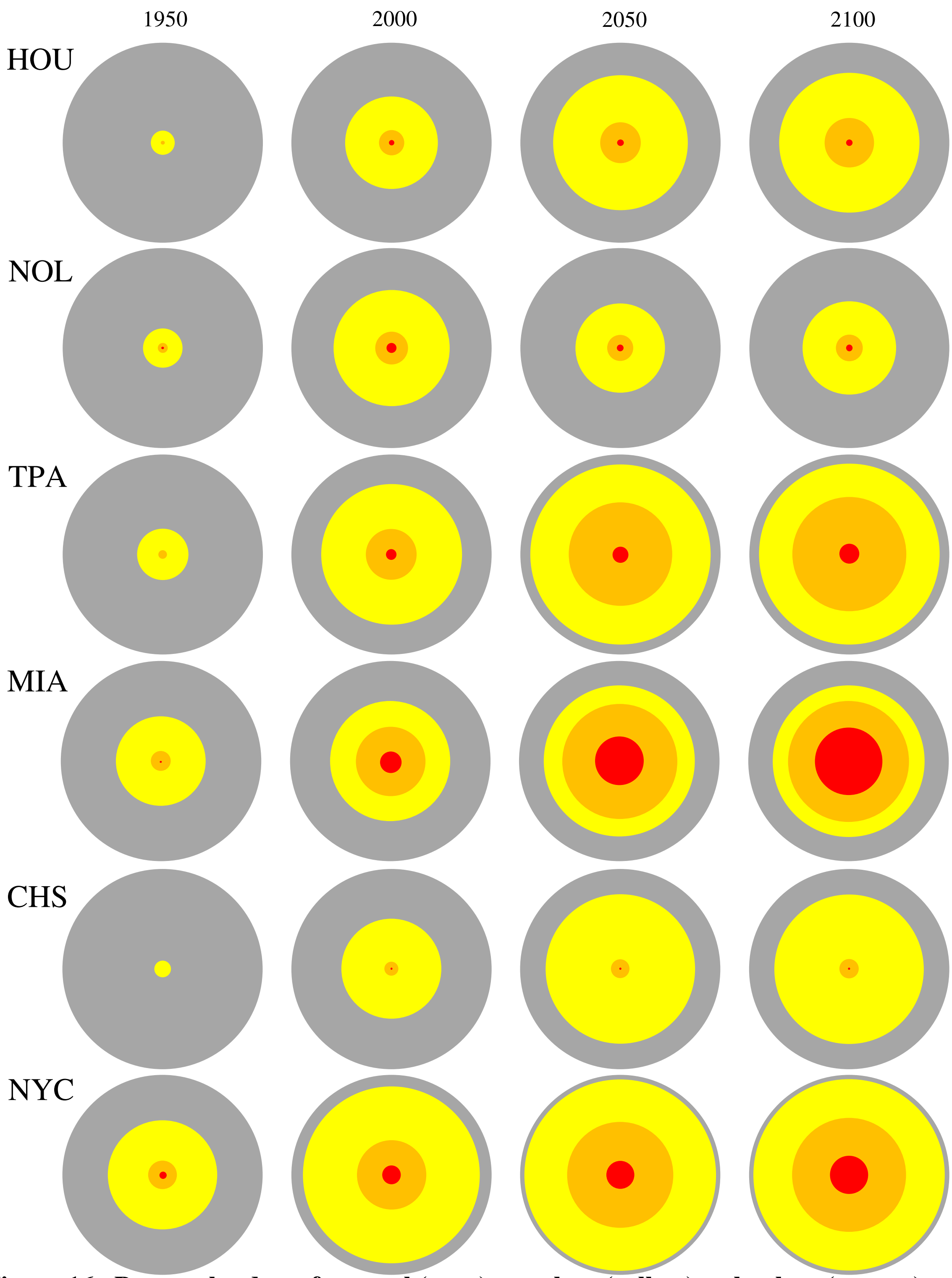

Figure 16. Percent land use for rural (gray), exurban (yellow), suburban (orange), and urban (red) in the 2013 MSA of Houston, New Orleans, Tampa, Miami, Charleston and New York City for 1950, 2000, 2050 and 2100, where 2050 and 2100 are projected under the A1 scenario

Miami experienced growth within exurban and suburban, but urban showed the most prominent growth. Additionally, Miami is projected to experience more growth within urban morphology than the other LU classifications, and future growth will be highly dense within the MSA core. The geography of MSAs change over time and more counties may be added as the developed footprint of these metropolitan regions expand. In this study, the MSAs historical and future projections of LU composition are assumed under the 2013 definition of each MSA. Thus, the continual growth of HUs within the MSAs will increase the density over time (Figure 17). By 2100 under the A1 projection, New York City will remain the densest MSA in this study at 783.11 HU km-2; Charleston will continue to be the least dense MSA by 2100 at 51.39 HU km-2. New York City may be the densest MSA, but Miami is expected to experience the greatest change in density—nearly +9,700%—from 1940 to 2100. Tampa's density is projected to not change as much as Miami; however, Tampa's density by 2100 is 345 HU km-2, nearly as dense as Miami. The density results indicate that in the future, Miami may continue to be the most rapidly growing MSA of the areas investigated.

Figure 17. The housing unit density for each MSA from 1940 to 2100, where 2010 to 2100 is under the A1 projection.

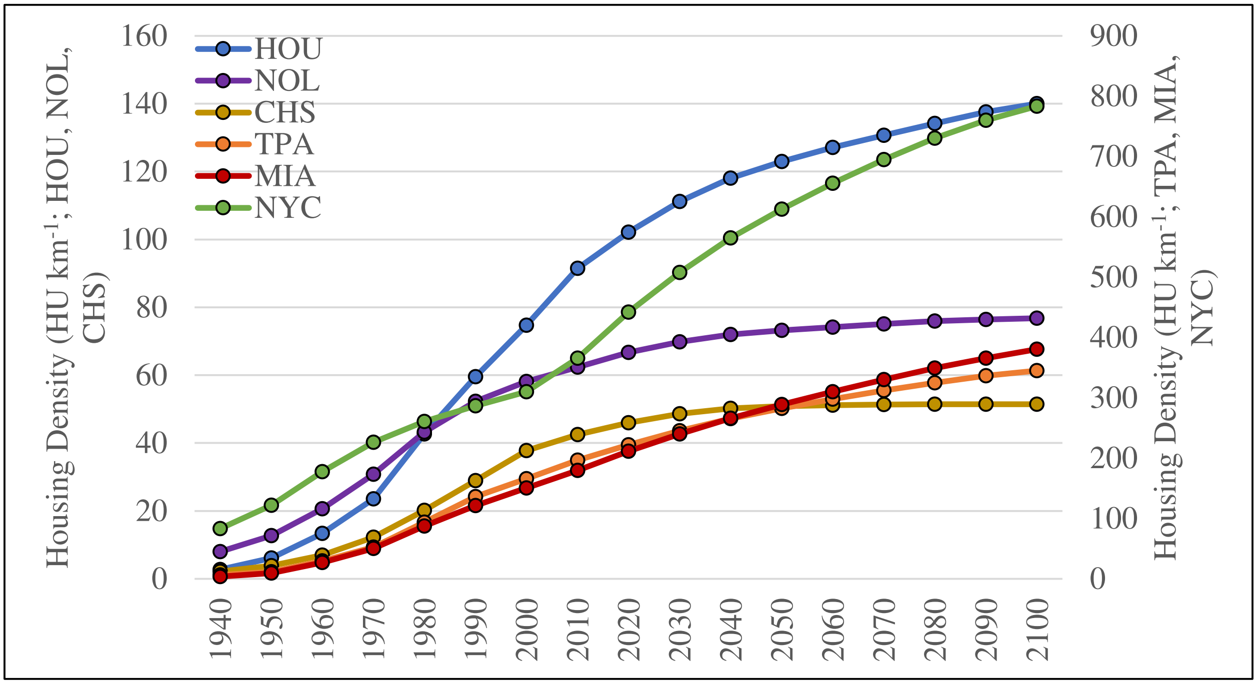

Hurricane Scenarios

In this study, the use of hurricane scenarios does not include the structural integrity of the underlying HUs within the storm swath. Simply, the scenarios examine the potential number of HU impacted by a hurricane synthetic. Although the impact of the hurricane will vary per HU, the central focus is to illustrate the residential disaster potential and how the development footprint changes the disaster potential over time. There are two hurricane synthetics that were created for this study: an "all landfalling" synthetic and a "major" synthetic (Figure 18). The "all landfalling" synthetic contains three wind swaths: 17 m s-1, 25 m s-1, and 34 m s-1 (Category 1).

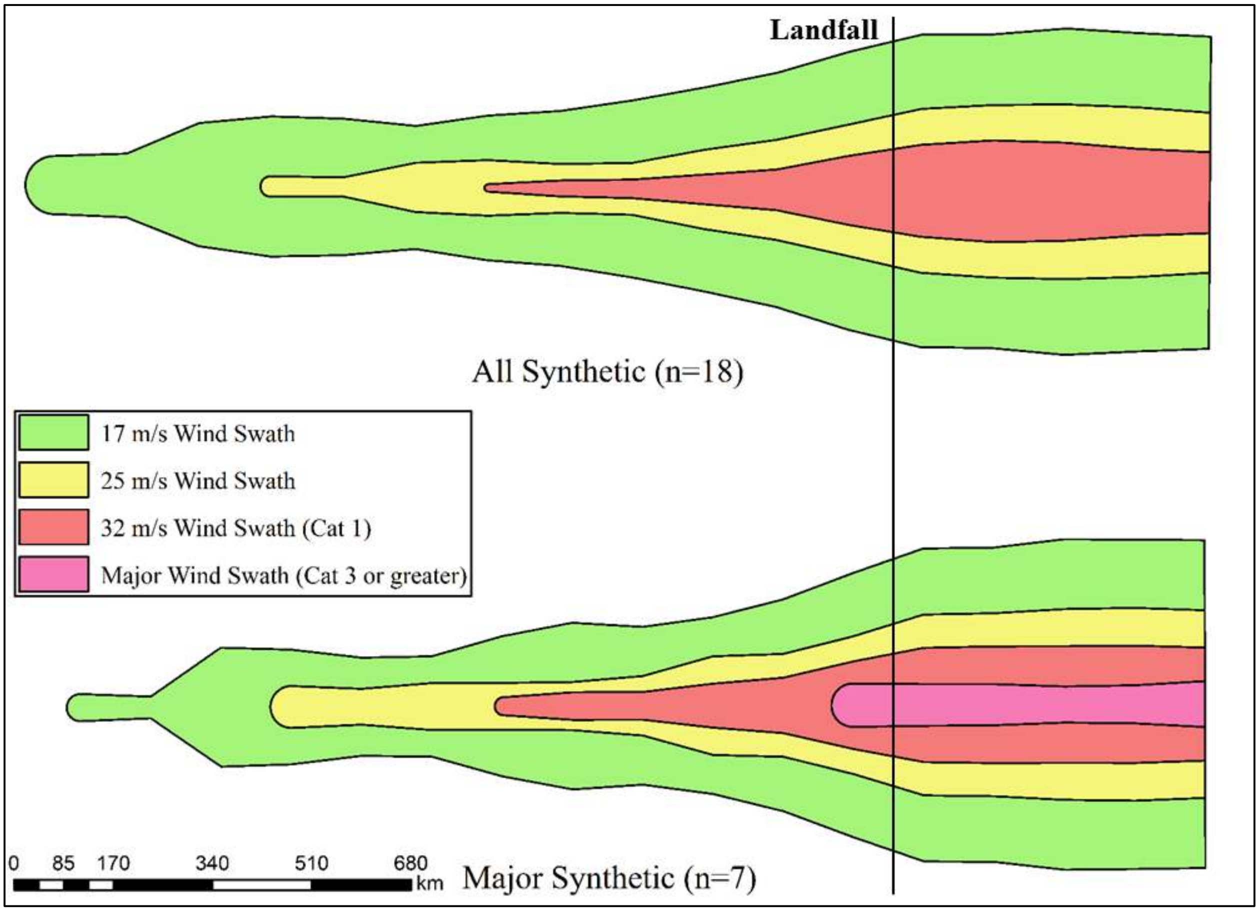

Figure 18. The hurricane synthetics—created from historical landfalling hurricanes from 2004 to 2014—used to assess the potential disaster impact.

The "major" synthetic contains the same three wind swaths and an additional major swath of 50 m s-1 or greater wind speed (Category 3 or greater). The hurricane synthetics were placed over the developed core of each MSA to assess "worst-case" scenarios (Clarke 2005). The angle of the synthetic's landfall was determined by examining previous hurricanes and how they made landfall near each corresponding MSA. In most cases, landfall was orthogonal to the coastline for each MSA, except for Tampa (Figure 19). Because of Tampa's location along the eastern

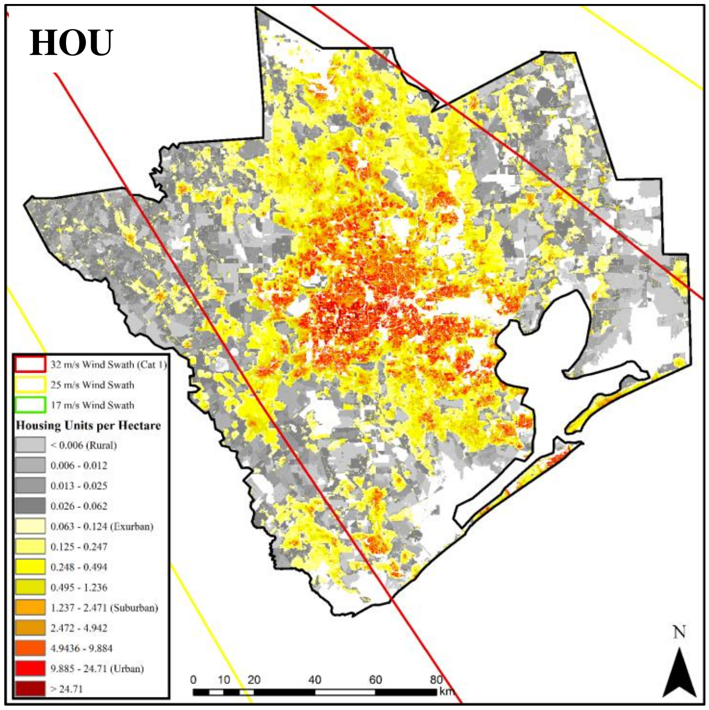

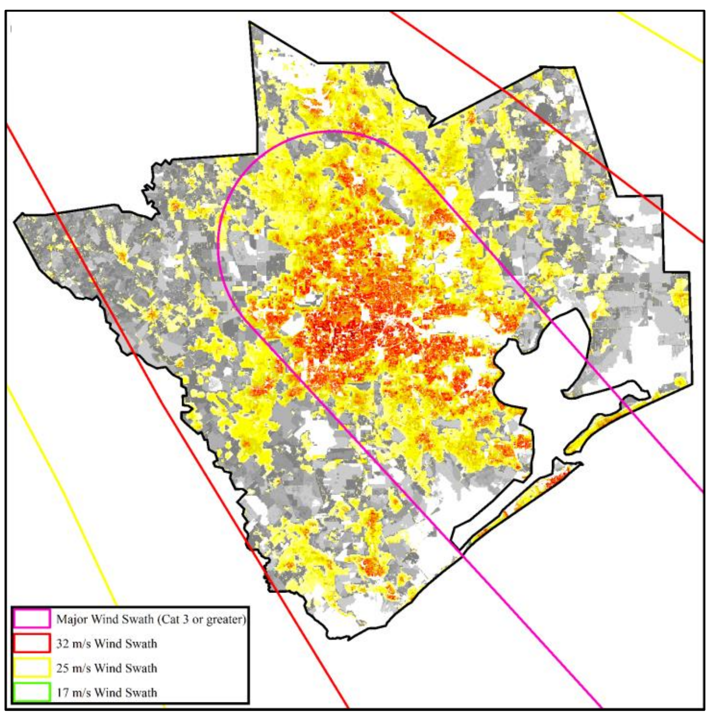

Figure 19. After Figure 4, where the hurricane synthetics ("all" synthetic, top; "major" synthetic, bottom) are superimposed on the A1 2010 projection of the six MSAs.

(continued on following page)

Figure 19 (continued)

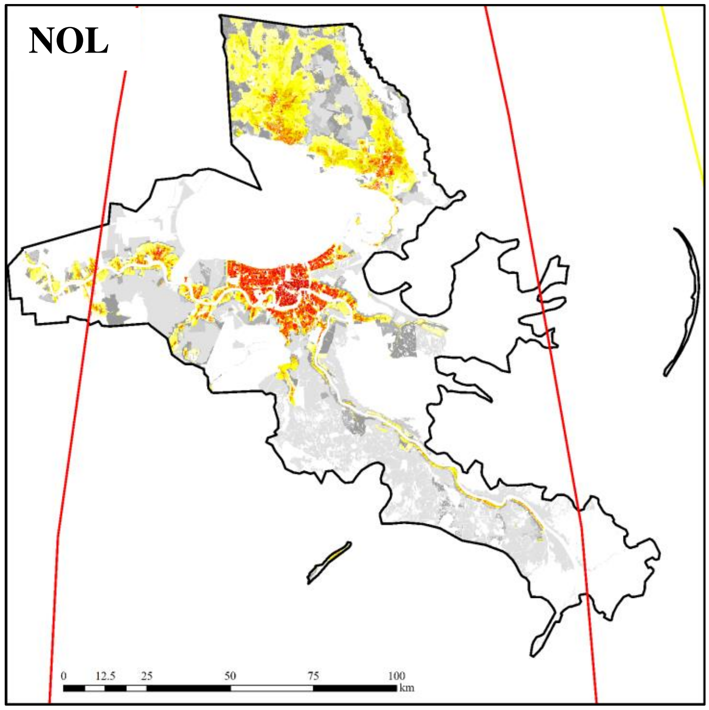

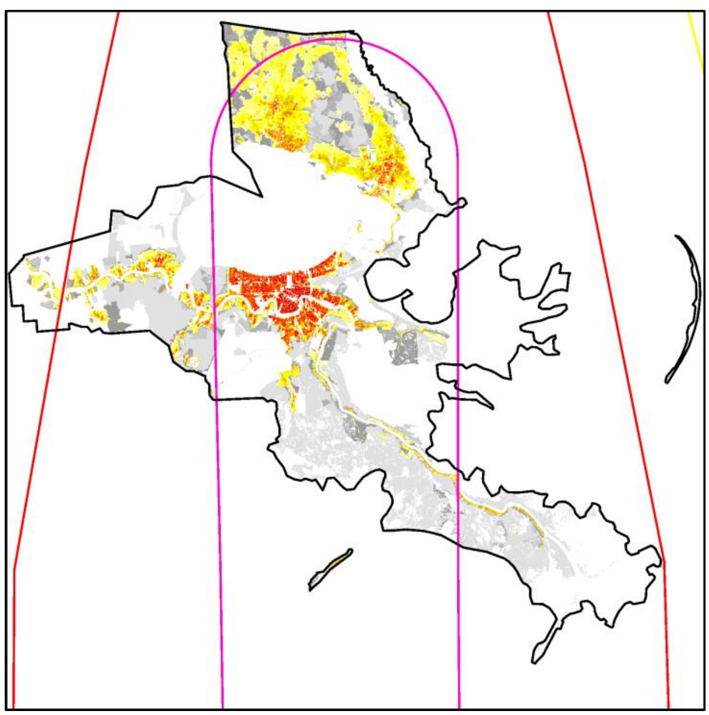

(continued on following page)

Figure 19 (continued)

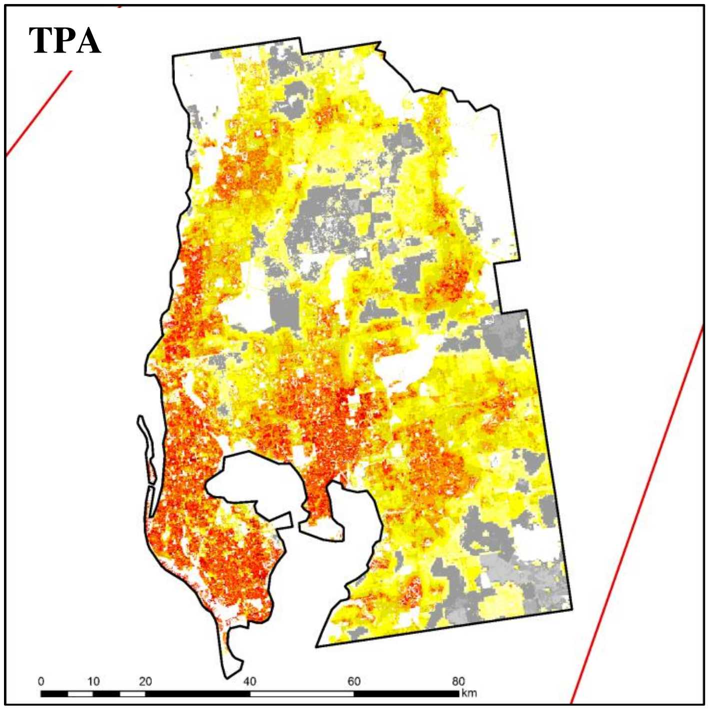

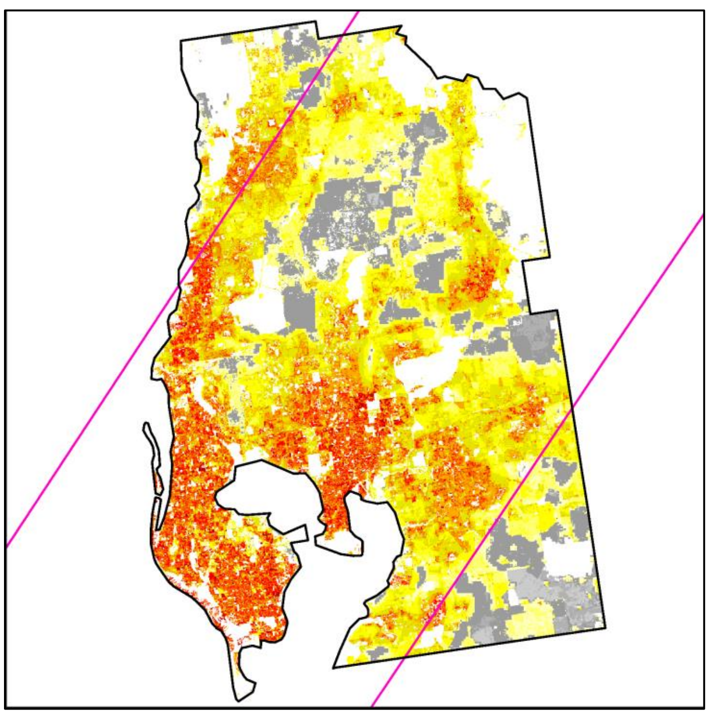

(continued on following page)

Figure 19 (continued)

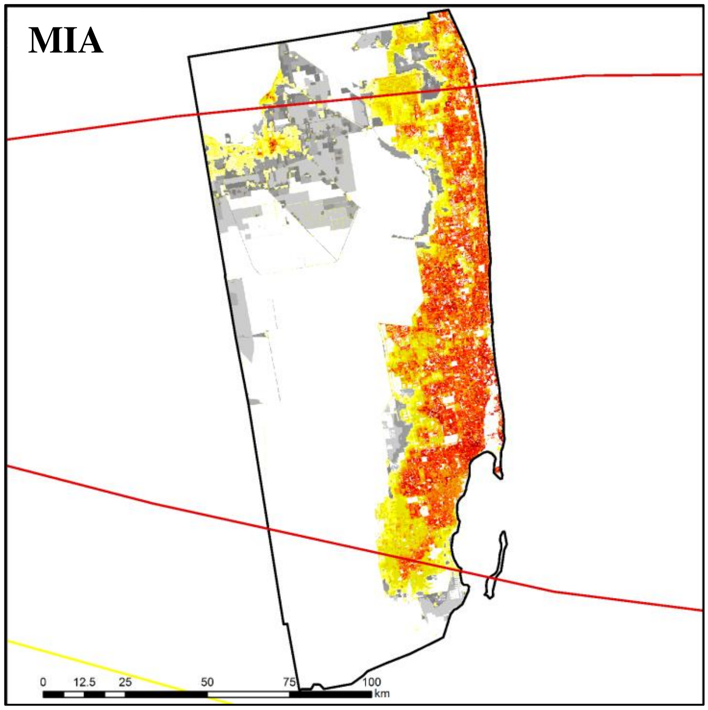

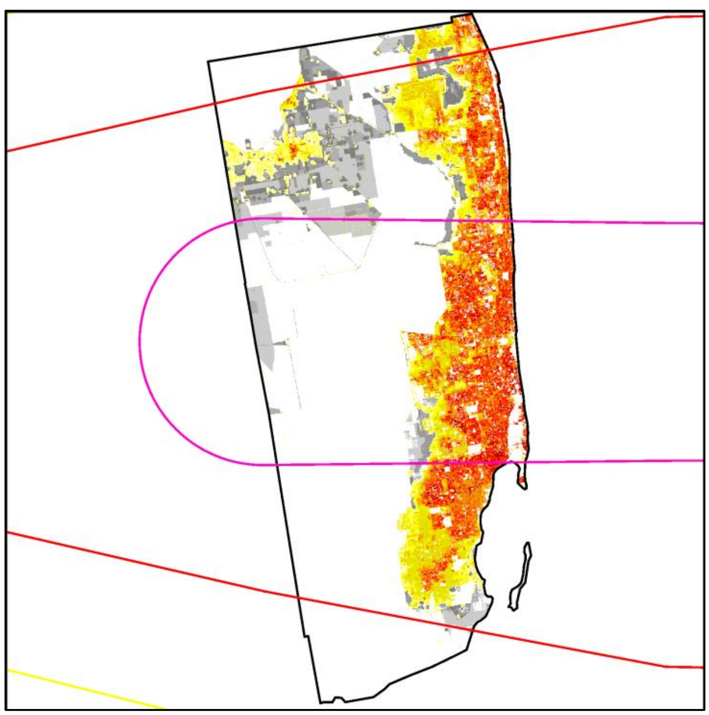

(continued on following page)

Figure 19 (continued)

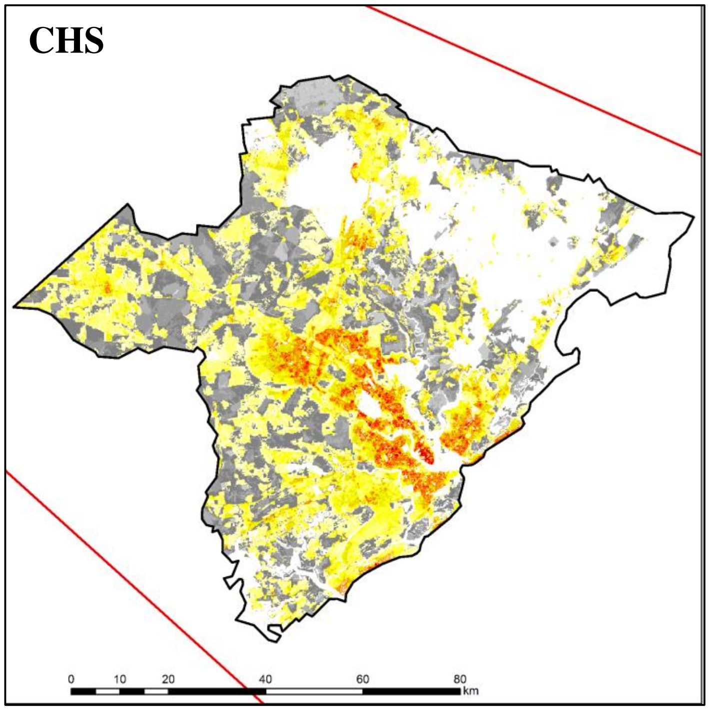

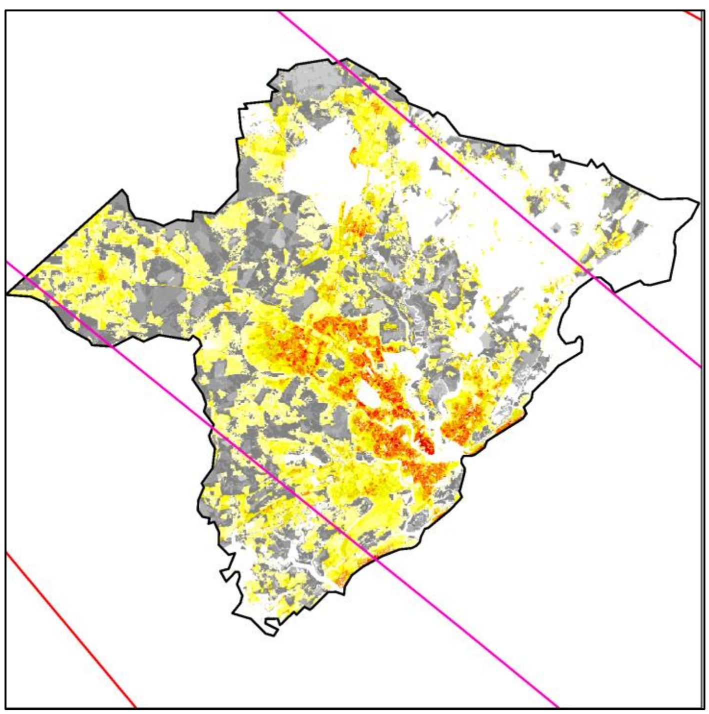

(continued on following page)

Figure 19 (continued)

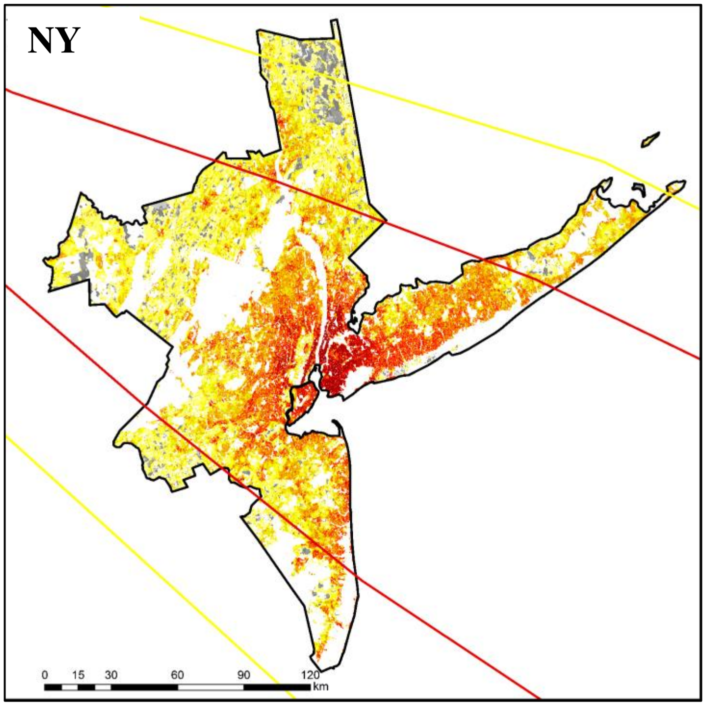

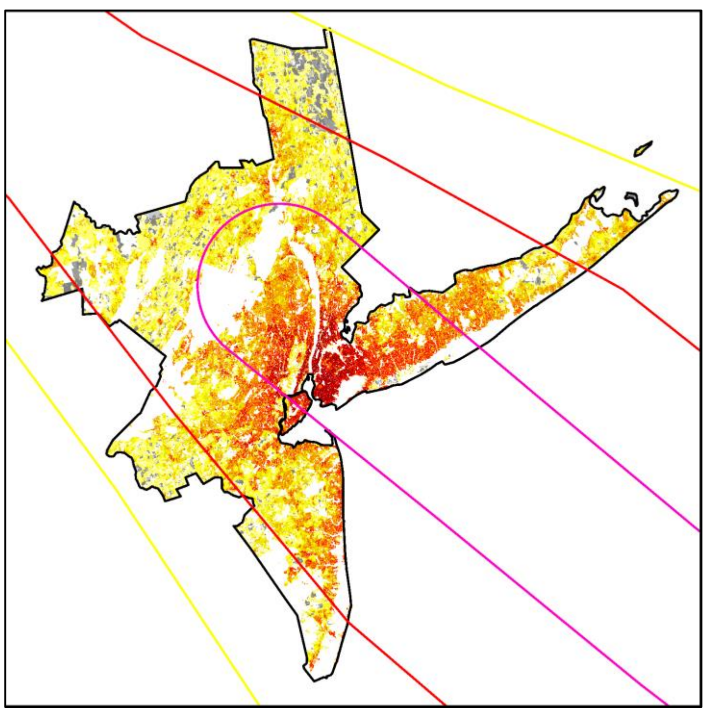

Gulf Coast, an orthogonal landfall would be improbable; therefore, the hurricane synthetic was placed over Tampa in likeness to Hurricane Charley in 2004. The following analysis is separated into two parts: "all" synthetic (All Storm hereafter) analysis and "major" synthetic (Major Storm hereafter) analysis.

All Storm Analysis

For all MSAs, the hurricane synthetic encompassed the entire MSA, including the largest MSA, New York City (Figure 20). Tampa and Charleston reside completely within the 32 m s-1 (Category 1) swath of the all storm, indicating that a hurricane impact would cause disastrous effects for the entirety of the MSAs. The New Orleans MSA is almost completely within the Category 1 wind swath, with about 99% of the MSAs HU within the swath from 2010 to 2100. The number of HU that exists within each MSA's swath changes over time. For example, the number of HUs within Houston is projected to grow from 2010 to 2100. In 2010, 3% of Houston's HUs are within the 25 m s-1 wind swath; by 2100, 5.4% of the HU within the MSA will lie within the 25 m s-1 wind swath under the A1 pathway. In the same period, the percentage of HU within the Category 1 swath decreased from 97% to 95%. The decrease within the Category 1 swath indicates that the areas surrounding the MSA core are growing at a faster rate than the core itself; however, the core of the MSA is forecast to experience a growth in HU, as well.

Another metric that provides an assessment of an MSA's developed footprint and character is the "developed density", which is the number of HUs classified as suburban and urban divided by the total area of the land classified as suburban and urban. The Houston MSA

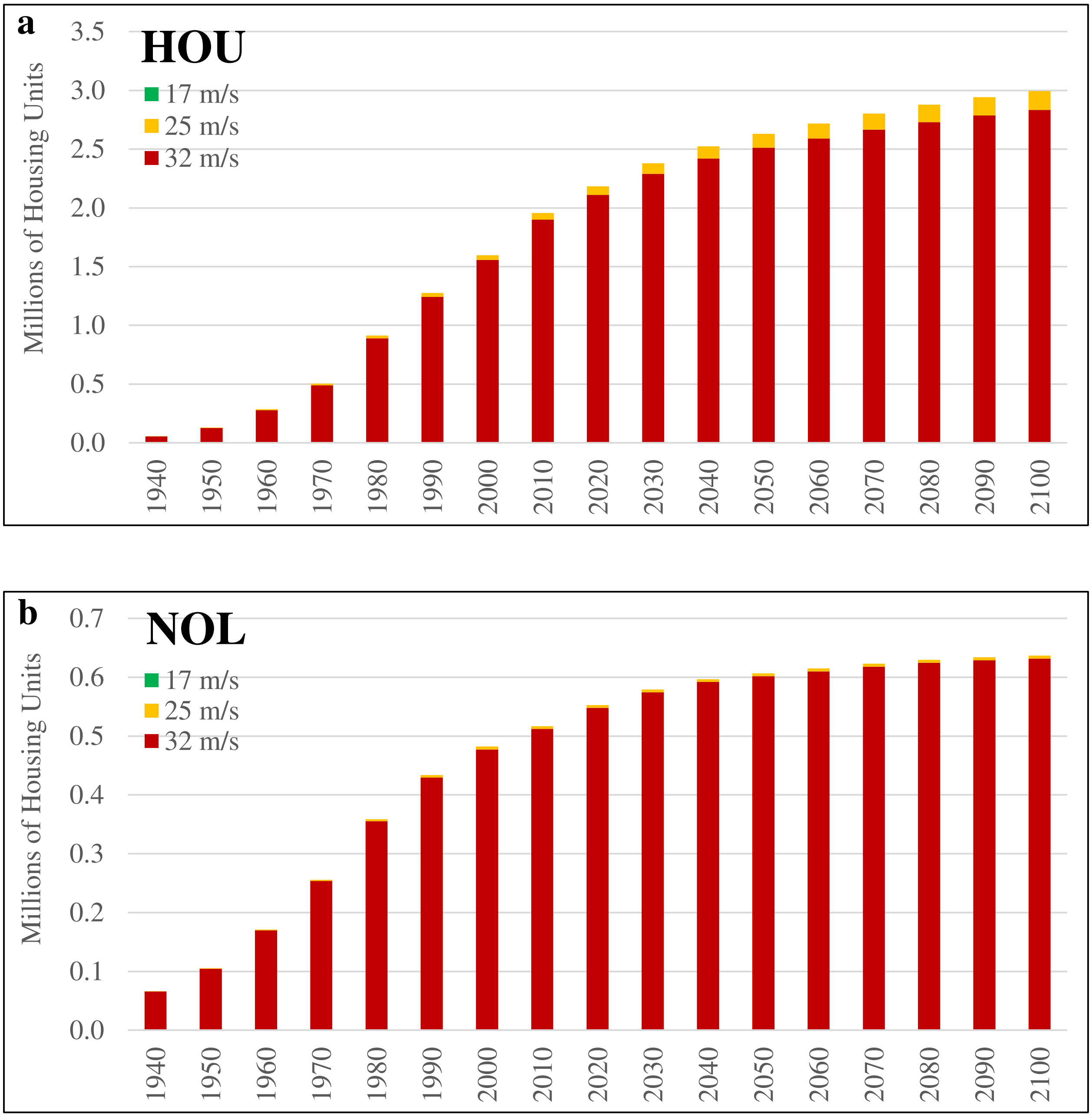

Figure 20. The number of housing units impacted historically from 1940 to 2000 and from 2010 to 2100 under the A1 projection by each wind swath within the All Storm for a Houston, b New Orleans, c Tampa, d Miami, e Charleston, f New York City.

(continued on following page)

Figure 20 (continued)

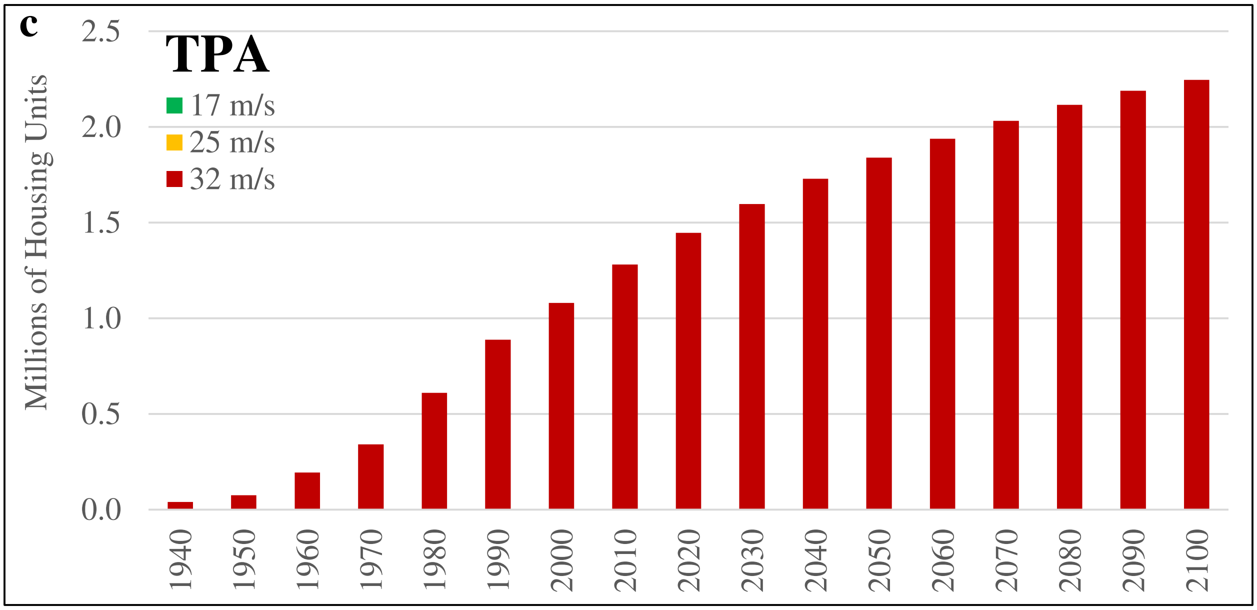

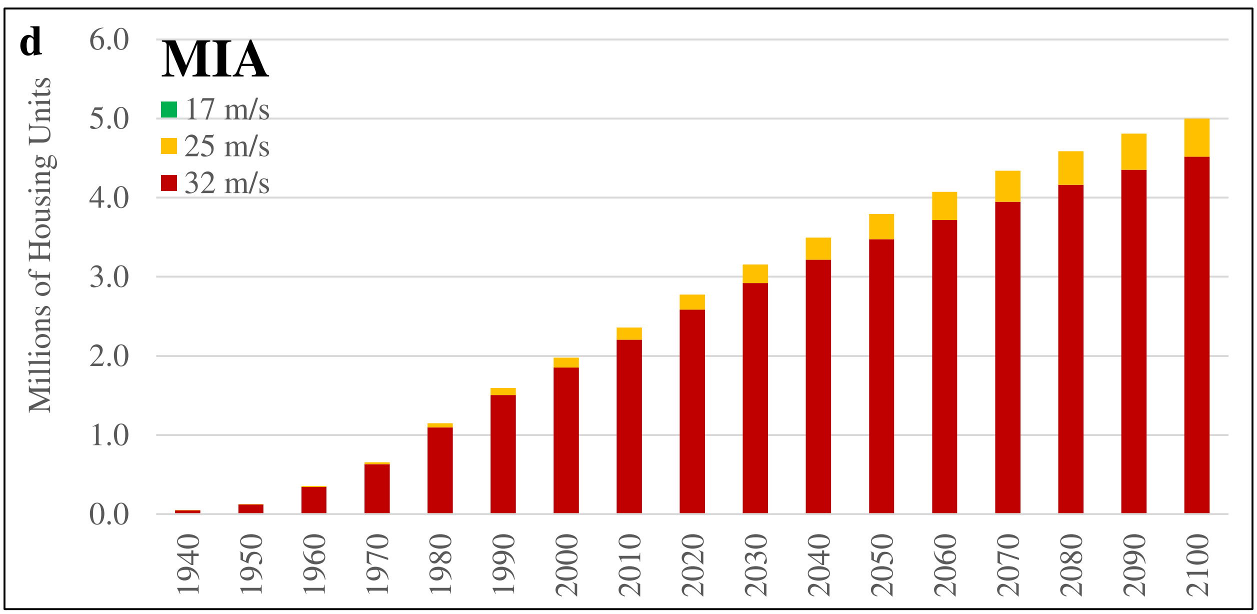

(continued on following page)

Figure 20 (continued)

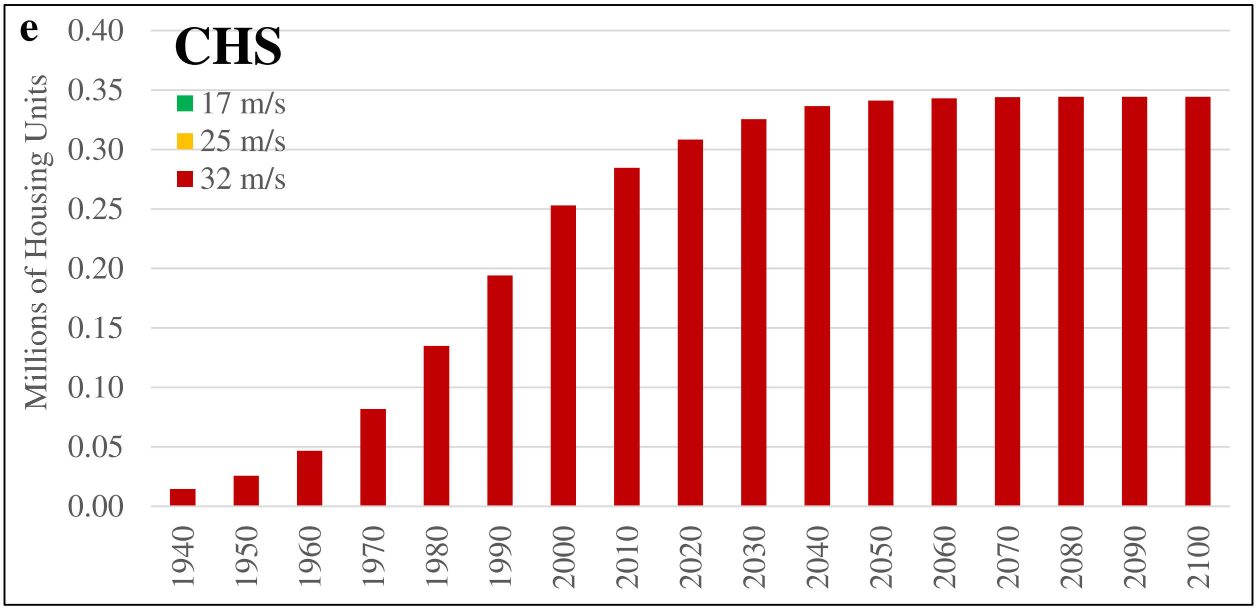

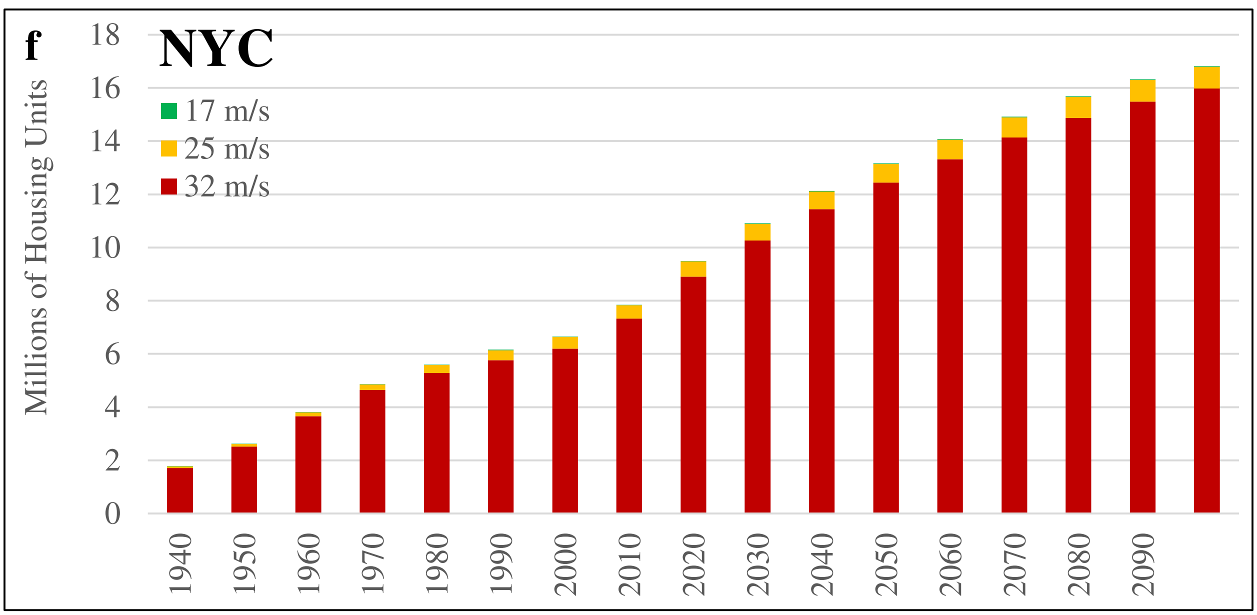

is projected to decrease in developed density by 13% from 2010 to 2100, indicating that development in the area will exhibit a dominant sprawl morphology. Because of the size of Houston, a direct impact of a hurricane is likely to consume the MSA entirely; under the A1 projection, the number of HUs within the All Storm synthetic is forecast to increase from 1.9 million to 2.9 million, or 53%, from 2010 to 2100. About 95% of the growth will be within the Category 1 swath, but tropical storm winds can be damaging as well. In addition, other disastrous impacts can arise from less-intense, landfalling tropical storms, such as heavy rainfall and flooding (e.g., Tropical Storm Allison in 2001; Stewart 2001).

The Miami MSA, which has the second most HUs of the MSAs observed, exhibits a similar result to Houston, primarily because of the unique north-to-south linear nature Miami's primary development corridor. HUs are expected to grow more rapidly in the 25 m s-1 wind swath than the Category 1 wind swath; however the number of HU within the Category 1 wind swath is projected to increase by 104.9% from 2010 to 2100. The absolute number of HU with the Category 1 wind swath is projected to be ten times larger than the number of HU with the 25 m s-1 wind swath. By 2100, 90% of the HU in Miami will reside within the Category 1 wind swath. Overall, the number of HUs within the All Storm synthetic is projected to increase from 2.3 million to 4.9 million, or 112%, from 2010 to 2100 under the A1 projection. It is unknown what the underlying impacts will be, given the different variables of a hurricane; however, if a storm similar to this hurricane scenario were to impact Miami, 90% of the HUs in the MSA would theoretically experience hurricane force winds. Because these data do not include radii of winds stronger than Category 1, it is possible that areas within the Category 1 wind swath would be stronger than 32 m s-1. Additionally, the hurricane synthetics assume uniform wind speeds throughout the swaths and do not consider the different strengths that can characterize each quadrant. Therefore, the Category 1 swath is the minimum strength of the swath, meaning that stronger winds would likely exist near the middle, and poleward, of the swath.

Because the New York City MSA is much larger than the other MSAs, it was the only MSA to experience all three swaths within the All Storm synthetic (17 m s-1, 25 m s-1, and 32 m s-1). About 93% of the HUs within New York City were within the Category 1 wind swath in 2010; by 2100, the number of HUs within the Category 1 swath increased to 95%, indicating that the core of the MSA is growing more rapidly than other regions of the MSA. New York City is known as the gateway for immigration; more than 2.5 million immigrants settled in New York City within the last four decades (Foner 2001). Additionally, New York City is ranked as one of the top cities in the world for economic function, research and development, and cultural interaction, as well as a career hub for artists, actors, and researchers (Hall et al. 2009). The city's suburban and urban development is expected to densify from 2010 to 2100; the developed density is projected to increase from 1,298 HUs km-2 to 1,911 HUs km-2, or 47%. Since the number of HUs is increasing faster than the developed area, New York City is developing up more than out, indicating that the central business district (CBD) of Manhattan is particularly attractive to new residents. From 2010 to 2100, the number of HUs within the Category 1 swath is projected to increase from 7.3 million to 15.9 million HUs, or 118.1%, in the A1 projection. Because the storm was intentionally placed over the heart of the MSA, the number of HUs within the Category 1 swath was the greatest of the wind swaths.

Overall, the impact of a Category 1 storm is projected to increase based on the rising exposure within all of the MSAs (Figure 21). From 1940 to 2100, the number of HUs impacted by the entire All Storm synthetic increases from 51,000 to 5,000,000, or 9,695%. Although New York City has the highest number of HUs impacted by the All Storm synthetic, the MSA changed the least in terms of HU potentially impacted—or, about 845%—of the MSAs from 1940 to 2100. The Houston, Tampa, Miami, and New York City MSAs are all projected to have over 2 million HUs impacted by the All Storm synthetic by 2100. These analyses, illustrate that the growing exposure within the MSAs is, and will continue to, amplify disaster potential.

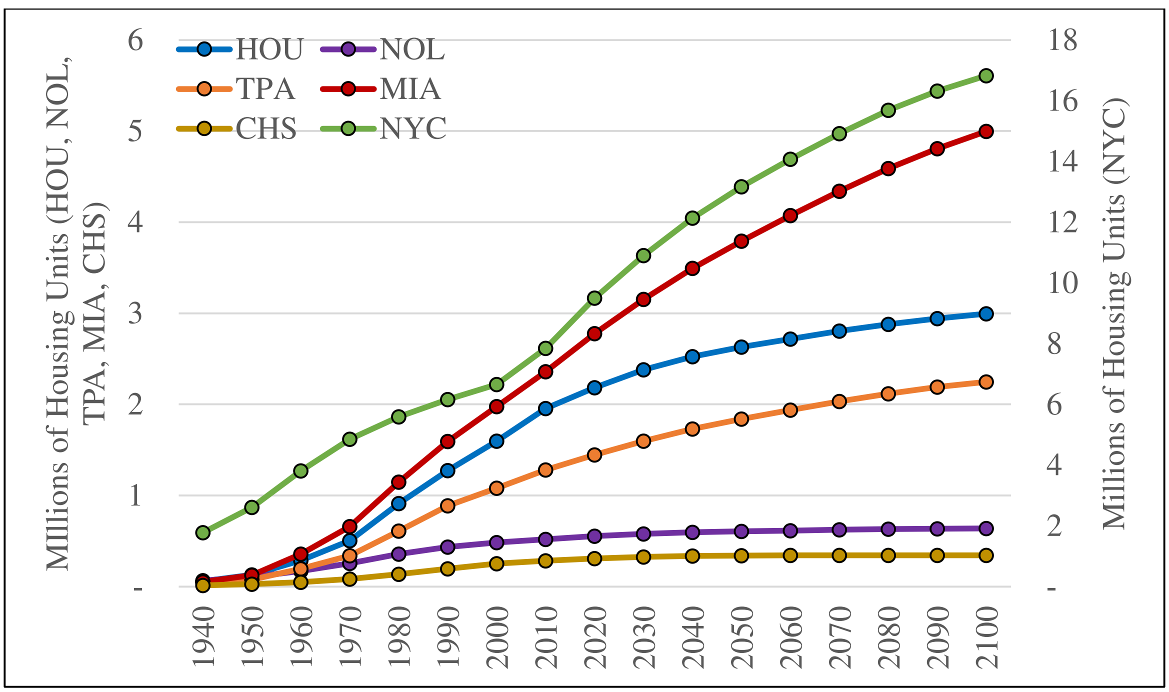

Figure 21. The total number of housing units (HUs) impacted by the All Storm for all MSAs from 1940 to 2100, where 2010 to 2100 is forecast under the A1 projection.

Major Storm Analysis

Similar to the All Storm synthetic, the Major Storm synthetic encompassed each MSA entirely. Tampa and Charleston resided completely within the major swath (Category 3 or greater) and the 32 m s-1 (Category 1) wind swath, similarly to the All Storm synthetic. Unlike the All Storm synthetic, the number of HUs in each MSA is distributed differently within the swaths. For example, all of the MSAs impacted by the All Storm scenarios had about 90% of their HU with the Category 1 wind swath. For the Major Storm synthetic, the percentage of HU within the major swath ranges from about 60% to 95% (Figure 22). Houston, Miami, and Tampa are expected to have a decrease in the percentage of HU within the major swath, primarily because of the HU growth within the Category 1 swath. Simply, areas within the Category 1 swath are growing faster than the area within the major swath. From 2010 to 2100, the number of HUs within the Category 1 swath is projected to increase from about 250,000 HUs to 740,000 HUs, or 189%, under the A1 projection. In the same period, Tampa and Miami are projected to experience roughly the same result, increasing by 180.8% and 196.1%, respectively. For Houston, Miami, and Tampa, the HUs in the major swath are not growing as rapidly, but the number of HUs within the major swath is much greater. By 2100, the number of HUs within the major swath is expected to grow to about 2 million HUs for those three MSAs. If a major hurricane were to landfall atop the CBD of the MSAs (like this study demonstrates), over 2 million HUs will be impacted by winds greater than 50 m s-1.

In the worst-case scenario, approximately 91% of New Orleans HUs will be within the major swath from 2010 to 2100. This illustrates that the HU growth rate across the MSA is relatively uniform; the number of HUs within the major swath and the Category 1 swath are

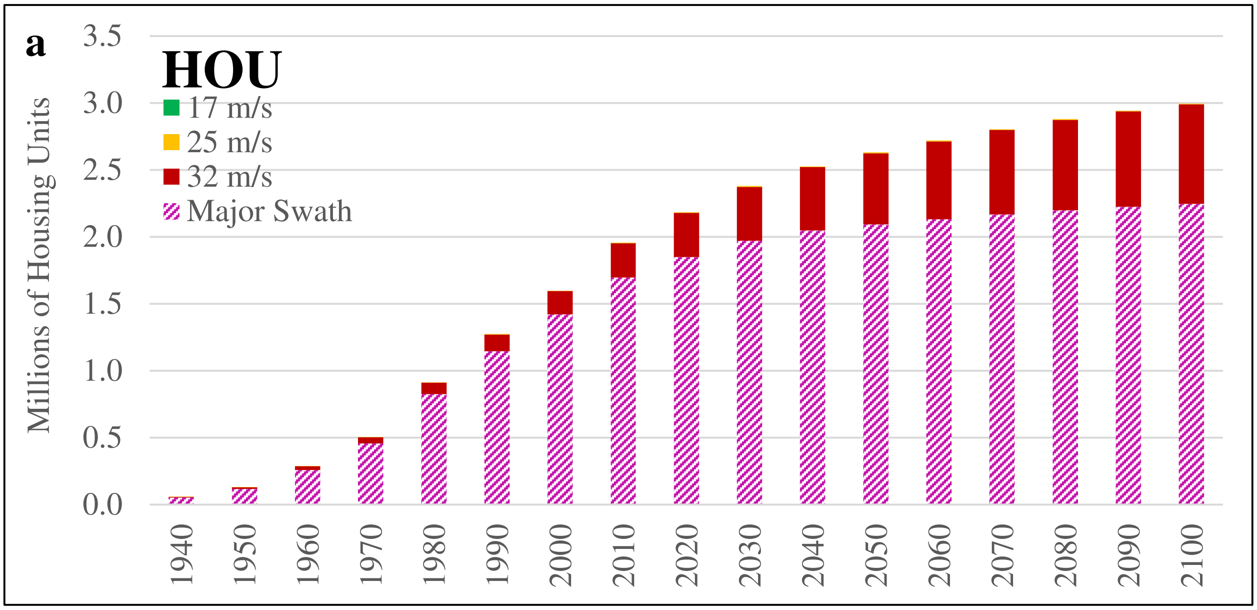

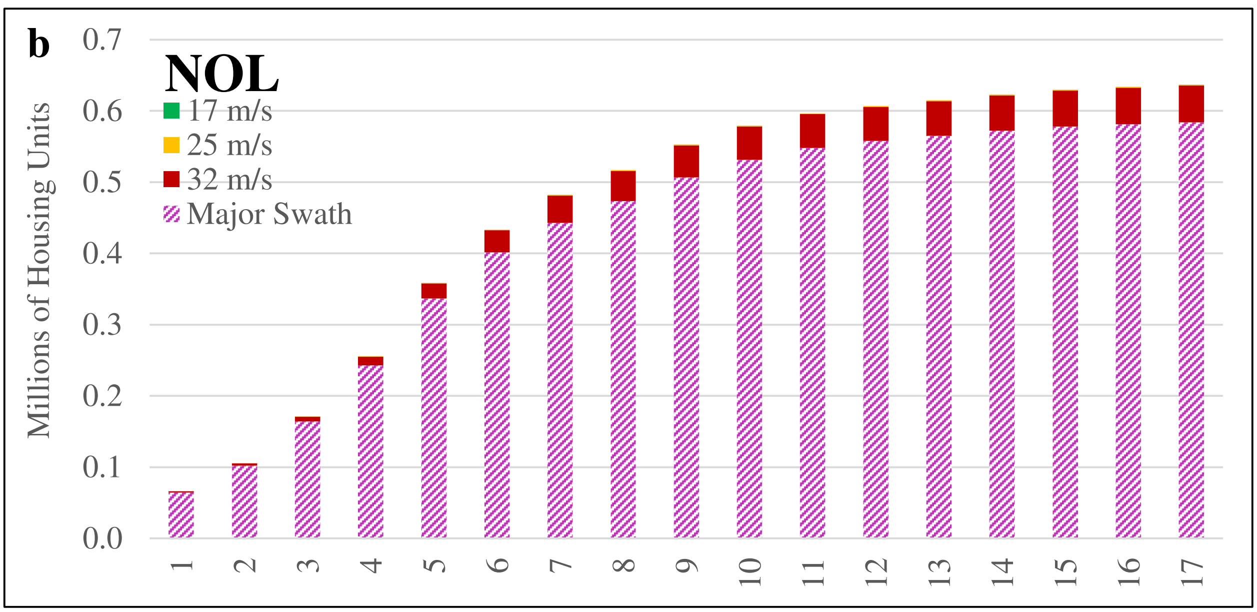

Figure 22. The number of housing units impacted historically from 1940 to 2000 and from 2010 to 2100 under the A1 projection by each wind swath within the Major Storm for a Houston, b New Orleans, c Tampa, d Miami, e Charleston, f New York City.

(continued on following page)

Figure 22 (continued)

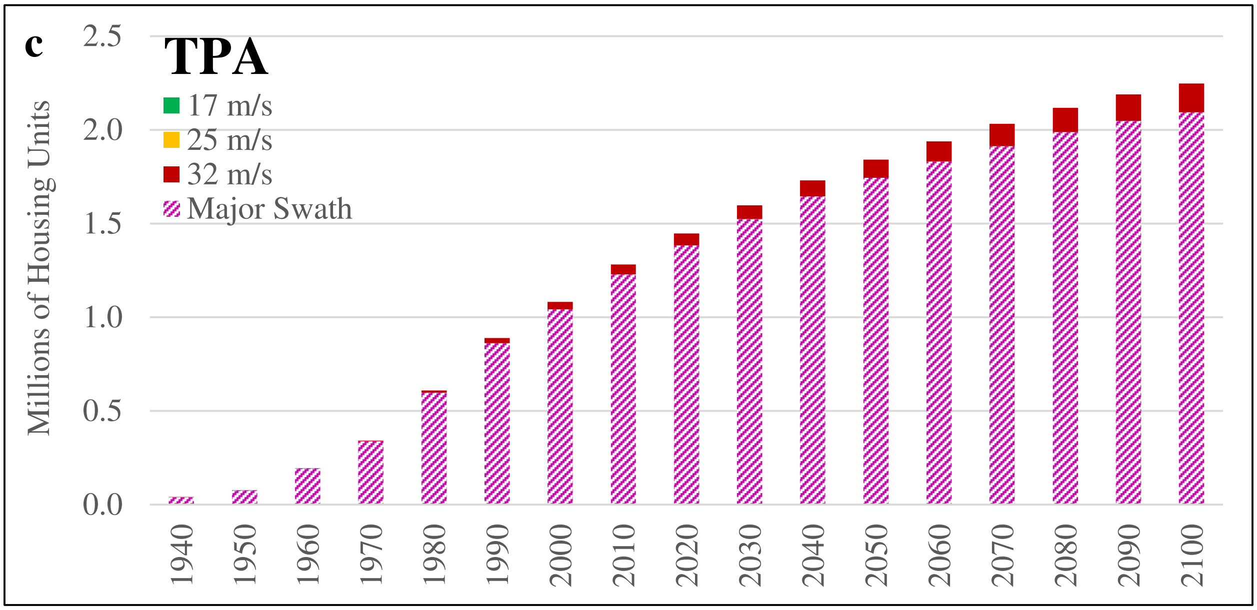

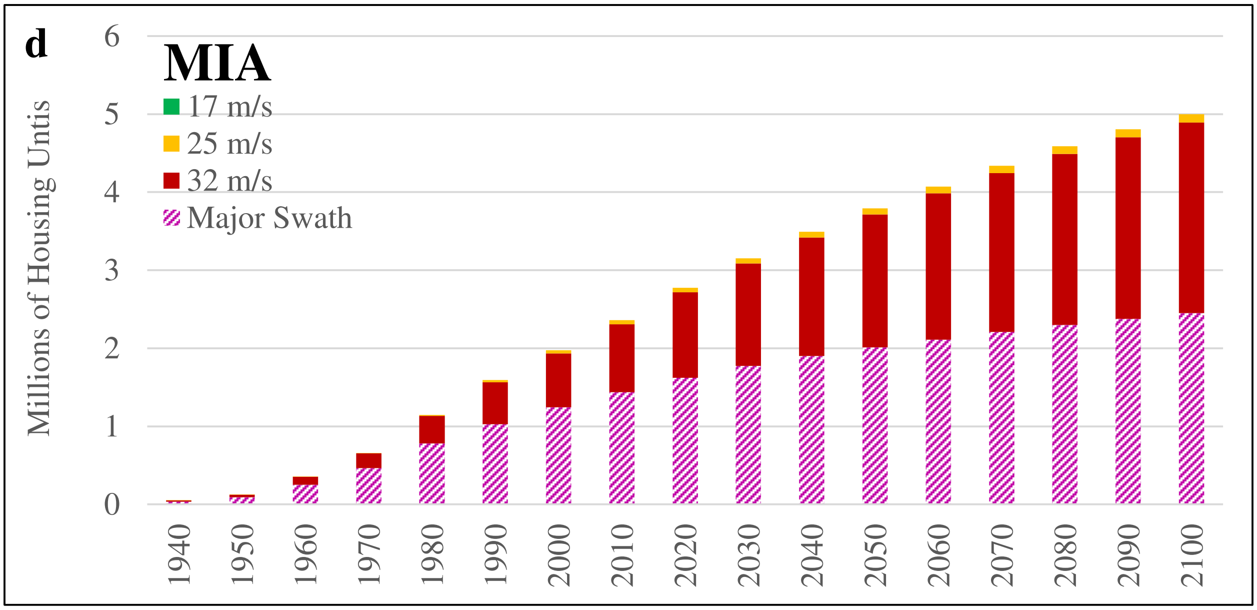

(continued on following page)

Figure 22 (continued)

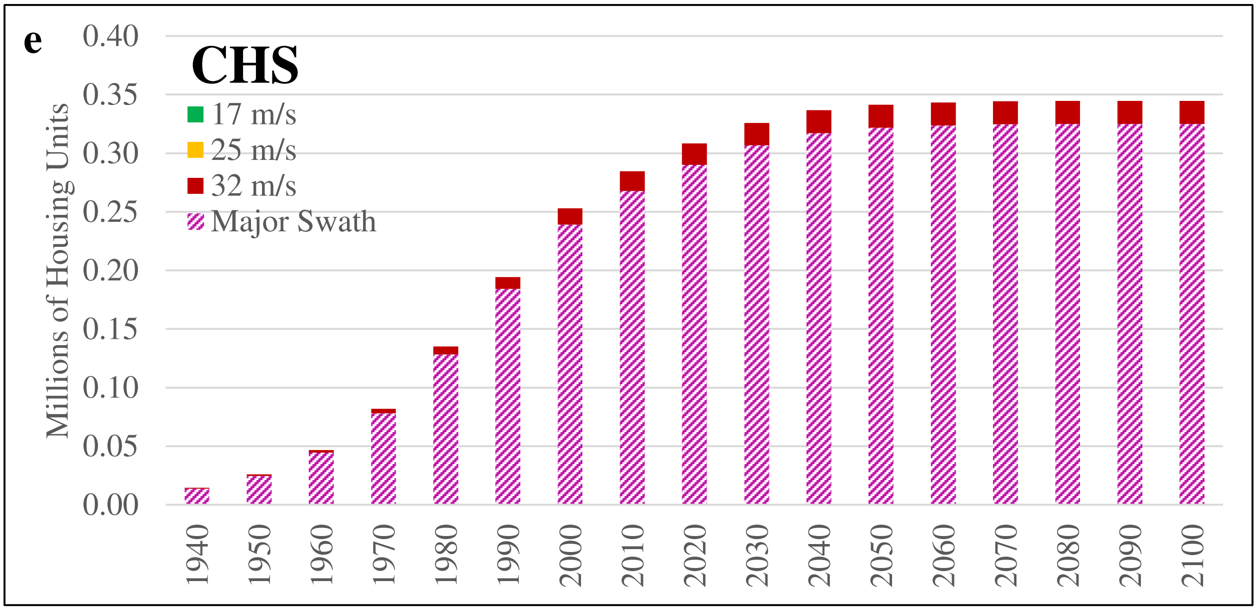

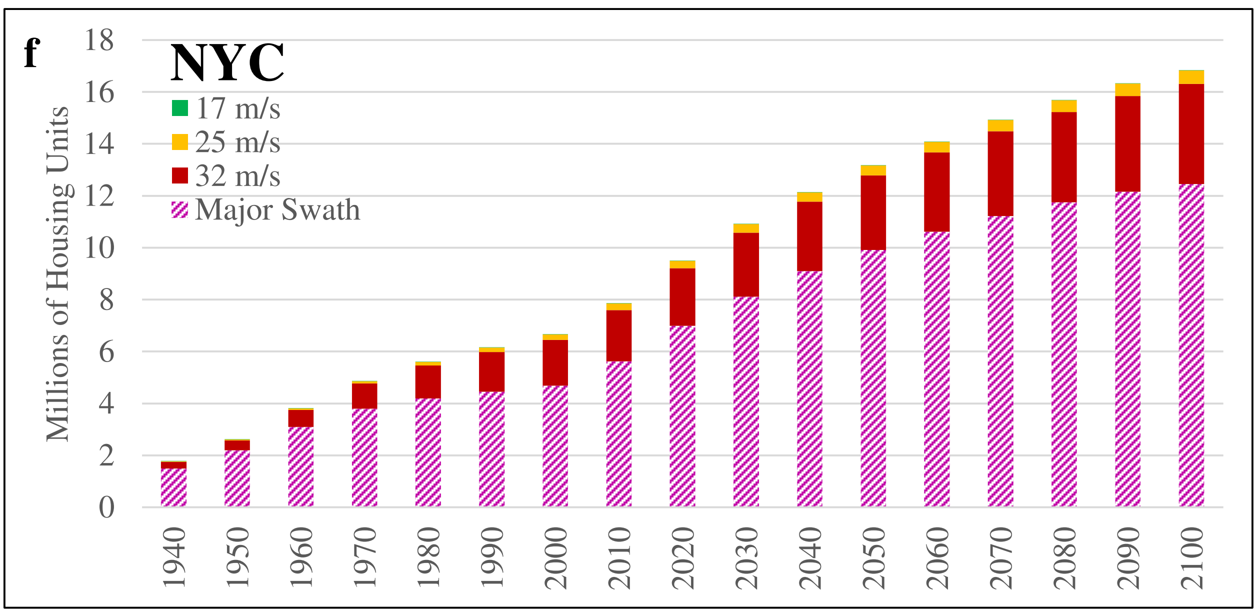

forecast to increase by 21% Charleston's pattern is very similar to New Orleans; about 94% of the HUs within Charleston are located within the major swath from 2010 to 2100. Also, the number of HUs within Charleston is expected to increase by about 21.4% in the major swath and about 15.5% in the Category 1 swath. Once again, the MSA of New York City was the only MSA to reside within all four synthetic swaths; in 2010, about 71.6% of the HUs resided in the major swath, 25% resided in the Category 1 swath, 3.2% resided in the 25 m s-1 swath, and the remaining percentage in the 17 m s-1 swath. The number of HUs within the major swath account for about 75.2% of New York City's HUs by 2100, indicating that the MSA's core is growing more rapidly than the others. Overall, there is growth within each of the swaths; from 2010 to 2100, the number of HUs within the major swath grows from 5.6 million to 12.4 million, or 121.3%. The major swath in New York City is projected to experience a faster rate of growth than the other swaths and contain at least three times more HUs than that of the Category 1 swath. If a major hurricane affects New York City, the damage could be catastrophic, especially since New York City does not experience hurricanes as often as other locations along the coast (Pielke 1997; Mileti 1999; Blake and Gibney 2011; Cangialosi and Berg 2012). The Great New England Hurricane in 1938 made landfall at Long Island, New York as a Category 3 hurricane (Spignesi 2002) and provides a perspective on the possibility of a high-end event occurring in this MSA. There were more than 600 deaths, over 1,700 injuries, and approximately 23,000 structures damaged in this hurricane. The number of buildings impacted was relatively low compared to the potential built environment damage tallies if a similar storm were to occur again today. If a storm similar to the Great New England Hurricane occurred again today, it would be one of the greatest disasters in U.S. history in terms of HU impacts alone (Spignesi 2002).

The Major Storm scenario under the A2 projection—the "worst-case"—produced the largest disaster potential for the MSAs studied from 2010 to 2100(Figure 23). For all MSAs, A2 has the largest increase of the projections for the four swaths that characterize the Major Storm synthetic. For New Orleans and Charleston, the number of HUs impacted by the major swath rises from 2010 to 2100 instead of remaining constant as A1 projects. Also, Houston, Miami, and Tampa exhibit faster growth in the Category 1 swath than the major swath; however, the number of HUs within the major swath is much larger and increases by at least 100% from 2010 to 2100. The Houston, Miami, and Tampa MSA cores are growing rapidly; however, locations around the core are growing much more rapidly, resulting in a sprawl morphology. The number of HUs within the major wind swath is expanding out into the Category 1 wind swath, further illustrating the expanding bull's-eye effect (Ashley et al. 2014; Strader and Ashley 2015). Because all of the MSAs are completely encompassed within the All Storm and Major Storm synthetics, any growth that the MSAs experience in the future would be impacted by both theoretical storms. All MSAs illustrate the amplification of exposure, an important predictor of disaster consequences.

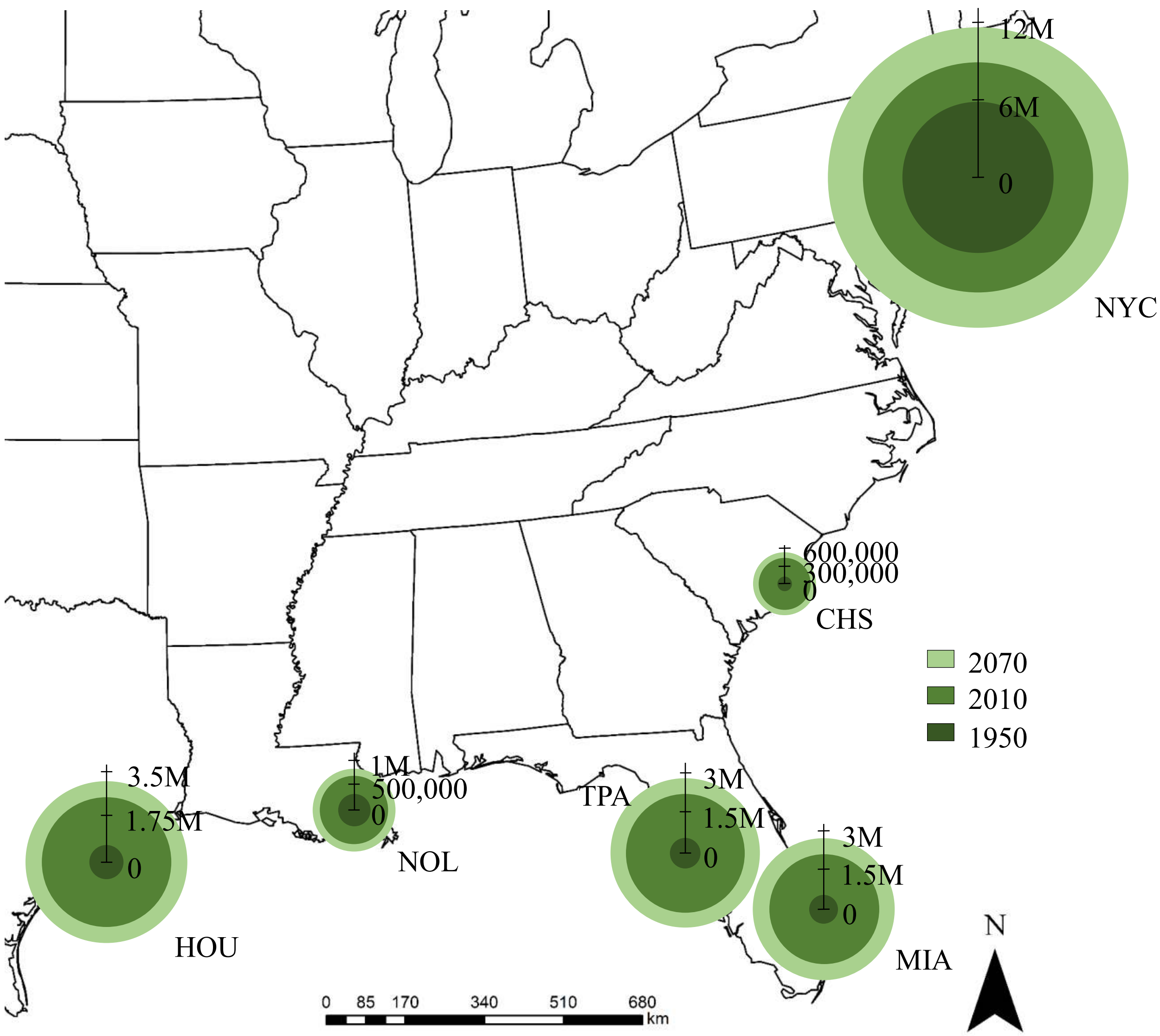

Figure 23. The number of housing units impacted by the major swath for each MSA from 1950 to 2070 under the A2 "worst-case" scenario.

Disaster Potential

Tropical cyclones are natural phenomena that can develop into disasters if they interact with human and physical environmental systems (Mileti 1999; Abramovitz 2001; Reilly 2009). Increasing the number of HUs along and near the coastline places more potential “targets” in the path of a tropical cyclone; however, without a climatological risk of tropical cyclone hazard, there is no disaster potential. Further insight into tropical cyclone disaster potential can be gained by combining climatological risk and coastal exposure into a single metric. In this calculation, disaster potential is a product of the theoretical HU exposure and the tropical cyclone climatological risk of an MSA. The climatological risk is defined by the Tropical Hazard Index (THI; Keim et al. 2007), which is derived from the intensity and frequency of landfalling storms from 1901 to 2005. In this index, a tropical storm strike is awarded two points, a Category 1 to 2 is awarded four points, and a Category 3 or greater is awarded eight points. Though the THI has a relatively limited historical period of record, it does provide a simple geographical index that may be used to denote the risk of the Atlantic and Gulf Coastlines to tropical cyclones. The number of HUs that were within an MSAs developed footprint (exurban, suburban, and urban) are summed and used as the exposure constituent in disaster potential calculation. Each MSAs developed exposure value is multiplied by the MSA’s Tropical Hazard Index to derive the disaster potential metric for the area over time (Figure 24). Naturally, there are a considerable number of caveats in using this disaster metric. For instance, the calculation does not assess the plethora of social, physical, and non-residential, built-environment vulnerabilities that can either magnify or attenuate disaster potential. Additionally, each MSA has distinct physical characteristics (e.g., differences in bathymetry, bay and estuary system, hazard reduction infrastructure, etc.) that could greatly modify the disaster potential. The goal here is to provide a synoptic view to disaster potential, providing a basis for additional future interrogation of other important disaster constituent variables.

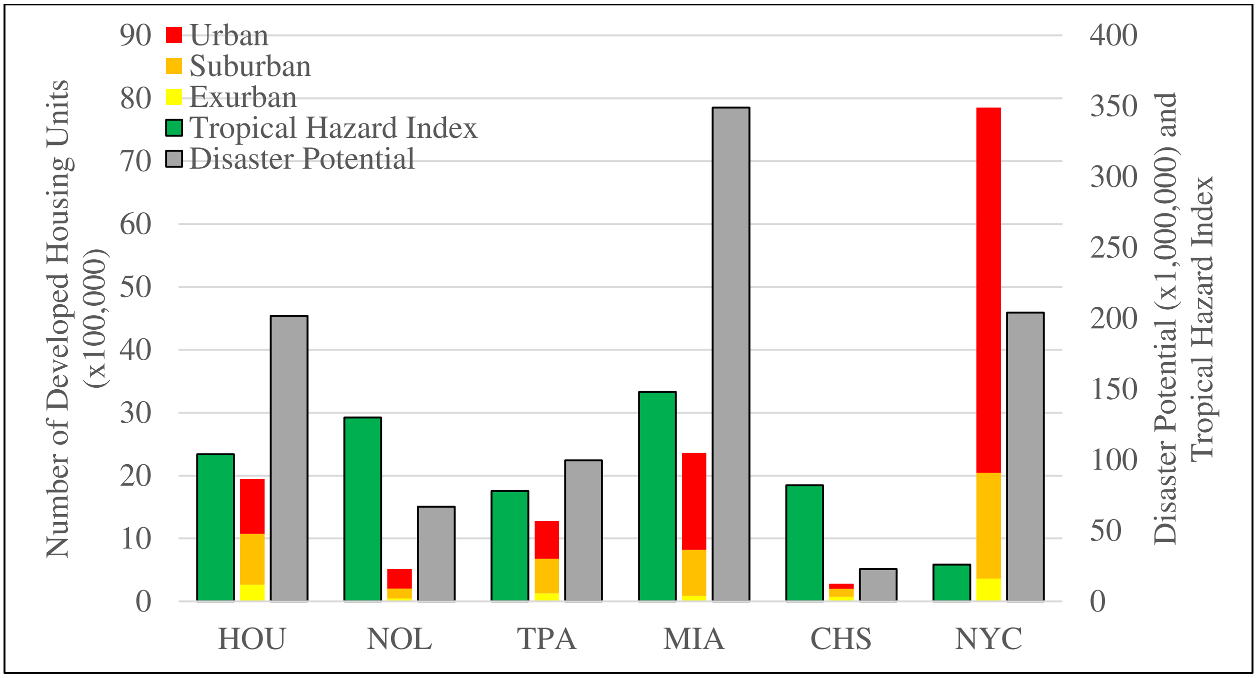

Figure 24. The Tropical Hazard Index (green; Keim et al. 2007), the number of housing units in 2010 by land use (where yellow is exurban, orange is suburban, and red is urban), and a combined disaster potential (gray), which is calculated by multiplying the number of housing units (i.e., residential exposure) by the Tropical Hazards Index (i.e., risk) in each MSA.

In 1940, the New York City MSA had the highest disaster potential because of its high exposure at the time compared to the other MSAs (Figure 25). By 1980, the Miami MSA surpassed New York City and became the MSA with the highest disaster potential, primarily due to Miami's elevated tropical cyclone risk combining with the area's rapid exposure growth.

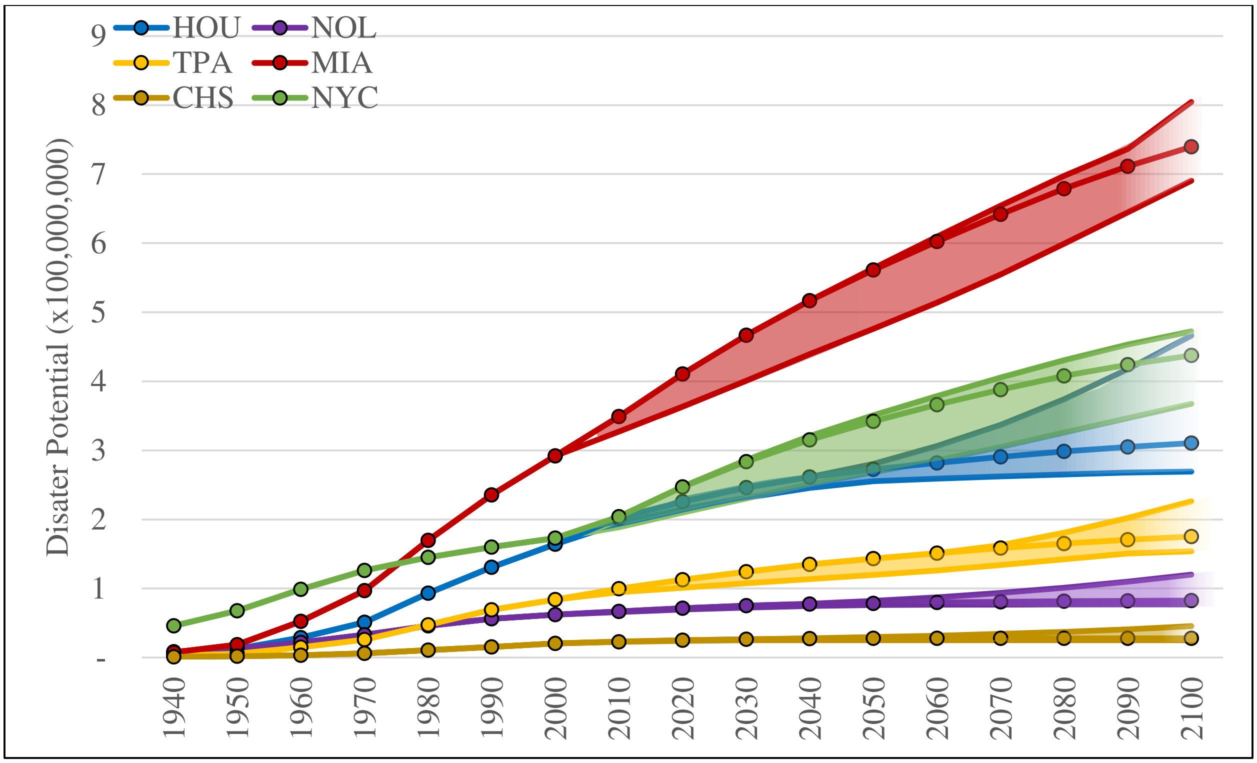

Figure 25. The change in disaster potential from 1940 to 2100, where the upper bound is the highest potential of the projections, the lower bound is the lowest potential of the projections, and the marked line is the A1 projection.

Miami's disaster potential has intensified more rapidly than the other MSAs; it is expected to see a hundredfold increase in disaster potential from 1940 to 2100. New York City has the second greatest disaster potential through 2100 because of the large number of HUs within the developed footprint of the MSA. New York City's tropical cyclone risk was the lowest of the MSAs (Figure 24), indicating that the disaster potential of the MSA is largely driven by exposure. However, as Hurricane Sandy and the Great New England Hurricane illustrate, a low risk does not equate to zero risk. The Houston and Tampa MSAs experience a substantial disaster potential increase, growing by 5,522% and 5,739%, respectively. Compared to the other MSAs, New York City had the smallest change and is forecast to experience an 853% growth in disaster potential from 1940 to 2100. The Charleston MSA has a higher climatological tropical cyclone risk than the New York City MSA and Tampa MSA, but has the fewest number of developed HUs. Because of the relatively low exposure, the disaster potential is smaller than the other MSAs. Overall, there is a statistically significant ($t=2.68$; $p=0.04$) increase in the disaster potential from 1940 to 2100 for all MSAs. Thus, all MSAs are forecast to experience an increase in disaster potential over time, and that potential is largely driven by the exposure of residential development (Figure 25). The analysis provides evidence that the disaster potential will continue to increase into the future and that the next landfalling hurricane may be far more disastrous than the U.S. has experienced to date.

Research Constraints

As with any research, there are constraints to the data and methodologies employed. For instance, in this study, there are a number of caveats associated with extracting data from

HURDAT2. First, the wind radii data "best-tracked" is only available beginning in 2004, which provided a limited sample to investigate—18 landfalling storm, of which 7 were considered major. The number of landfalling hurricanes from 2004 to 2014 provided sufficient data to construct a synthetic hurricane, but may not be fully representative of landfalling hurricane potential. Additionally, compared to alternative wind swath data from, for example, H*Wind and QuikScat, HURDAT2 underestimates the operational wind radii, which, in turn, underestimates the wind radii used for the hurricane synthetics (Moyer et al. 2007). Further, "best-track" radii are based on a "survey" approach, and these data do not include other observational datasets, such as Doppler radar (Landsea and Franklin 2013). Overall, the database is incomplete and limited, but efforts are being made to re-analyze and expand the dataset (Landsea and Franklin 2013).

The five ICLUS scenarios provide snapshots of potential residential and land use growth in the 21st century; however, these deterministic scenarios are not the only possible futures in a large spectrum of societal and environmental possibilities. It is likely that residential growth will deviate from the predicted ICLUS scenarios. There are model inputs and assumptions that can modify the overall projection of each scenario. For instance, the model assumes that growth rates and patterns will be similar to those of recent years (1990s to 2000; U.S. EPA 2009). The model begins with an initial population at year t and develops a new population based on demographic transition for year t+1. It is important to recognize that ICLUS data are employed to estimate the potential impact of hurricanes if HU trends continue to grow, and not provide a single deterministic solution or expectation. Rather than employing the residential built environment impacts calculated in this study as absolutes, the data should be used to explore evolution in land use and the relative importance of exposure change to the disaster landscape.

This study examined solely residential exposure theoretically impacted by a landfalling hurricane. There are a number of vulnerability factors beyond residential exposure that can amplify or attenuate disaster consequences. For instance, future research should assess additional socioeconomic vulnerabilities of MSAs, including variables such as age, race, poverty, etc. Though many of these variables are now collected by the Census Bureau, the enumerations often change from one census to the next, making spatiotemporal comparisons—which was a hallmark of this thesis—difficult. Research has revealed that communities with high proportions of, for instance, minorities and elderly are particularly vulnerable to disaster impacts (Cutter et al. 2003; Cutter et al. 2007; Flanagan et al. 2011). Race and ethnicity poses potential language and cultural barriers that can affect how a person copes with disaster (Cutter et al. 2003). The elderly tend to have more mobility constraints that can affect abilities to react to an impending disaster. Other particularly vulnerable populations include those of low income status, women and children, and those of high social dependence (Cutter et al. 2003).

Understanding how vulnerable segments of the population have changed, and will possibly change in the future, will provide a better estimate potential tropical cyclone disaster impacts. Additionally, identifying the type of residential unit, as well as its age, alters the fundamental exposure and vulnerability constituent investigated in this study. For example, mobile homes are far more vulnerable than timber frame build homes because they cannot withstand high winds, whether hurricane, thunderstorm, or non-thunderstorm induced (Cutter et al. 2003; Donner 2007). Also, assessing how building codes are implemented and enforced at the local level would promote a greater understanding of the true vulnerability of the built-environment (Simmons and Sutter 2008). If building codes are not applied or enforced, a residential unit is more likely to be constructed inadequately and, therefore, more probable to sustain structure failure affiliated with hurricanes and other wind hazards (Burby 2006; Tansel and Sizirici 2011). Destruction to other critical infrastructure—such as bridges, hospitals, or power plants—can influence a disaster as well and should be considered in future disaster potential assessment. The research assumes that the built-environment is uniform for each MSA, when in reality, this is not the case. Ultimately, this research provided a broad understanding of both historical and future exposure changes for the residential built environment at threat to a hurricane disaster. A more sophisticated, and arguably more complex, research model incorporating additional variables—storm attributes such as rainfall rate and surge measurements; a full census of the built-environment and integrity of that environment; important socioeconomic and demographic factors; etc.—would promote a more robust disaster potential assessment.

CHAPTER 5

DISCUSSION AND CONCLUSION

This study provided an assessment of historical and future exposure to tropical cyclones in the U.S. and evidence that the change in the residential built-environment continues to alter the disaster landscape. At the regional level, residential density within 50 km of the coastline was greater than the rest of the CONUS, and this highly vulnerable region is expected to continue to experience substantial future exposure growth. Spatiotemporal trends of residential exposure in six at-risk MSAs along the Atlantic and Gulf Coasts were also assessed, revealing how disaster potential has evolved in these areas over a 160-year period. Results revealed immense growth in housing and land use—both historically and in future projections through 2100—within all MSAs studied. Each MSA has unique growth rates and patterns, but all MSAs experienced statistically significant growth in housing exposure from 1940 to 2010. The number of HUs in New York City increased the most of the MSAs, but Miami had the greatest change in HUs during the period. The sustained residential growth uncovered is expected to further expose coastal regions to tropical cyclones and their affiliated hazards.

The increasing tropical cyclone disaster potential varies across time and space; generally, MSAs in the lower latitudes are at a greater risk of tropical cyclone hazards than areas more poleward (Brettschneider 2008; Keim et al. 2007; Blake and Gibney 2011; Czajkowski et al. 2011; Cangialosi and Berg 2012). The frequent occurrence of hurricane landfalls and the rapid growth of the MSA increases the risk of disaster now and in the future. Due to the juxtaposition of exposure, its growth, and the highest landfall risk of any MSA along the Atlantic and Gulf Coasts (Kiem et al. 2007), Miami currently has the highest disaster potential of the MSAs investigated and is forecast to have the highest disaster potential in the future. Aside from the climatological risk factor, hurricanes can landfall anywhere along the Atlantic and Gulf Coasts. The possibility of more intense hurricanes in a warming world (Knutson et al. 2010; Nordhaus 2010; IPCC 2012; Wong et al. 2014; NAS 2016; Walsh et al. 2016), in conjunction with rapidly increasing exposure along the coastline, will create higher magnitude tropical cyclone disasters than the U.S. has ever experienced (Pielke 1997; Mileti 1999).

While wind swaths were the tropical storm hazard used to explore impact potential, other tropical cyclone hazards such as storm surge and flooding will exacerbate any event. In addition, studies reveal that sea-level rise is an impending issue that will have potentially disastrous consequences in the future (Pielke et al. 2008, Maloney and Preston 2014; Hay et al. 2015; Carson et al. 2016; Hauer et al. 2016). The already substantial storm surge hazard associated with landfalling hurricanes will amplify as the elevated sea level will combine with storm-induced surges to create greater coastal flooding and catastrophic wave action in the future. With the global mean sea level projected to rise more than 1.5 meters by 2100 (DeConto and Pollard 2016), storm surge amplification due to sea level rise will induce a greater threat to all coastal locations, including those that were once thought to be safe from surge impacts (Rowley et al. 2007; Hauer et al. 2016). Low-lying areas, which characterize all of the MSAs investigated in this study, are becoming more exposed to tropical inundation as sea level rises, which is increasing the likelihood of disaster when a tropical cyclone event occurs.

As the built-environment footprint continues to swell in areas exposed to possible tropical storm hazards, the threat of U.S. hurricane disaster increases. If, for example, the U.S. coast lacked people and their assets, a landfalling hurricane would not pose a significant threat to local, regional, and national socioeconomic systems. In general, the coast has experienced an influx of people because of the area's idyllic features; there may be a gained mindset that the benefits outweigh the cost. This optimism bias is where people believe their personal risk is less than the risk faced by others (Weinstein et al. 2000). Additionally, people typically only plan for the immediate future, overestimate their capability of recovering from a disaster, and heavily rely on emergency relief (Mileti 1999). The government subsidizes disaster relief, flood insurance, and coastal infrastructure improvements through tax dollars, providing a "back up plan" for those living in risk-prone areas (Steinburg 2000; Sutter 2007). Could this be a contributor to the lack of perceived disaster threat?

Minimizing loss of life and costs is a general goal of U.S. hurricane policy (Pielke 1997), but it is important to consider actions that reduce vulnerability, and therefore, reduce disaster potential. There have been proposals to reduce U.S. vulnerability, including: changes in land use (Cutter 2007); adjustments in federal disaster assistance and mitigation policies; improvements to hurricane forecasting; and new evacuation strategies (Pielke 1997). On average, every $1 used for mitigation strategies can prevent $7 in disaster recovery costs (Abramovitz 2001). Retrofitting structures is an effective mitigation method that allows buildings to be reinforced and become more hazard-resistant (Smith 2013). Many residents along the coast may experience normalcy bias, where they do not realize the true disaster risk because they have never experienced a hurricane disaster, and they believe it will never occur. Communicating effectively tropical cyclone disaster risk to residents in these areas will promote a more informed, risk-averse populace that may be more motivated to employ hazard mitigation and adaptation strategies. By understanding the effects of hazards and working together, society can reduce the consequences of future disasters Abramovitz 2001).

In conclusion, the Atlantic and Gulf Coasts, as well as all MSAs investigated, have experienced significant increases in exposure to tropical cyclones and will continue to become more exposed in the future. The inflation of this major disaster constituent suggests that the potential for catastrophic tropical cyclone events in the future. Results from the study may be used to inform policy makers, catastrophe modelers, emergency management, and the public on how increasing residential growth can lead to a catastrophe, especially if effective mitigation strategies are not implemented.

REFERENCES

Abramovitz JN (2001) Unnatural Disasters. Worldwatch Institute 1-62

Adger WN, Huq S, Brown K, Conway D, and Hulme M (2003) Adaptation to climate change in the developing world. Progress in Development Studies **3**(3):179-195

Ashley WS, Strader S, Rosencrants T, Krmenec A (2014) Spatiotemporal Changes in Tornado Hazard Exposure: The Case of the Expanding Bull's Eye Effect in Chicago, IL. Weather Climate Society 6:175–193. doi: 10.1175/WCAS-D-13-00047.1

Ashley W, Strader S (2015) Recipe for Disaster: How the Dynamic Ingredients of Risk and Exposure are changing the Tornado Disaster Landscape. B Am Meteorol Soc In Press. doi: 10.1175/BAMS-D-15-00150.1

Bender MA, Knutson TR, Tuleya RE, Sirutis JJ, Vecchi GA, Garner ST, Held IM (2010) Modeled Impact of Anthropogenic Warming on the Frequency of Intense Atlantic Hurricanes. Science 327:454-458

Bierwagen BG, Theobald DM, Pyke CR, Choate A, Groth P, Thomas JV, Morefield P (2010) National Housing and Impervious Surface Scenarios for Integrated Climate Impact Assessments. P Natl Acad Sci USA 107(49):20887-20892. doi: 10.1073/pnas.1002096107

Blake ES, Gibney EJ (2011) The Deadliest, Costliest, and Most Intense United States Tropical Cyclones from 1851 to 2010 (and other frequently requested hurricane facts). NOAA/National Weather Service, National Centers for Environmental Prediction, National Hurricane Center 1-47

Blake ES, Kimberlain TB, Berg RJ, Cangialosi JP, Beven II JL (2013) Tropical Cyclone Report, Hurricane Sandy (AL182012), 22-29 October 2012. National Hurricane Center. United States National Oceanic and Atmospheric Administration's National Weather Service

Borden KA, Schmidtlein M, Emrich C, Piegorsch WW, Cutter SL (2007) Vulnerability of U.S. Cities to environmental Hazards. J Homel Secur Emerg 4(2): 1-21

Bouwer LM (2011) Have Disaster Losses Increased Due to Anthropogenic Climate Change? B Am Meteorol Soc 92:39-46

Bouwer LM (2013) Projections of Future Extreme Weather Losses under Changes in Climate and Exposure. Risk Anal 33(5):915-930

Brettschneider B (2008) Climatological Hurricane Landfall Probability for the United States. J Appl Meteorol Clim 47:704-716

Burby R J (2006) Hurricane Katrina and the Paradoxes of Government Disaster Policy: Bringing about Wise Governmental Decisions for Hazardous Areas. Annals 604(1):171-191

Burton CG (2010) Social Vulnerability and Hurricane Impact Modeling. Natural Hazards Review 11:58-68

Cangialosi J, Berg R, (2012) Hurricane Life Cycle and Hazards. National Hurricane Conference 26 March 2012

Carson M, Köhl A, Stammer D, Slangen ABA, Katsman CA, van de Wal RSW, Church J, White N (2016) Coastal Seal Level Changes, Observed and Projected During the 20th and 21st Century. Climatic Change 134(1-2):269-281

Casson E, Coles S (2000) Simulation and Extremal Analysis of Hurricane Events. J Roy Stat Soc C-App 49(3):227-245

Changnon SA, Pielke RA, Changnon D, Sylves RT, Pulwarty R (2000) Human Factors Explain the Increased Losses from Weather and Climate Extremes. B Am Meteorol Soc 81(3):437-442

Changnon SA (2008) Temporal and Spatial Distributions of Damaging Hail in the Continental United States. Phys Geogr 29(4):341-350

Christensen JH, Krishna Kumar K, Aldrian E, An SI, Cavalcanti IFA, de Castro M, Dong W, Goswami P, Hall A, Kanyanga JK, Kitoh A, Kossin J, Lau NC, Renwick J, Stephenson DB, Xie SP, Zhou T (2013) Climate Phenomena and their Relevance for Future Regional Climate Change. In: Climate Change 2013: The Physical Science Basis. Contribution of Working Group I to the Fifth Assessment Report of the Intergovernmental Panel on Climate Change [Stocker TF, Qin D, Plattner GK, Tignor M, Allen SK, Boschung J, Nauels A, Xia Y, Bex V, Midgley PM (eds.)]. Cambridge University Press, Cambridge, United Kingdom and New York, NY, USA

Clarke L (2005) Worst-Case Thinking: An Idea Whose Time Has Come. Natural Hazards Observer 29(3): 1-3

Coale A, Trussell J (1996) The Development and Use of Demographic Models. Pop Stud-J Demog 50(3):469-484

Crossett KM, Culliton TJ, Wiley PC, Goodspeed TR (2004) Population Trends Along the Coastal United States: 1980-2008. NOAA's National Ocean Service 1-47

Cutter SL, Boruff BJ, Shirley WL (2003) Social Vulnerability to Environmental Hazards. Soc Sci Quart 84(2):242-261

Cutter SL, Emrich CT, Webb JJ, Morath D (2009) Social Vulnerability to Climate Variability Hazards: A Review of the Literature. Final Report to Oxfam America 1-44

Cutter SL, Johnson L, Finch C, Berry M (2007) The U.S. Hurricane Coasts: Increasingly Vulnerable? Environment: Science and Policy for Sustainable Development 49(7):8-21

Cutter SL, Emrich C (2005) Are Natural Hazards and Disaster Losses in the U.S. Increasing? Eos, Transactions American Geophysical Union 86(41):381-389

Cutter SL (1996) Vulnerability to Environmental Hazards. Prog Hum Geog 20:529-539

Czajkowski J, Simmons K, Sutter D (2011) An Analysis of Coastal and Inland Fatalities in Landfalling U.S. Hurricanes. Nat Hazards 59:1513-1531

DeConto RM, Pollard D (2016) Contribution of Antarctica to Past and Future Sea-Level Rise. Nature 531:592-597. doi: 10.1038/nature17145

Donner WR (2007) The Political Ecology of Disaster: An Analysis of Factors Influencing U.S. Tornado Fatalities and Injuries 1998-2000. Demography 44(3):669-685

Demuth J, DeMaria M, Knaff JA (2006) Improvement of advanced microwave sounder unit tropical cyclone intensity and size estimation algorithms. J Appl Meteorol 45:1573-1581

Emanuel K (2006) Climate and Tropical Cyclone Activity: A New Model Downscaling Approach. J Climate 19:4797-4802

Emanuel K, Ravela S, Vivant E, Risi C (2006) A Statistical Deterministic Approach to Hurricane Risk Assessment. B Am Meteorol Soc 87(3):299-314

Flanagan BE, Gregory EW, Hallisey EJ, Heitgerd JL, Lewis B (2011) A Social Vulnerabilty Index for Disaster Management. Journal of Homeland Security and Emergency Management 8(1):1-22

Foner N (2001) New Immigrants in New York. Columbia University Press. 1-321

Frey WH, Singer A (2006) Katrina and Rita Impacts on Gulf Coast Populations: First Census Findings. Washington: Brookings Institution, Metropolitan Policy Program

Georgiou PN (1986) Design Windspeeds in Tropical Cyclone-Prone Regions. Dissertation, University of Western Ontario

Hall P, Takenaka H, Bender R, Sassen S, Ichikawa H (2009) Global Power City Index 2009. Mori Memorial Foundation 1-38

Hall SG, Ashley WS (2008) Effects of Urban Sprawl on the Vulnerability to a Significant Tornado Impact in Northeastern Illinois. Natural Hazards Review 9(4):209-219

Hall TM, Jewson S (2007) Statistical Modelling of North Atlantic Tropical Cyclone Tracks. Tellus A **59**(4):486-498

Hallegatte S (2007) The Use of Synthetic Hurricane Tracks in Risk Analysis and Climate Change Damage Assessment. J Appl Meteorol Clim 46:1956-1966

Hauer ME, Evans JM, Mishra DR (2016) Millions Projected to be at Risk from Sea-Level Rise in the Continental United States. Nature Climate Change Accepted

Hay CC, Morrow E, Kopp RE, Mitrovica JX (2015) Probabilistic Reanalysis of Twentieth-Century Sea-Level Rise. Nature 517:481-484

Intergovernmental Panel on Climate Change (IPCC) (2012) Summary for Policymakers. In: Managing the Risks of Extreme Events and Disasters to Advance Climate Change Adaptation [Field CB, Barros V, Stocker TF, Qin D, Dokken DJ, Ebi KL, Mastrandrea MD, Mach KJ, Plattner GK, Allen SK, Tignor M, Midgley PM (eds.)]. A Special Report of Working Groups I and II of the Intergovernmental Panel on Climate Change. Cambridge University Press 3-21.

Keim BD, Muller RA, Stone GW (2007) Spatiotemporal Patterns and Return Periods of Tropical Storm and Hurricane Strikes from Texas to Maine. J Climate 20:3498-3509

Knutson TR, McBride JL, Chan J, Emanuel K, Holland G, Landsea C, Held I, Kossin JP, Srivastava AK, Sugi M (2010) Tropical Cyclones and Climate Change. Nat Geosci 3:157-163

Landsea CW, Franklin JL (2013) Atlantic Hurricane Database Uncertainty and Presentation of a New Database Format. Mon Weather Rev 141:3576-3592

Maloney MC, Preston BL (2014) A Geospatial Dataset for U.S. Hurricane Storm Surge and Sea-level Rise Vulnerability: Development and Case Study Applications. Climate Risk Management 2:26-41

Mendelsohn R, Emanuel K, Chonabayashi S, Bakkensen L (2012) The Impact of Climate Change on Global Tropical Cyclone Damage. Nature Climate Change 2(3):205-209

Mileti DS (1999) Disasters by Design: A Reassessment of Natural Hazards in the United States. Joseph Henry Press 1-4.

Miller S, Muir-Wood R, Boissonnade A (2008) An Exploration of Trends in Normalized Weather-Related Catastrophe Losses. Climate Extremes and Society, Cambridge University Press 225-247

Morss RE, Wilhelmi OV, Meehl GA (2011) Improving Societal Outcomes of Extreme Weather in a Changing Climate: An Integrated Perspective. Annu Rev Env Resour 36(1):1-52

Moyer AC, Evans JL, Powell M (2007) Comparison of Observed Gale Radius Statistics. Meteorol Atmos Phys 97(1-4):41-55. doi:10.1007/s00703-006-0243-2

Nakamura J, Lall U, Kushnir Y, Rajagopalan B (2015) HITS: Hurricane Intensity and Track Simulator with N. Atlantic Ocean Applications for Risk Assessment. J Appl Meteorol Clim 54(7):1620-1636. doi:10.1175/JAMC-D-14-0141.1.

National Academies of Sciences, Engineering, and Medicine (NAS) (2016) Attribution of Extreme Weather Events in the Context of Climate Change. The National Academies Press. doi: 10.17226/21852

National Ocean Service (2014) What percentage of the American population lives near the coast? http://oceanservice.noaa.gov/facts/population.html. Accessed 28 January 2016

Nelson AC, Lang RE (2007a) The Next 100 million. Planning 73(1):4-6

Nelson AC, Lang RE (2007b) The Rise of the Megapolitans. Planning 73(1):7-12

Nicholls RJ, Small C (2002) Improved Estimates of Coastal Population and Exposure to Hazards Released. Eos, Transactions American Geophysical Union, 83(28):301-305

Nordhaus WD (2010) The Economics of Hurricanes and Implications of Global Warming. Climate Change Economics 1(1):1-20

Noy I (2016) Tropical Storms: The Socio-economics of Cyclones. Nature Climate Change 6:343-345. doi:10.1038/nclimate2975

Office of Management and Budget (OMB) (2013) Revised Delineations of Metropolitan Statistical Areas, Micropolitan Statistical Areas, and Combined Statistical Areas, and Guidance on Uses of the Delineations of These Areas. OMB Bulletin NO. 13-01. https://www.whitehouse.gov/sites/default/files/omb/bulletins/2013/b-13-01.pdf. Accessed 15 February 2016

Rasch RJ, Blake ES, Cobb III HD, Roberts DP (2006) Tropical Cyclone Report, Hurricane Wilma (AL252005), 15-25 October 2005. National Hurricane Center, United States National Oceanic and Atmospheric Administration's National Weather Service.

Paulikas M, Ashley W (2011) Thunderstorm Hazard Vulnerability for the Atlanta, Georgia Metropolitan Region. Nat Hazards 58:1077-1092

Pielke Jr. RA (1997) Refraining the U.S. Hurricane Problem. Society and Natural Resources: An International Journal 10(5): 485-499

Pielke Jr. RA (2007) Future Economic Damage from Tropical Cyclones: Sensitivities to Societal and Climate Changes. Philos T Roy Soc A 365:2717-2729

Pielke Jr. RA, Landsea C, Mayfield M, Laver J, Pasch R (2005) Hurricanes and Global Warming. B Am Meteorol Soc 86(11):1571-1575

Pielke Jr. RA, Gratz J, Landsea CW, Collins D, Saunders MA, Musulin R (2008) Normalized Hurricane Damage in the United States: 1900-2005. Natural Hazards Review 9:29-42

Reilly B (2009) Disasters in Human History: Case Studies in Nature, Science, and Catastrophe. McFarland and Company Inc. Publishers 159-172

Rowley RJ, Kostelnick JC, Braaten D, Li X, Meisel J (2007) Risk of Rising Sea Level to Population and Land Area. EOS, Transactions American Geophysical Union 8(9):105-116

Rumpf J, Weindl H, Höppe P, Rauch E, Schmidt V (2007) Stochastic Modelling of Tropical Cyclone Tracks. Math Method Oper Res 66(3):475–490

Rumpf J, Weindl H, Höppe P, Rauch E, Schmidt V (2009) Tropical Cyclone Hazard Assessment Using Model-based Track Simulation. Nat Hazards 48:383-398

Satterthwaite D (2007) Adapting to Climate Change in Urban Areas: The Possibilities and Constraints in Low- and Middle-Income Nations. IIED

Shepherd JM, Knutson T (2007) The Current Debate on the Linkage between Global Warming and Hurricanes. Geography Compass 1(1):1-24

Simmons KM, Sutter D (2008) Manufactured Home Building Regulations and the February 2, 2007 Florida Tornadoes. Nat Hazards 46:415-425

Smith K (2013) Environmental Hazards: Assessing Risk and Reducing Disaster. Routledge

Spignesi SJ (2002) The 100 Greatest Disasters of All Time. Citadel Press 194-196

Steinburg T (2000) Acts of God: The Unnatural History of Natural Disaster in America. Oxford University Press

Strader S, Ashley WS, Irizarry A, Hall S (2014) A Climatology of Tornado Intensity Assessments. Meteorol Appl 22(3):513-524. doi: 10.1002/met.1482

Strader SM, Ashley WS (2015) The Expanding Bull's-Eye Effect. Weatherwise 68:23-29

Sutter D (2007) Ensuring Disaster: State Insurance Regulation, Coastal Development, and Hurricanes. Mercatus Policy Comment No. 14 http://ssrn.com/abstract=1350550 Accessed 14 April 2016

Sutter D (2009) Hurricane Damage and Global Warming. Issue Analysis, Competitive Enterprise Institute 4:1-20

Tansel B, Sizirici B (2011) Significance of Historical Hurricane Activity on Structural Damage Profile and Posthurricane Population Fluctuation in South Florida Urban Areas. Natural Hazards Review 12(4):196-201

Theobald DM (2005) Landscape Patterns of Exurban Growth in the USA from 1980 to 2020. Ecol Soc 10(1):1-34

State of the Coast (2013) National Coastal Population Report: Population Trends from 1970 to 2020. National Ocean Service, National Oceanic and Atmospheric Administration, developed in partnership with the U.S. Census Bureau. http://stateofthecoast.noaa.gov/features/coastal-population-report.pdf Accessed 6 May 2015

United States Census Bureau (2010a) http://www.census.gov/popclock/ Accessed 26 January 2016

United States Census Bureau (2010b) http://quickfacts.census.gov/qfd/index.html Accessed 27 January 2016

United States Census Bureau (2014) 2010-2014 American Community Survey 5-Year Estimates. http://factfinder.census.gov Accessed 31 March 2016

United States Environmental Protection Agency (U.S. EPA) (2010) ICLUS Tools and Datasets (Version 1.3.2). U.S. Environmental Protection Agency, Washington D.C. EPA/600/R-09/143F

United States Environmental Protection Agency (U.S. EPA) (2009) Land-Use Scenarios, National-Scale Housing-Density Scenarios Consistent with Climate Change Storylines (Final Report). EPA/600/R-08/076F

Vickery PJ, Skerlj PF, Twisdale Jr. LA (2000) Simulation of Hurricane Risk in the US Using an Empirical Track Model. J Struct Eng-ASCE 126(10):1222–1237

Vigdor J (2008) The Economic Aftermath of Hurricane Katrina. J Econ Perspect 22(4):135-154

Walsh KJE, McBride JL, Klotzbach PJ, Balachandran S, Camargo SJ, Holland G, Knutson TR, Kossin JP, Lee T, Sobel A, Sugi M (2016) Tropical Cyclones and Climate Change. WIREs Climate Change 7:65-89. doi: 10.1002/wcc.371

Weinkle J, Maue R, Pielke Jr. R (2012) Historical Global Tropical Cyclone Landfalls. J Climate 25:4729-4735

Weinstein ND, Lyon JE, Rothman AJ, Cuite CL (2000) Changes in Perceived Vulnerability Following Natural Disaster. Journal of Social and Clinical Psychology 19(3):372-395

Wilson SG, Fischetti TR (2010) Coastline Population Trends in the United States: 1960 to 2008. U.S. Census Bureau 1-27

Wong PP, Losada IJ, Gattuso JP, Hinkel J, Khattabi A, McInnes KL, Saito Y, Sallenger A (2014) Coastal systems and low-lying areas. In: Climate Change 2014: Impacts, Adaptation, and Vulnerability. Part A: Global and Sectoral Aspects. Contribution of Working Group II to the Fifth Assessment Report of the Intergovernmental Panel on Climate Change [Field CB, Barros VR, Dokken DJ, Mach KJ, Mastrandrea MD, Bilir TE, Chatterjee M, Ebi KL, Estrada YO, Genova RC, Girma B, Kissel ES, Levy AN, MacCracken S, Mastrandrea PR, White LL (eds.)]. Cambridge University Press, Cambridge, United Kingdom and New York, NY

Wurman J, Robinson P, Alexander C, Richardson Y (2007) Low-Level Winds in Tornadoes and Potential Catastrophic Tornado Impacts in Urban Areas. B Am Meteorol Soc 88:31–46

Yonekura E, Hall TM (2011) A Statistical Model of Tropical Cyclone Tracks in the Western North Pacific with ENSO-dependent Cyclogenesis. J. Appl. Meteorol. Clim 50:1725-1739